UNIVERSITÀ DI PARMA

UNIVERSITA' DEGLI STUDI DI PARMA

DIPARTIMENTO DI MEDICINA E CHIRURGIA

DOTTORATO DI RICERCA IN

Scienze Mediche e Chirurgiche Traslazionali

CICLO XXXV

Immunomodulating effects and response prediction of the combined treatment with anti-angiogenic agents and immunotherapy in preclinical models of renal cell carcinoma

Coordinatore:

Chiar.mo Prof. Nicola Sverzellati

Relatore:

Chiar.ma Prof. Mara Bonelli

Dottoranda:

Dott.ssa Silvia Zoppi

ANNI ACCADEMICI 2019/2020 - 2020/2021 - 2021/2022

Alla mia famiglia

TABLE OF CONTENTS

ABSTRACT

The introduction of immunotherapy revolutionized the clinical approach of Renal Cell Carcinoma (RCC). RCC is the most common type of kidney cancer, accounting for 80 to 85% of all renal neoplasms and for 2% of all cancer diagnosis worldwide. The clear cell RCC (ccRCC) is the most represented subtype, accounting for approximately 70% of all RCCs. Metastatic ccRCC has long been considered an immunogenic malignancy, susceptible to the effect of immunotherapy. However, in spite of the little success observed with the use of cytokines, the approval of anti-angiogenic tyrosine kinase inhibitors (TKIs) from 2005 followed by the development of immune checkpoint inhibitors (ICIs) represented a real breakthrough in the management of ccRCC. In addition, the demonstration that TKIs as axitinib, whose main targets is VEGFR, play a role in the immune modulation provided the rationale for the association of TKIs and ICIs and between 2019 and 2021 several of these associations were approved as first line treatment in RCC patients.

In this rapidly evolving scenario, there is still scarcity of evidences concerning the best strategy to adopt in patients that progress after a first line treatment consisting of the association of TKIs and immunotherapy. To date, the second line therapy should be any VEGF target therapy that has not already be used in association with immunotherapy. Therefore, it is imperative to define new tailored approaches able to identify the better treatment to choose among further TKIs, ICIs, or also mTOR inhibitors after a previous axitinib-based first line setting. In this context, preclinical *in vitro* and *in vivo* studies could help identify immunomodulating mechanisms, revealing the molecular and immune context generated by the drug exposure in the tumor and the host.

To this end, our study aims to evaluate *in vitro* and *in vivo*, in a syngeneic murine RCC model, the effect of the combination of axitinib and avelumab or pembrolizumab (anti-PD-L1 or anti-PD-1 antibodies, respectively), in terms of modulation of the immune response and anti-cancer efficacy to search for preclinical hints that could lead the future clinical choices. Our research focused on the investigation of the immunomodulatory effect of axitinib alone or in combination with anti-PD-(L)1 agents on a panel of RCC cell lines and PBMCs, both human and murine. Particularly we observed that axitinib treatment induced the expression of the immune checkpoint PD-L1 on the whole panel of tumour cells (769-P and Caki-2, human and

RENCA, murine). In addition to its effect on cancer cells, axitinib exposure reduced the activity of murine T cells activity, while it diminished the surface expression of proteins involved in the down regulation of the immune response as PD-1, TIM-3 and LAG-3 on both human and murine PBMCs, thus preventing T cell exhaustion. Notably, the addition of avelumab or its murine analogue resulted in the amplification of this effect.

Overall, the increase in PD-L1 induced by TKI could induce a stronger effect of the anti-PD-L1 or PD-1 antibodies, providing the biological rationale for their combination. The setting of a syngeneic co-culture system of RENCA cells and murine PBMCs allowed us to obtain a better picture of the complex landscape of interactions happening between tumor and immune cells. Under this condition we demonstrated that the addition of an anti-PD-1 agent to axitinib-treated cells produced an increase lymphocyte activity, quantified both as cytotoxic activity against tumor cells, and as IFN-g production.

These findings underline the immunomodulatory role of axitinib both on tumor cells as well as on lymphocytes activation status.

The second part of the research was focused on the study of the relationship between gut microbiota and responsiveness to treatment. Indeed, in the last few years, emerging data are demonstrating the role of the intestinal microbiota in response to therapy, and how gut bacteria composition could influence the clinical outcome.

With regards to RCC, it has been demonstrated that among gut bacteria population, the relative abundance of a beneficial commensal, *Akkermansia muciniphila*, is associated with the elicitation of immune responses beneficial against cancer. On these bases we evaluated whether standard therapies could induce a taxonomic deviation of stool composition in Balb/c mice treated with a sequential approach that mimics the first- and second-line standard approaches adopted for RCC. In addition, we evaluated the impact of gut microbiota on first line standard therapies, exploring the role of different strains of *Akkermansia muciniphila* to ICIs therapies in avatar mouse model. Our findings demonstrated that the presence of *Akkermansia* strains SGB9228 and SGB9226 in gut microbiota increased mice survival in animals treated with ICIs, suggesting the beneficial role of this commensals in the response to the standard ICI treatment, and indicating that the evaluation of the gut microbiota composition could represent a valuable tool to stratify patients.

INTRODUCTION

1. RENAL CELL CARCINOMA

Renal Cell Carcinoma (RCC) is an insidious neoplasm accounting for the 2% of all cancer diagnosis worldwide, with more than 400,000 new cases around the world [1,2] and 13,500 new cases registered in Italy in 2020 (AIOM 2021). It represents the most common type of kidney cancer, accounting for 80 to 85% of all renal neoplasms[3]. More in depth, RCC is not a single disease but comprises a group of several tumors of renal epithelial origin classified by different histology. Among them, the most represented one is clear cell RCC (ccRCC), accounting for approximately 70% of all RCCs [4,5,6.] At the time of diagnosis approximately two thirds of patients present with localized disease. However, in about 30% of patients with a localized disease cancer will metastasize, and in one third of patients cancer is already metastatic at the time of diagnosis[3,7.]

The better understanding of the pathogenesis of RCC and the development of new agents and treatment options led to a 5-year survival rate among patients with kidney cancer increase from 57% to 74% in the last 15 years. However, not all patients respond to the therapy and there is still an unmet need of clinical biomarkers for predicting the clinical response to treatment [7]. Therefore, RCC is still one of the most lethal urologic malignancies.

EPIDEMIOLOGY

Worldwide, RCC is the sixth most common cancer in men and the tenth in women, accounting for the 5% and 3% of new cancer diagnosis respectively [8]. The male to female ratio is 1.7 : 1 [1]. RCC incidence is higher in Europe and North America, with the highest mortality rate is reported in European countries, and positively correlated with the human development index and gross domestic product [9] (Figure 1).

RCC is the most lethal of all kidney cancers, with a 5-year relative survival rate of about 75%. According to GOBOCAN statistics, RCC caused almost 175.000 deaths in 2018, representing the 1.8% of global cancer deaths[2].

Survival is strongly dependent on tumor staging, consisting of 93% for stage I (localized disease), 75,2% for stage II/III (disease with local lymph node involvement) and of only 12% for a stage IV RCC [1]. In spite of a marked increase in 5-year survival rate, that went from a deceiving 48% in 1970s to a 75,2% of 2015, about 20-50% will progress to a metastatic disease regardless of the nephrectomy [1,7].

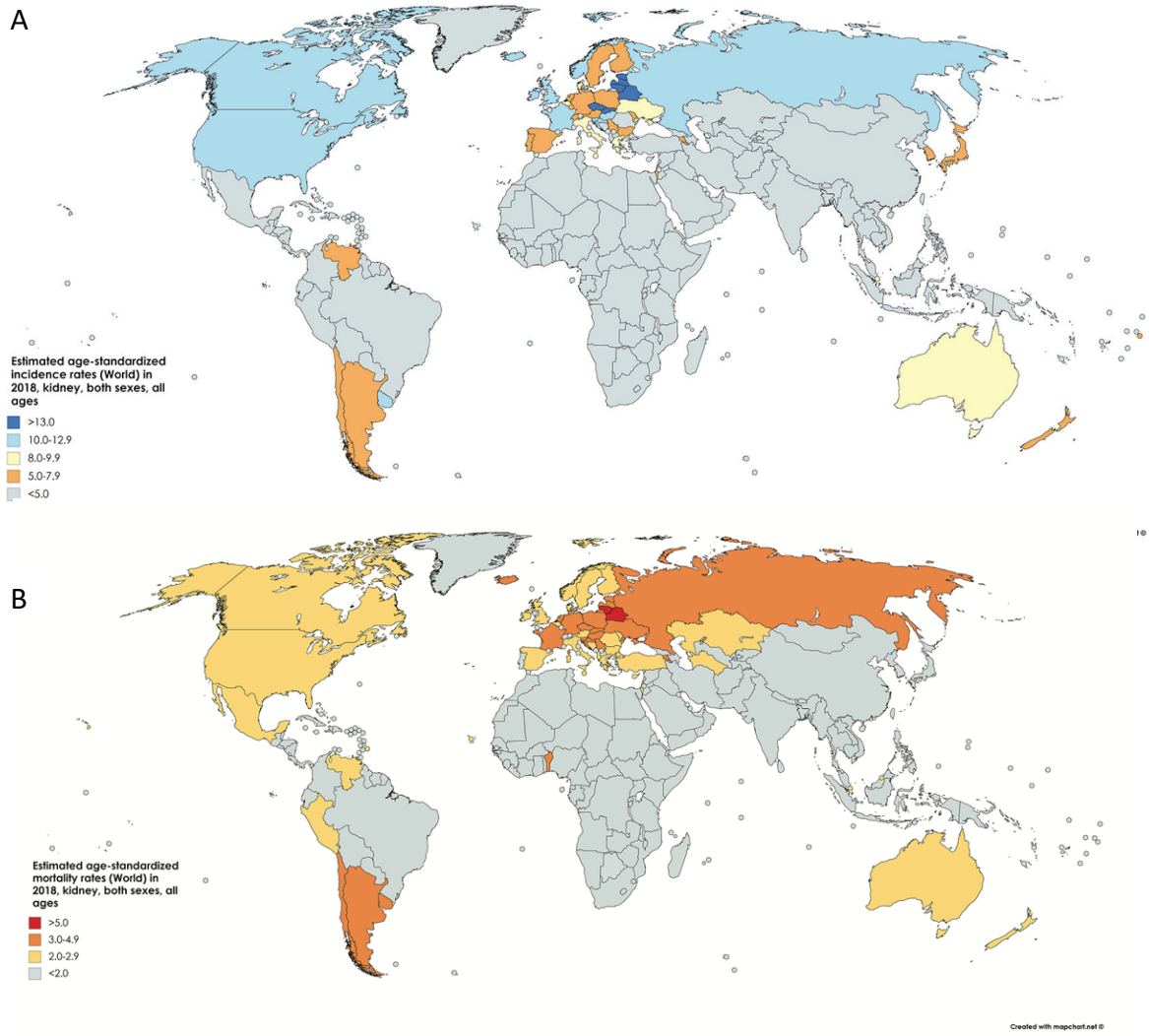

Figure 1. Map showing estimated age-standardized incidence rates (A) and mortality rates (B) for kidney cancer worldwide in 2018, in males including all ages. Created with mapchart.net. Data obtained from GLOBOCAN 2018[1].

RISK FACTORS

RCC incidence varies internationally: incidence is higher in more developed regions like Europe and North America compared to Africa and South America where RCC diagnosis are less than a half. This remarkable variation depends on a combination of factors: surely in Europe and North America there are more tumors incidentally discovered through computerized tomography scan, ultrasound, and magnetic resonance imaging, however this incidence peak is also due to the improvement of quality of life in western countries. RCC is strongly related also to common carcinogenic factors like cigarette smoking, hypertension, obesity and radiation [10].

More in detail, RCC risk factors can be divided into unmodifiable and modifiable.

Non modifiable risk factors are:

Age and sex: Gender and age are strongly correlated with the risk of developing RCC. Sporadic RCC is diagnosed in older adults, with an age-standardized rate (ASR) per 10000 of 0.5 below the age of 40, that increases to 35.0 in over 75 years old. Most patients are diagnosed between the age of 65 and 79 [1,11,12].

Moreover, there is higher prevalence in men, accounting for about two thirds of diagnoses and deaths. The incidence gap remains constant across all age groups [1,11].

Genetic predisposition: RCC occurs in both sporadically and hereditary forms. Although the majority of RCC diagnosis comprises a sporadic disease, several familial syndromes involving the mutations of oncogenes or tumor suppressor genes have been associated with RCC[13]:

- Von Hippel Lindau (VHL) disease, depending on the germline loss of function of the VHL gene on at chromosome 3p25-26[14]. VHL loss represents the most common cause of familial RCC.
- Hereditary papillary RCC (HPRCC), associated with germline mutations on *MET* proto-oncogene and to type 1 papillary RCC (PRCC).
- Birt-Hogg-Dubé (BHD) syndrome, an autosomal dominant inherited cancer syndrome linked to germlines mutations on the folliculin (*FLCN*) gene, a tumor suppressor gene.
- Cowden syndrome, an autosomal dominant disorder caused by germline loss-of-function of the *TSC1* gene.

- Tuberous sclerosis complex, an autosomal dominant disorder associated with mutations of a number of genes, including *PTEN, TSC1* and *TSC2*[15].
- Hereditary leiomyomatosis and renal cancer (HLRCC) an autosomal dominant condition associated with *fumarate hydrase* (*FH*) mutations and type 2 PRCC [16].

Investigations into familial RCC have uncovered mutations in genes that have also been implicated in sporadic RCC development.
More in detail it is known that at least 17 different genes are involved in familial RCC development, among which germline and somatic alterations of genes as *VHL*, *FH*, *MET*, *FLCN*, *PTEN*, *TSC1*, *TSC2*, *BAP1*, *PBRM1*, *MITF*, *FH* and *CDKN2B* are also involved in the development of sporadic RCC [9].

Modifiable risk factors for renal cell carcinoma include:

Cigarette smoking: smoking is a major risk factor for RCC, as for lung cancer and bladder cancer. Cigarette smoke contains polycyclic aromatic hydrocarbons and beta-naphthylamine, classified as group 1, carcinogenic to humans, by IARC. Genetic alteration and inflammation induced by these compounds can increase the risk of RCC [1]. One large meta-analysis found that the risk of developing RCC is increased of about 50% for current smokers, compared to never smokers. Increasing the number of cigarettes per day has also been associated to an increase in Relative Risk (RR) (up to 2.03 for patients smoking 21 or more cigarettes per day), underlying a strong dose-dependent effect on RR [17]. Continued cigarette smoking after RCC diagnosis and during therapy has proved to reduce the PFS and the OS of about 7 and 15 months respectively, and overall to be associated with less clinical benefit [18]. With regards to the histological subtype, there is a correlation between tobacco exposure and the increased risk of developing ccRCC (23%) or papillary RCC (26%) [19]. Overall, active smokers or individuals with a history of tobacco exposure present with more aggressive forms and experience a less overall survival or progression free survival.

Obesity: Obesity is a complex disease, defined as a body mass index (BMI)≥30 kg/m^2 for adults, and characterized by an excessive growth and accumulation of white adipose tissue. Obesity is the second modifiable cause of carcinogenesis after smoking [20].

With regards of RCC, there is a proportional correlation, equally strong in men and women, between the increase in BMI and the risk of developing RCC [21,22]. The association proved to be linear with an increase in the risk of 4% for every increase of 1 kg/m^2 (Wang F. and Xu Y., 2014) and of 25% for every 5 kg/m^2 more [23]. The mechanisms that associate cancer risk and excess weight are not fully elucidated: obesity promotes resistance to insulin and insulin-like growth factor 1 (IGF-1) and an increase in the leptin hormone levels that result in a promoted tumor growth. The disruption of adiponectin levels and the chronic inflammation that characterize obesity may also play a role in tumor initiation and progression [24–26].

Notably, several retrospective studies uncovered a possible positive effect of a BMI>25 on OS, PFS and cancer survival and even for TKI or immunotherapy-treated patients [27–29].This phenomenon is known as the "obesity paradox" and has also been demonstrated in other chronic disease for which obesity is a risk factor. The mechanisms by which obesity could provide a better outcome are not clear. However, using the BMI as a surrogate parameter to evaluate adiposity is not sufficient to evaluate the patient body composition. In addition, changes in BMI that may happen during the therapy are not taken into account in these studies: the role of adipose tissue as a prognostic factor for RCC still has to be elucidated [26].

Diet and exercise: Physical activity may have a protective role against RCC by reducing obesity, blood pressure, insulin resistance (through the reduction of circulating insulin and IGF-1) and lipid peroxidation. According to a meta-analysis physical activity can reduce the risk for RCC by 22% [30].

Some studies suggested that a diet rich in cruciferous consumption could reduce the relative risk (RR) of RCC of about 27% [31], while a diet rich in barbecued meat increases the risk for RCC [32]. Nonetheless, the European Prospective Investigation into Cancer and Nutrition (EPIC) and the VITAmins and LIfestyle (VITAL) study study disputed this result as no significant association between diet and RCC risk was assessed [33,34].

Alcohol: Although there is a significant consensus around the association of alcohol consumption and increase of cancer development [35,36], a moderate alcohol intake showed a protective effect on RCC incidence [37]. Notably, alcohol intake has been correlated with a decrease in RCC risk in a dose-dependent manner, with an estimated 28% reduction in

individuals consummating ≥15g/day of alcohol, equivalent to slightly more than one alcoholic drink per day [37]. Pelucchi et al., found a significant inverse trend in risk even when evaluating an intake >100 g/day, comparable to more than 8 drinks [38]. Conversely, in the VITAL study no association between alcohol intake and RCC was found [34].

Hypertension: there is evidence that hypertension predisposes to RCC [13,34,39]. In the VITAL study hypertension was independently correlated with RCC (HR 1.70) [34], while several studies consistently report a dose-dependent relationship between hypertension and the risk of RCC: in a recent meta-analysis, an increase of 10 mmHg in blood pressure corresponds to an increased risk of RCC of 10%-22% [33,40].

The association between RCC and hypertension is independent of smoking and BMI, and the risk of developing RCC is higher for individuals that are both obese and have hypertension than for those who suffer from only one of these conditions [33,39–41].

The role of statins is controversial. A reduction in blood pressure reduces the kidney cancer risk [39,40], however Sanfilippo and colleagues found that kidney cancer was more frequently diagnosed in women with treated hypertension than among untreated patients [41]. Altogether, the risk of RCC could be reduced with a better blood pressure control.

Diabetes: Diabetes mellitus is associated with increased risk of several types of cancer, including RCC [42–44]. Interestingly, an independent biologic effect of diabetes comorbidities was reported in several studies [42]. A history of diabetes could correlate with 42% of risk of RCC [42].

Occupational exposure: Although RCC is not considered an occupational disease as bladder cancer and mesothelioma, several risks has been linked to occupational exposure to specific agents. Among them, the most studied is trichloroethylene, a substance most known for its use as a metal cleaner and degreaser and whose occupational exposure is classified as carcinogenic to humans by IARC[45]. Exposure to trichloroethylene confers 30% to 40% additional risk to develop RCC [46].

In addition, other occupational substances that can relate with RCC induction are asbestos, benzene, vinyl chloride, cadmium, and an overdose of acetaminophen [1].

HISTOPATHOLOGICAL FEATURES

Increasing evidences over the years suggested that RCC represent a group of histologically heterogeneous diseases. In this scenario, the histological classification is of outmost importance considering that every specific histologic variant is related to a different prognosis [47,48]. Currently, according to the 2022 WHO classification, several histological RCC subtypes have been identified (Table 1)[49].

WHO Classification of Renal Cell Tumors
ccRCC
Clear Cell Renal Cell Carcinoma
Multilocular cystic renal neoplasm of low malignant potential
Papillary renal tumors
Papillary adenoma
Papillary renal cell carcinoma
Oncocytic and chromophobe renal tumors
Oncocytoma
Chromophobe cell renal carcinoma
Other oncocytic tumors of the kidney
Collecting duct carcinoma
Other renal tumors
Clear cell papillary renal cell tumour
Mucinous tubular and spindle cell carcinoma
Tubulocystic renal cell carcinoma
Acquired cystic disease–associated renal cell carcinoma
Eosinophilic solid and cystic renal cell carcinoma
Renal cell carcinoma, NOS
Molecularly defined renal carcinomas
TFE3-rearranged renal cell carcinomas
TFEB-altered renal cell carcinomas
ELOC (formerly TCEB1)-mutated renal cell carcinoma Fumarate hydratase–deficient renal cell carcinoma
Hereditary leiomyomatosis and renal cell carcinoma
Hereditary leiomyomatosis and renal cell carcinoma
Hereditary leiomyomatosis and renal cell carcinoma syndrome–associated renal cell carcinoma
Succinate dehydrogenase–deficient renal cell carcinoma
ALK-rearranged renal cell carcinomas
Medullary carcinoma, NOS

Table 1.

Adapted from 2022 WHO Classification of Renal Cell Tumors[49]

In particular, the most frequent RCC are:

Clear cell Renal Cell Carcinoma (ccRCC)

Clear cell Renal Cell Carcinoma (ccRCC) is the most common and aggressive histological subtype, comprising itself the 60-75% of all adult cancers of the kidney [47,48]. ccRCC originates from the epithelium of proximal tubules in the renal cortex and macroscopically it is a yellowish lesion with signs of necrosis and hemorrhage. Histologically, ccRCC cells are characterized by a lipid- and glycogen-rich cytoplasm, resulting in a typical clear color [47,48]. The majority of ccRCCs are sporadic (90%) while the remaining 5-7% is normally associated with hereditary syndromes as the VHL disease or the tuberous sclerosis [48].

Papillary RCC (pRCC)

The papillary variant is the second most common for RCC, accounting for 10 to 20% of all adult RCCs [47,48]. As for ccRCC it can occur sporadically or as a familial condition [48]. The fifth edition of the WHO classification of Tumors of the urinary system and male genital organs eliminated the previous categorization of pRCC in two subtypes (type 1 and type 2 pRCC), on the basis of the recognition of several individual entities with different molecular backgrounds within the type 2 pRCC [49]. pRCC patients have been reported to have a better prognosis compared to ccRCC patients [47].

Chromophobe RCC (ChRCC)

Chromophobe RCC is the third most common variant accounting for 5-7% of all RCCs and is associated to the Birt-Hogge-Dube syndrome. It is less aggressive and has a more favorable prognosis than ccRCC, metastasis occurs in only 7% of cases. ChRCC presents with a light orange to brown color, characterized by large pale cells with irregular nuclei and perinuclear halos [47,48].

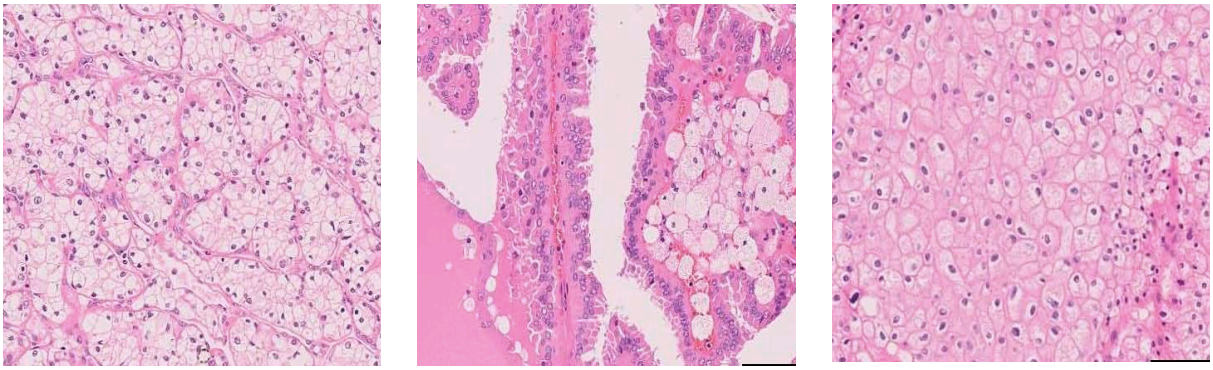

A B C

Fig 2. Morphology of the principal histotypes of RCC A) Clear Cell Renal Cell Carcinoma. B) Papillary Renal Cell Carcinoma. (C) Chromophobe Renal Cell Carcinoma [47].

CLASSIFICATION AND PROGNOSTIC FACTORS

Cancer staging is the process of determining the spread and growth of the primary tumor. It predicts prognosis and guides the management and treatment decisions. For many tumors the dissemination is the critical parameter to assess, as spreading beyond the origin site orientates the therapeutic strategy between cure and palliation. The American Joint Committee on Cancer (AJCC) tumor-node-metastasis (TNM) staging is the most commonly used and universally accepted staging system for cancer. This tumor classification has been initiated by Denoix in 1943 and firstly published in 1958. To date, the recommended version to utilize is the 8th, published in 2017, and resumed in the table below [50,51]. T descriptors designated as T1, T2, T3 and T4, provide precise anatomic definitions of the local extent of the primary tumor. The N descriptors are designated as N0, N1, N2 and N3. The stage groupings recognize new data about the better prognosis of T1 and N0 tumors and classify those tumors into stages I and II. The adverse impact of nodal metastases on survival noted in some recent surgical series warrants placing node positive tumors in stage III. Locally advanced unresectable (T4) tumors and N3 or M1 are classified as stage IV [52].

TNM 8th edition for RCC

T-primary tumor

Tx Primary tumor cannot be assessed
T0 No evidence of primary tumor

T1 limited to the kidney, < 7cm	T1a ≤ 4cm T1b >4cm - 7cm
T2 limited to the kidney, > 7 cm	T2a > 7cm - 10 cm T2b > 10 cm
T3 Tumour extends into major veins or perinephric tissues but not into the ipsilateral adrenal gland and not beyond Gerota fascia	T3a tumor grossly extends into the renal vein or its segmental (muscle-containing) branches, or tumor invades perirenal and/or renal sinus fat but not beyond the Gerota fascia T3b spread to infra diaphragmatic IVC T3c spread to supra diaphragmatic IVC or invades the wall of the IVC

T4 involves ipsilateral adrenal gland or invades beyond Gerota fascia

N- nodal involvement

N0 No nodal involvement
N1 Metastatic involvement of regional lymph node (s)

M- Metastasis

M0 No distant metastases
M1 Metastases

Stage grouping	T	N	M
Stage I	T1	N 0	M 0
Stage II	T2	N 0	M 0
Stage III	T3	N 0	M 0
	T1, T2, T3	N 1	M 0
Stage IV	T4	Any N	M 0
	Any T	Any N	M 1

Table 2 and 3. TNM classification, 8th edition; TNM staging system

The prognostic value of the anatomical information provided by the TNM staging system has been validated in both single and multi-institution studies, demonstrating that a higher stage correlates with worse prognosis [50,51]. Anatomical classification systems as PADUA (Preoperative Aspects and Dimensions Used for an Anatomical classification system), recently updated to the simplified versine SPARE (Simplified PAdua REnal), the R.E.N.A.L. (Radium, Exophytic/endophytic properties, Nearness of the tumor to the collecting system or sinus, Anterior/posterior, Location relative to the polar line) and the C-index have been proposed for the description and standardization of renal tumors [53,54].

Other parameters that could impact the prognosis are histopathological features, clinical and molecular factors.

Histological features include the Fuhrman nuclear grade, the histologic subtype, sarcomatoid features, vascular invasion, tumor necrosis and perirenal fat [51,55]. The Fuhrman score evaluates the prognostic significance of morphological parameters and its predictive value has been validated, nonetheless it is significant only for the clear cell subtype [50,56,57]. With regards to the histological subtype, ccRCC displays higher risk of death compared with pRCC type I and pRCC type II in the non-metastatic setting [58], reflecting the need of a tailored therapeutic strategy.

Clinical prognostic features include local symptoms and performance status, cachexia and anaemia [55]. Performance status is the most relevant, allowing a functional assessment of patients; it can be evaluated in different ways, the more common are through the Eastern Cooperative Oncology Group (ECOG) scale or the Karnofsky scale. The two scales are largely used as ways to classify a patient according to their functional impairment, compare the effectiveness of therapies, and assess a patient's prognosis (see the table below). Several post-operative risk- assessment nomograms have been tested to better predict the survival, but none have been validated yet [51].

In advanced kidney cancer the anatomical factors described above have limited prognostic significance, as the primary tumor features disappear once the tumor spread and become metastatic. ECOG and Karnosfky scales remain the most important prognostic tools for patients assessment in mRCC. Laboratory parameters could be added to clinical prognostic

assessment, these including high levels of calcium, leukocyte count, platelet count, c-reactive protein, low hemoglobin, lactate dehydrogenase (LDH), elevated pre-operative neutrophil to leukocyte ratio (NLR) [59]. These parameters have been shown to correlate with prognosis and in particular high calcium levels, preoperative anemia and neutrophil to lymphocyte ratio are associated with survival [59].

To better evaluate and define the prognosis, different tools were defined to address mRCC patients. The main prognostic clinical models adopted are the International Metastatic RCC database consortium (IMDC), the Memorial Sloan Kettering Cancer Center (MSKCC) model and the UCLA Integrated Staging System (UISS).

The IMDC score individuates six independent predictors of poor survival: performance status (Karnofsky performance status < 80%), time from diagnosis to start of treatment inferior than 1 year, low hemoglobin level (anemia), corrected serum calcium higher than normal level (hypercalcemia), neutrophilia (neutrophil count > upper limit of normal) and thrombocytosis (platelet count >upper limit of normal) [32]. Depending on the number of poor prognosis factors patients are categorized into good prognosis (lack of factors), intermediate risk of death with a median overall survival of about 23 months (one or two factors) and poor risk with median survival of about 8 months (more than three factors) [32,60].

The MSKCC model includes adverse independent prognostic factors as Karnofsky performance status less than 80%, LDH higher than 1.5 times the upper limit of normal, serum hemoglobin less than the lower limit of normal and the interval between diagnosis and beginning of systemic treatment less than 1 year [61]. Also in this model, patients are segregated into good, intermediate or poor-risk groups according to the number of pre-treatment factors, zero, one or two and more than two respectively. Patients with favorable prognosis did not reach OS, in the intermediate group OS was 27 months and in the poor-risk group OS was 8.8 months [61].

The University of California, Los Angeles Integrated Staging System (UISS) is a postoperative model based on TNM stage, Fuhrman grade, and ECOG performance status (PS), that defines three risk groups, favorable, intermediate and poor-risk, and it is validated for both localized cancer and metastatic tumor patients. The OS to three years related to this model, about the patient with metastatic cancer, is 37% in the favorable risk group, 23% in the intermediate-risk group, and 12% in the poor-risk group (Patard J.J. et al., 2004).

Several molecular markers are under evaluation for treatment selection in mRCC. Markers taken into account are either circulating, as VEGF and VEGF-correlated proteins, cytokines and angiogenic factors, circulating endothelial cells, LDH and the carbonic anhydrase IX (Ljungberg B. et al., 2022), or tissue located, as Ki67, p53, PTEN, P21, as well as gene mutations or gene expression profiling [51]. However, none of these has been able for now to yield significant data to improve the prognostic evaluation of patients [51].

In addition, several chromosomic alterations as 7q, 8q, 20q gain or loss of 9p, 9q and 14q have been related to a worse survival, with a prognostic role [62]. Notably, it has been reported that expression levels of *PBRM1*, a gene involved in chromatin stability, and *BAP*1, an important tumor suppressor gene involved in DNA damage response and regulaton of cell cycle and cell growth [63]are independent prognostic factors for mRCC: the concomitant loss of both genes is related to a worse prognosis [64]. Another study reports that patients with BAP1 mutations have a worse prognosis compared to patients with PBRM1 mutation [65].

The introduction of new therapies for mRCC treatment, as target therapy and immunotherapy, boosted the research for other molecular factors that could possibly have a prognostic and/or predictive role for patients. Particular relevance was paid to PD-L1 and the tumor mutational burden in this context. However, a meta-analysis investigating the role of PD-L1 expression in 6 studies and 1623 cases of RCC, at various stages and immunotherapy naïve, reported a negative prognostic role of PD-L1 expression and an increased risk of death (HR; 1.81, 95 % CI 1.31-2.49; $p < 0.001$) [66] and another meta-analysis reports that segregating patients depending on PD-L1 expression could be useful to identify patients that will later benefit of therapy in terms of PFS but not in terms of OS [67].

It appears that studying the ensemble of molecular features trying to identify a signature might be the key to identify patients that will later benefit from therapy. The IMmotion150 study (NCT01984242) compared the association of atezolizumab and bevacizumab vs sunitinib and reported that angiogenesis, T-effector/IFN-γ response, and myeloid inflammatory gene expression signatures were associated with PFS, suggesting that these signatures might be predictive of the response to VEGF inhibitors or to immunotherapy [68]. Similarly, a randomized phase III trial testing the combination of avelumab and axitinib vs sunitinib alone in mRCC patients (NCT 02684006) found that genes involved in angiogenesis, activation of T lymphocyte and IFNγ pathway and NK cells made a genetic signature able to predict the

response to immunotherapy. At the same time the study confirmed the signature found in the IMmotion150 trial [69]

SYMPTOMS

The majority of RCC patients only present with symptomatic disease (bone pain, deterioration of performance status, persistent cough are the more common) in advanced stages. Indeed, the most of RCC cases are detected incidentally during non-invasive imaging for the investigation of aspecific symptoms and abdominal diseases [70]. The classical triad of flank pain, gross hematuria and palpable abdominal mass is less frequent than in the past and generally correlates with a more aggressive disease[71], while paraneoplastic syndromes as hypercalcemia, unexplained fever, erythrocytosis and Stauffer's syndrome are relativey frequent [51,71].

2. ETIOPATHOGENESIS

RCC development could be considered as the complex interplay of different factors. Among them there are three elements particularly relevant: angiogenic alterations, metabolic reprogramming and the tumor microenvironment.

ANGIOGENIC ALTERATIONS

RCC, as many solid tumors, is characterized by a hypoxic condition due to the local imbalance between oxygen supply and consumption [72,73]. Mammalian cells exposed to conditions of low oxygen tension undergo an adaptative response that adjusts cellular metabolism to the limited availability of oxygen and triggers the formation of new blood vessels and the production of new blood cells to restore oxygen supply [74]. This adaptation is coordinated by the hypoxia inducible factors (HIFs), a family of heterodimeric transcription factors that respond to a decrease in oxygen levels in the cellular environment. HIF proteins consist of an α–subunit (either HIF-1α or HIF-2α) and a β–subunit, where the level of the α–subunit represent the rate-limiting step in their functions as its availability varies with the oxygen levels. In normoxic conditions, HIF-1α is hydroxylated by a series of prolyl hydroxylases in a process that requires molecular oxygen, while cytoplasmatic VHL forms a ubiquitin ligase complex with elongins B and C and cullin 2. The presence of a hydroxyl group at the proline

residues allows the binding of HIF-1α and the enzyme complex mediated predominantly by VHL and resulting in the ubiquitination of HIF-1α and its subsequent degradation [73].

By contrast, under hypoxic conditions HIF-1α is not hydroxylated and forms an heterocomplex with HIF-β in the nucleus, inducing the expression of genes that contain hypoxia-response elements (HRE) in the promoter, such the vascular endothelial growth factor (VEGF), the platelet derived growth factor β (PDGF-β) and the transforming growth factor α (TGF-α) genes [73–76].

In ccRCC, the hypoxia signaling pathway is permanently active, in part due to its solid tumor nature and in part due to the loss or mutation of *VHL*, which occurs in the 90% of all sporadic ccRCC cases and is nearly ubiquitous in familial cases of ccRCC [47], that maintains a condition of "pseudohypoxia" [15,74]. This results in a HIF-1α accumulation and a subsequent constitutive expression of HIF-induced proteins. Increased expression of many of the HIF targets is involved in cancer promotion through different mechanisms: VEGF and PDGF are known to induce angiogenesis and particularly VEGF expression correlates with micro vessel density, while TGF-β and the epidermal growth factor (EGF) are oncogenic growth factors that promote tumor growth and metastasis [77].

VEGF is a key player in the induction of (tumor-related) angiogenesis. The VEGF family includes several isoforms: *VEGF-A, VEGF-B, VEGF-C, VEGF-D, VEGF-E, VEGF-F* and the placenta growth factor (PGF) [78]. These factors exert their effect by binding with different affinities to their respective receptors (VEGFRs) and co-receptors that include neuropilins and sulfate proteoglycans [79]. VEGFRs are tyrosine kinases receptors (RTKs) among which are described three different receptor types: VEGFR-1, VEGFR-2 and VEGFR-3. VEGF-1 and 2 are mainly expressed on vascular endothelial cells, but can also be expressed on non-endothelial cells, while VEGFR-3 is predominantly expressed on endothelial lymphatic cells [78,80]. Binding of VEGF to the correspondent receptor causes the autophosphorylation of the tyrosine residues and the activation of several signaling pathways involved in proliferation and survival of endothelial cells, as phospholipase-Cγ (PLCγ)/protein kinase C (PKC), Ras/Raf/ERK/MAPK pathways and PI3K/Akt pathway [81–84]. The activation of VEGFR-1 has been associated with the promotion of inflammatory cells migration and inflammatory cytokines secretion, such as: tumor necrosis factor α (TNF-α), interleukin-1 β (IL-1β), IL-6, monocyte chemoattractant protein-1, macrophage inflammatory protein-1β [85,86].

Altogether, tumor-associated angiogenesis results in an abudanttumor microvasculature characterized by fenestrations between the endothelial cells of capillaries and venule. This results in the promotion of mobilization of inflammatory cells to the tumor site, maintaining the local inflammatory processes [77,78].

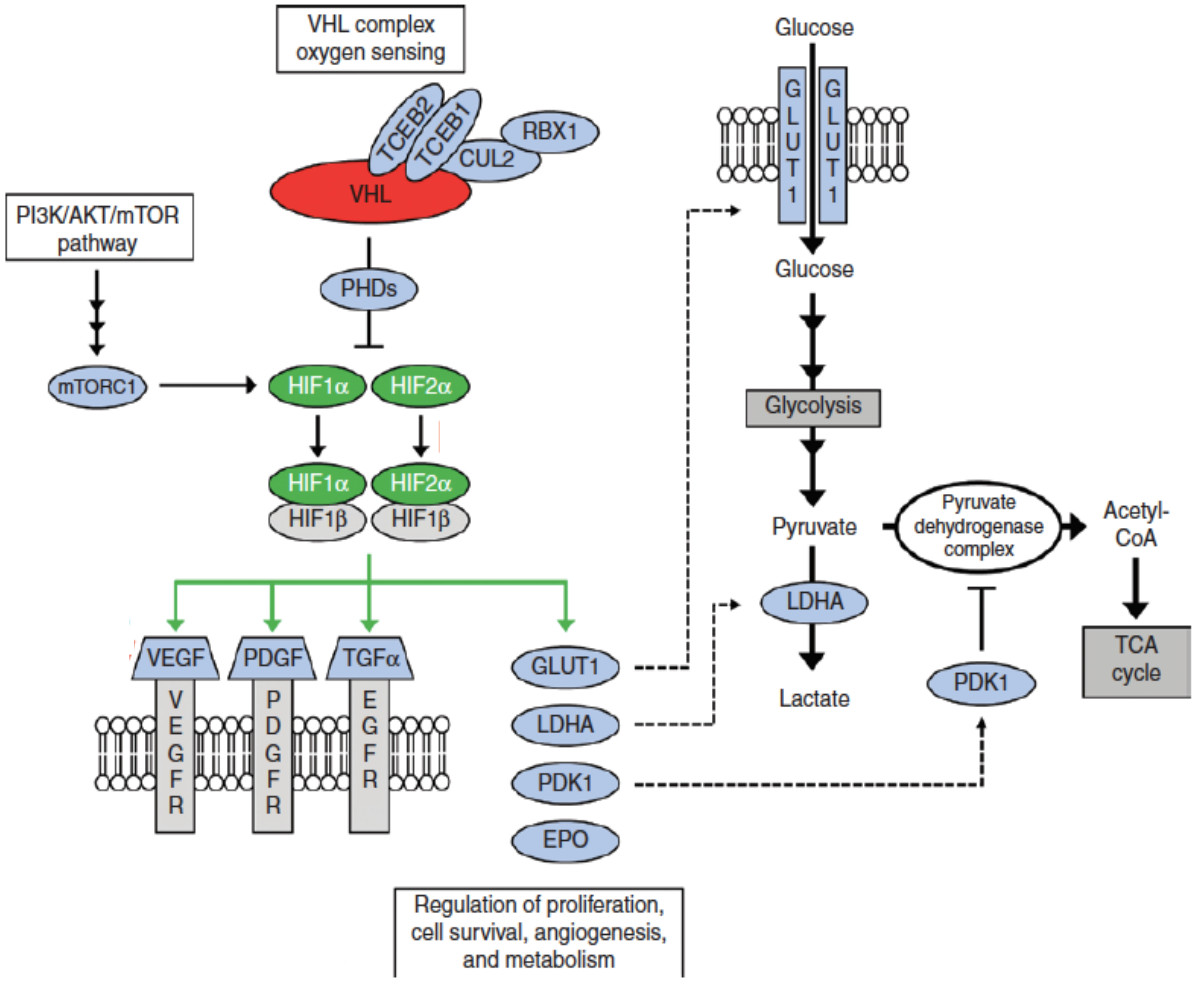

Figure 3. The VHL/HIF pathway modulation in ccRCC*. In normoxic conditions, the VHL complex targets the HIF proteins for degradation after the hydroxylation of the HIF proteins. In ccRCC characterized by VHL loss of function, the VHL protein is inactivated, thus resulting in the loss of degradation and stabilization of HIF1α and HIF2α. The HIFs upregulate the expression of several growth factors, including VEGF, PDGF, and TGFα, that modulate angiogenesis and proliferation through the binding with their respective receptors tyrosine kinases (RTKs). The expression levels of the HIF transcription factors are also regulated by the PI3K/AKT/mTOR pathway. The impact of the HIF transcription factors on metabolic adaptation comprehends also the upregulation of the expression of several genes involved in glucose metabolism regulation*[15].

METABOLIC REPROGRAMMING

In addition to its transcriptional role, activated HIF-1 plays a crucial role in determining the cellular adaptive response to oxygen concentration changes though the modulation of metabolic pathways. HIF-1 sustains the metabolic shift from the oxidative phosphorylation to the less efficient glycolysis in tumor, inducing a more relevant glucose consumption. Indeed, the regulation of several genes involved in the regulation of glucose consumption are under HIF-1 control, such as *GLUT1* that increases the expression of glucose transporters 1 (GLUT-1) on cellular surfaces, and *PFK1*, that encodes for the phosphofructokinase 1 and aldolase, inducing an increase in the glycolytic breakdown of intracellular glucose [77,87]. The adaptation to the reduced oxygen concentration is also promoted through the downregulation of the oxidative phosphorylation by activation of *PDK1,* a gene encoding for the pyruvate dehydrogenase kinase 1, the enzyme inhibiting the activity of the pyruvate dehydrogenase, and MAX interactor 1 [87]. The global effect is the reduced oxygen demand.

Moreover, HIF-1 activation is induced upon the PI3K/AKT/mTOR pathway downstream signaling, thus implicating a large crosstalk between the two pathways contributing to RCC development [88,89]. As HIF, the PI3K/AKT/mTOR pathway controls the activation of receptor tyrosine kinases (RTKs) and plays an important role in the regulation of metabolic adaptations of the cells [89]. Besides its role in the downstream activation of HIF-1, this pathway it is considered to be a major determinant of the glycolytic phenotype through AKT1 and mTOR signaling [89].

PI3Ks are a unique family of intracellular lipid kinases that phosphorylate the 3'-hydroxyl group of the inositol ring of phosphatidylinositides (PtdIns). PI3K stimulates the conversion of membrane-bound phosphatidylinositol-(4,5)-bisphosphate (PIP_2) to phosphatidylinositol-(3,4,5)-trisphosphate (PIP_3). PIP_3 acts as a secondary messenger, facilitating the recruitment and activation of kinases such as PI3K-dependent kinase-1 (PDK1) and protein kinase B (PKB), also known as AKT. The signalling duration of PIP_3 is subject to regulation by PTEN, which acts to oppose PI3K activity. AKT activation is a key step in this pathway, regulating apoptosis, cell cycle progression and activation of mTOR. Phosphorylation by both PDK1 and mTORC2 is essential for full AKT activation. Activated AKT is a well-established survival factor, exerting antiapoptotic activity through several mechanisms such as preventing the release of cytochrome c from the mitochondria [90]. It also phosphorylates and inactivates the

proapoptotic factors BAD and procaspase-9 and the FOXO transcription factors, which mediate the expression of genes critical for apoptosis. AKT also activates IkB kinase (IKK), a positive regulator of NF-kB, which allows cell proliferation. Lastly, AKT promotes the phosphorylation and translocation of MDM2 into the nucleus, where it induces p53 degradation and thereby promoting cell cycle progression [91,92]. In addition, AKT controls the stability of cyclin D1, through the phosphorylation and consequent inhibition of glycogen synthase kinase 3b (GSK3B) [93]. AKT also directly antagonizes the action of the cell cycle inhibitors $p21^{WAF1}$ and $p27^{Kip1}$ by inducing their cytoplasmic retention [94]. Moreover, phosphorylation of AKT/mTOR kinases also results in increased translation of cyclin D1, D3, and E transcripts [95]. Lastly, AKT upregulates expression of the glycolytic enzyme PKM2, thus contributing to the Warburg effect. Particularly, AKT activation promotes the glycolytic metabolism through the AKT-induced translocation of glucose transporters and through the activation of hexokinase and phosphofructokinase. In addition, AKT induces the de novo fatty acid synthesis [89].

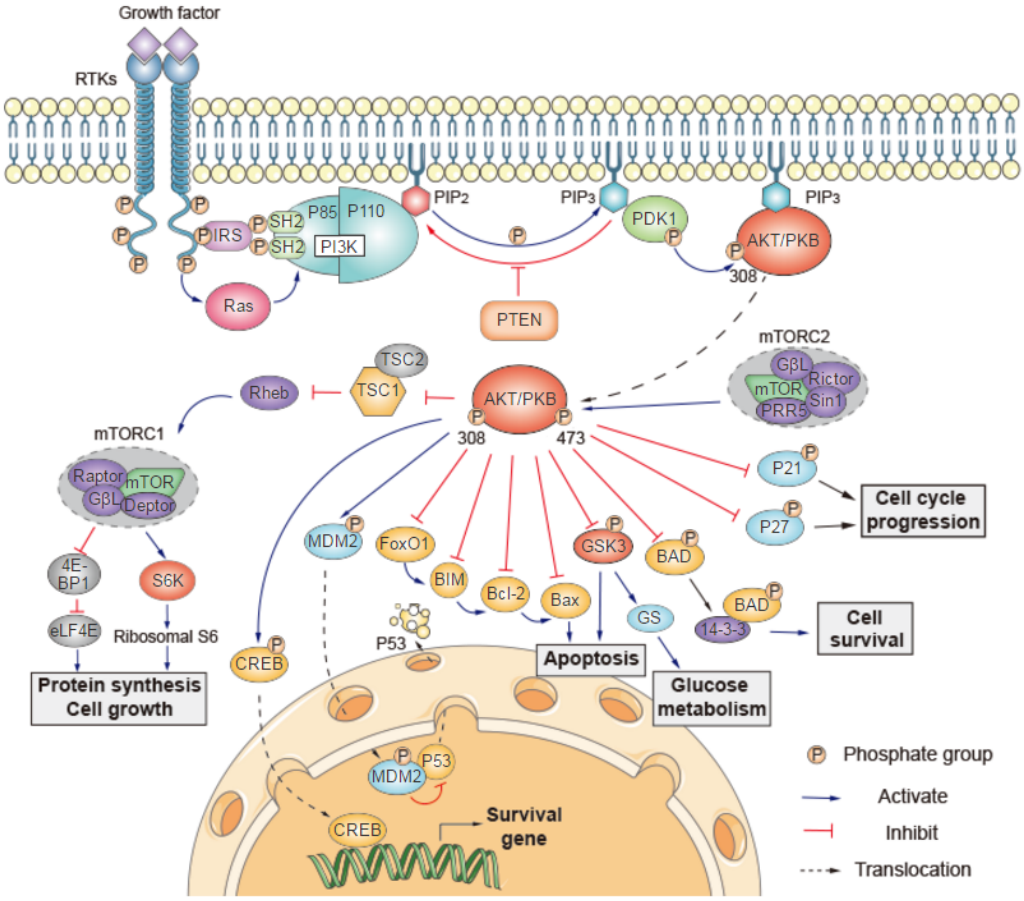

Figure 4. The PI3K/AKT signaling pathway. Components of these pathways recurrently targeted by genetic/epigenetic alterations in cancer are depicted with a red asterisk. (CD creative diagnostics).

AKT activates the downstream mTOR kinase by inhibiting a complex formed by the tumour suppressor proteins TSC1 and TSC2, also known as hamartin and tuberin. mTOR is an evolutionarily conserved serine/threonine protein kinase that belongs to the PI3Krelated kinase family (PIKK). The accessibility of the mTOR active site is governed in part by mTOR-associated proteins that form two distinct complexes: mTOR complex 1 (mTORC1) and 2 (mTORC2). These complexes differ in their composition, mode of activation and rapamycin sensitivity [96,97]. mTORC1 activation status is affected through a variety of environmental cues, including growth factors (as transmitted via the PI3K/AKT pathway for example), energy status, amino acids, and oxygen levels. mTOR broadly mediates cell growth and proliferation by regulating protein synthesis and can regulate response to nutrients by restricting cell cycle progression in the presence of suboptimal growth conditions. In brief, mTOR controls the synthesis of cyclin D1, Myc, and vascular

endothelial growth factor (VEGF) by phosphorylating p70S6 kinase (p70S6K) and eIF4E binding proteins 1, 2, and 3 (4E-BPs) [98]. Constitutively activated mTOR functions in supplying carcinoma cells with oxygen and nutrients by increasing the translation of HIF-1. mTOR also aids in another metabolic adaptation of cancerous cells to support their increased growth rate: activation of glycolytic metabolism. The downstream effectors of mTORC2 identified thus far are mainly members of the AGC kinase family, including AKT, protein kinase C (PKC) and serum and glucocorticoid-induced kinases, which modulate cytoskeleton organization, cell survival, lipid homeostasis and metabolism [99].

The complete mTOR activation and downstream pathway is described in Figure *5.*

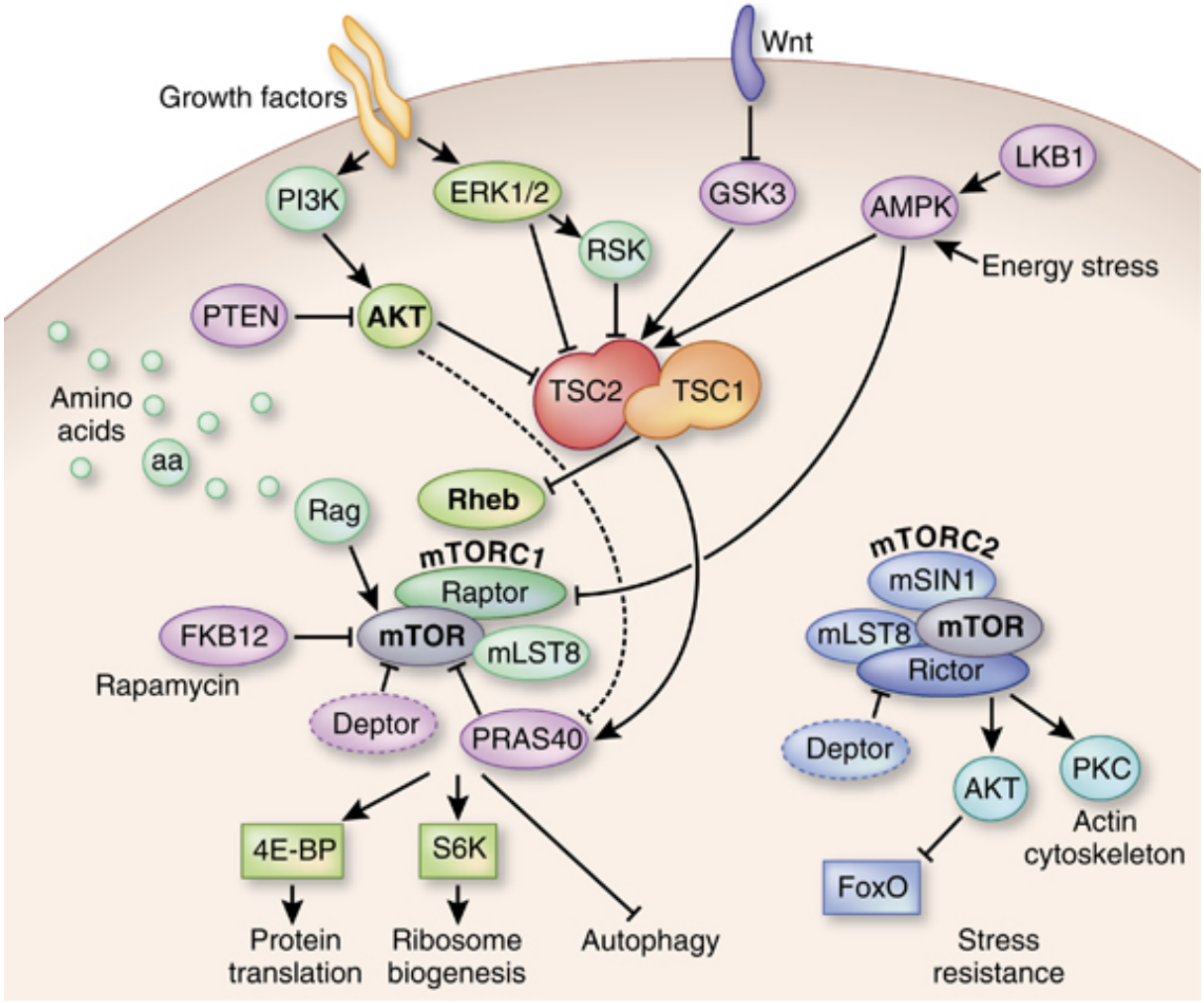

Figure 5. mTOR signalling cascade. The mTOR protein is part of two protein complexes: mTORC1 and mTORC2. mTORC1 is activated by growth factor signaling to phosphorylate 4E-BP and S6K, resulting in ribosome biogenesis and protein translation. mTORC1 is negatively regulated by the TSC complex. Activating proteins are shown in

green, inhibiting proteins in red. mTORC2 is activated to phosphorylate AKT and to regulate the actin cytoskeleton through PKC [100].

In ccRCC, between the VHL/HIF and PI3K/AKT/mTOR pathways exist an extended crosstalk that sustains tumor progression. The activation of the mTORC1 complex, which regulates the expression of several cellular proteins as 4E-BP1 and S6K, leads to the expression of a number of transcription factors as the above-mentioned HIF and c-Myc [89]. In addition, ss already mentioned, HIF upregulation due to VHL loss of function induces the expression of several growth factors, as VEGF, which in turn may activate the PI3K/AKT/mTOR pathway through the receptor tyrosine kinases. The subsequent activation of mTOR promotes itself HIF expression, therefore inducing a feedback loop resulting in the constitutive activation of the signaling network [88]. Overall, despite the total mutation rate for the PI3K/AKT pathway is lower than in other cancer types, the activation of this pathway is reported to be high among all cancers [101]. At the same time, other metabolic alterations frequently reported for RCC are a decreased expression of the components of the tricarboxylic acid (TCA) cycle, the suppressed entry of the pyruvate into the TCA and an impaired oxidative phosphorylation [15].

The TCA cycle is a chore metabolic pathway representing the main source of energy for cells. It takes place predominantly in the mitochondrial matrix, aiming to produce nicotinamide adenine dinucleotide (NADH) and flavin adenine dinucleotide (FADH) in their reduced form. NADH and FADH would subsequently be oxidized by the mitochondrial electron transfer chain (ETC), for ATP biosynthesis (Figure 6).

Particularly, in RCC it has been reported a decreased level of fumarate and malate and an opposite increase in succinate, isocitrate and citrate levels [15,102]. These alterations could be explained by the reductive carboxylation observed in VHL deficient ccRCC cell lines [103], shown to convert α–ketoglutarate, derived from the absorbed glutamine converted to glutamate, to citrate [103]. It has additionally been reported an increase in the expression of the oxidative pentose phosphate pathway for RCC, necessary for the production of NADPH and the ribose sugars necessary for replication [15]. There are evidences supporting the correlation between

metabolic reprogramming (decreased TCA cycle and AMPK gene expression and increase in penthose phosphate pathway and fatty-acid synthesis), and patients outcome[15,104].

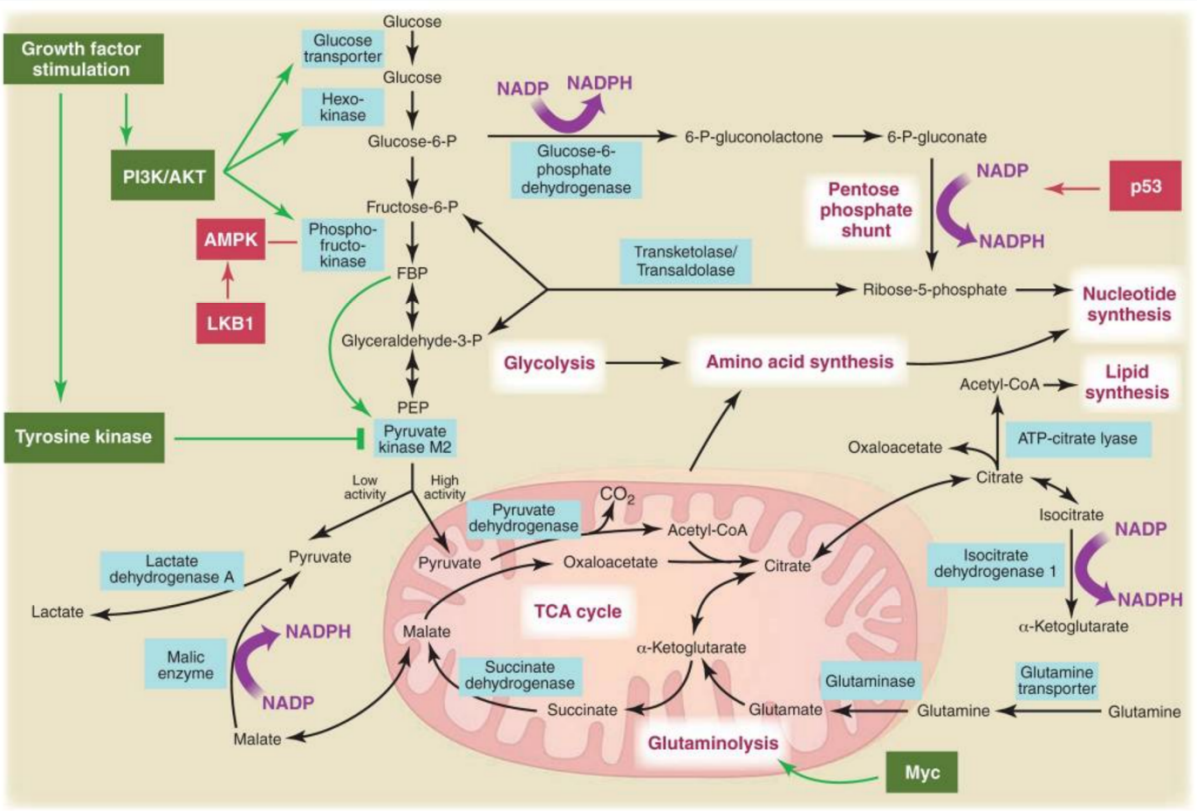

Figure 6. The main cellular metabolic pathways [105]

Lastly, a deeper analysis of the genes related to kidney cancer underscored that at least 17 different genes (among which *VHL*, *MET*, *FLCN*, *TSC1*, *TSC2*, *FH* and *SDH*) are involved in cellular pathways that regulate the energy, nutrient, iron or oxygen sensing [15,106]. Alterations in these pathways result in profound changes not only in glucose and glutamine utilization but also in lipid metabolism and mitochondrial function [74]. Collectively these modifications are known as "metabolic reprogramming", a phenomenon typical of RCC, which promotes cellular proliferation and tumor growth and resilience [74]. On these bases, kidney cancer can be considered a metabolic disease [106].

TUMOR MICROENVIRONMENT

The third element playing a fundamental role is the tumor microenvironment (TME) and its immune context. It is well recognized that tumor cells stimulate significant changes in their host tissues at a molecular, cellular and physical level, to obtain an environment that support

tumor growth and progression. Therefore, the tumor is an heterogenous complex of infiltrating and resident host cells, secreted factors and an extracellular matrix: a continuous evolving entity, supporting tumor progression, metastasis and determining the ability of the immune cells to recognize and eradicate tumor cells.

With regards to kidney cancer, its TME has peculiar features, compared to other tumor types: the rich VEGF-driven vascularization, and a dense leukocyte infiltrate [107].

Tumor infiltrating immune cells form an organized landscape composed of several cellular types inside the tumor microenvironment that has been associated with RCC patients prognosis. Lymphocytes T and macrophages are located both in the center of the lesion and at the margins, while natural killer (NK) cells, myeloid-derived suppressor cells (MDSCs), mast cells and neutrophils remain at the tumor margins. B lymphocytes and mature dendritic cells preferably host tumor-adjacent lymphoid islets [108]. Vascular and lymphatic vessels, as well as the fibroblastic stromal support, guide the disposition of these cells in the microenvironment [108]. A dense immune infiltrate is a common characteristic of solid tumors with favorable prognosis, as colorectal carcinoma, ovarian cancer, melanoma, breast, hepatocellular, head and neck, lung, bladder, pancreatic and gastric cancer [109–111].

A common characteristic of ccRCC tumors reported both by clinical and DNA expression studies is the rich leukocyte infiltrate [112,113]. The most prevalent component of the ccRCC immune infiltrate are $CD8^+$ and $CD4^+$ cells, NKs, myeloid cells with characteristics of macrophages and neutrophils [6,114]. Surprisingly, the abundance of $CD8^+$ and $CD4^+$ T cells at the invasive margins has been reported to be associated with higher tumor grade and a shorter patients' survival [6,108]. The inability of tumor-infiltrating lymphocytes (TILs) to mediate anti-tumor function has been extensively studied and its restoration has been proposed as a mean to enhance the efficacy of anti-tumor therapies.

Changes in classical and non-classical human leukocyte antigens (HLA) class I antigens expression on tumor cells have been associated with the dysregulation of TILs. A proper HLA class I expression is necessary for the presentation of antigens to $CD8^+$ cytotoxic T cells. Downregulation or loss of HLA I or other mediators involved in antigen processing such β_2-microglobulin, antigen peptide transporter 1 (TAP1), low molecular mass protein 2 (LMP2) and 7 (LMP7) have been reported for RCC [115]. Conversely, an upregulation of the non-classical HLA-G and E has also been found in RCC [116,117]. HLA-G exerts its direct immunomodulatory function through the interaction with inhibitory immunoglobulin-like receptors such as the

immunoglobuline like transcripts (ILT) 2 and 4, and KIR2DL4. These receptors are differentially expressed on B and T cells as well as in NK cells, dendritic cells, monocytes and macrophages [115,116]. These interactions result in a broad spectrum of immunosuppressive functions: the inhibition of $CD8^+$ T cells toxicity, activity of NK cells and the allogenic proliferative response of $CD4^+$ T cells, in addition to an impairment in chemotaxis [115]. HLA-E is the major ligand of the CD94/NKG2 family of receptors, expressed mainly on NK cells and on a subset of $CD8^+$ T cells [117]. The binding of HLA-E to its receptors reduces the immune effector cellular mediated cytotoxicity [117]. Increased expression of HLA-G and HLA-E has been reported to be associated with a worse prognosis and reduced immunogenicity, negatively impacting on T cell function[116,117].

The inability of tumor-infiltrating lymphocytes to mediate anti-tumor responses can additionally be related to the phenotype. A large-scale mass-cytometry analysis of RCC reported the infiltrating T cells to predominantly have an exhausted phenotype, characterized by expression of programmed death 1 (PD-1), T cell immunoglobulin and mucin domain-containing protein 3 (TIM3) and inducible T cell costimulator (ICOs) [118]. T cell exhaustion could explain how RCC progresses despite a rich T cell infiltrate, and thus the non-favorable prognosis associated with the infiltrate. Although there are several mechanisms that concur to induce T cell exhaustion or to prevent the induction of an anti-tumoral immune response, the one that has been mostly investigated is the expression of key surfaces molecules that prevent full T cell activation. Among these proteins, known as immune checkpoints, the most relevant are the cytotoxic T-lymphocyte associated antigen 4 (CTLA-4) and programmed death 1 (PD-1)/programmed death ligand 1 (PD-L1).

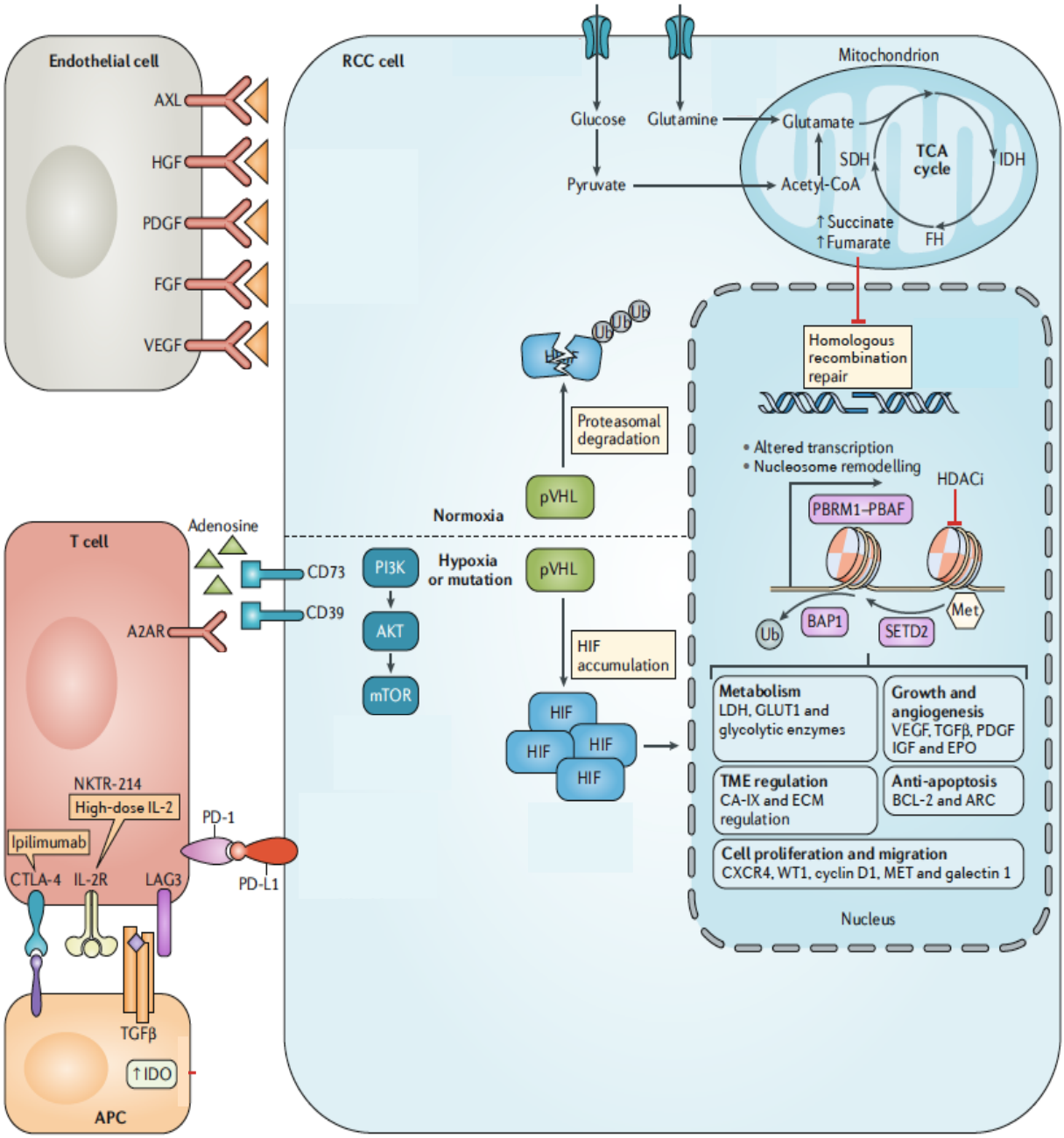

Figure 7. Tumorigenesis related signaling in RCC TME[119]

IMMUNE CHECKPOINTS:

T cell exhaustion or dysfunction is considered a key mechanism impairing a proper T cell response.

The full activation of T cells requires two signals: the recognition of the antigen peptide presented by MHC to the T cell receptor (TCR) (signal 1) and the binding of the costimulatory molecule CD28 expressed on T cells with B7-1 (CD80) or B7-2 (CD86) ligands expressed on antigen presenting cells (APCs) (signal 2). Inhibitory checkpoint molecules modulate the process in order to prevent the risk of immunopathology or autoimmunity [6,120].

Several mechanisms contribute to exhaustion, nonetheless the most studied is surely the overexpression of the immune checkpoints as the above mentioned CTLA-4, PD-1, the lymphocyte activation gene 3 (LAG3), T-cell immunoglobulin and ITIM domain (TIGIT) and T-cell immunoglobulin 3 (TIM3) [120].

CTLA-4 was one of the first immune suppressive molecules reported to have an inhibitory effect on T cell responses [120]. Constitutively expressed on Treg cells, APCs, and to a lower extent on activated T cells, it is structurally similar to CD28. CTLA-4 has high affinity for the B7 antigens CD80 and CD86, thereby competing with CD28 for B7 binding. CTLA-4 engagement with CD80 or CD86 results in the activation of a downstream inhibitory signaling that reduces T cell proliferation and full T cell activation [120,121]. It has been shown *in vivo* that a high expression of CTLA-4 is crucial for the suppressive function of Tregs and that blockage of CTLA-4 demonstrated a promotion of antitumor immunity through the enhancement of the effector T cells functions [122]. PD-1 is an inhibitory receptor expressed on several immune cellular types, mainly on activated T cells, B cells, NK and myeloid cells, nonetheless its role is better characterized on T cells. Its main function is to limit their activity in primary lymphoid organs during the inflammatory response to infections and to limit autoimmunity, which translates into an immune resistance mechanism in the TME [123]. Similarly to CTLA-4, PD-1 is absent on resting T cells, however while CTLA-4 regulates primarily T cell activation in lymphoid organs, PD-1 inhibits T cell function mostly in tissue and tumors and it is more broadly expressed [123,124].

Two ligands of PD-1 have been identified: PD-L1 (also known as B7-H1 or CD274) and PD-L2 (also known as B/-DC or CD273), upregulated on tumor cells, APCs and infiltrating T lymphocytes [6,124]. PD-L1 expression in tumor cells can be exptressed constitutively or induced by several different mechanisms. In some cancers as NSCLC and Hodgkin lymphoma genomic

rearrangements of the *CD274* region, located on chromosome 9p24.1, result in the induction PD-L1 expression[125,126].

Also, epigenetic regulations play a role in PD-L1 induction mainly through methylation and histone acetylation. The tri-methylation of histone H3 on lysine 4 (H3K4me3) has been reported to induce PD-L1 expression, as the recruitment of bromodomains and extra terminal proteins induced by the histone acetylation[125,126]. Due to its role as negative feedback immune response regulator, PD-L1 is upregulated by several inflammatory signaling pathways. Among them, the IFN-g pathway is the prominent up regulator of PD-L1 expression. IFN-g is a pro inflammatory cytokine secreted by activated T cells and NK cells which enhances the major histocompatibility complex expression to increase neoantigen presentation on tumor cells[125]. IFN-g bind to the type II interferon receptor and activates the JAK/STAT signaling, mainly involving STAT1, thus inducing the expression of several transcription factors[126]. It is worth noting that *JAK2* is located on chromosome 9 as *CD274*, therefore mutations happening in this site cause upregulation of PD-L1 either directly either via the stimulation of the JAK/STAT pathway[127]. Besides IFN-g, upregulation of PD-L1 mRNA can be induced upon stimulation of TNF-a, TLRa, IFN-a/b, TGF-b, IL-4, IL-6[125,128].

In addition to the inflammatory stimuli, hyperstimulation of several oncogenic pathways, as MYC, ALK, HIF1α, NF-κB pathway, MAPK pathway, PTEN/PI3K pathway, and EGFR pathway., has been reported to be involved in the induction of PD-L1 expression[125,126]. MYC is a transcription factor important for the regulation of cell growth and proliferation which is overexpressed in about 70% of tumors[125,129]. MYC knock down or pharmacological inactivation has been reported to reduce PD-L1 mRNA an protein levels, although some studies evidenced a direct binding of MYC to the promoter of PD-L1[130]. Another driver of PD-L1 induction is the anaplastic lymphoma kinase (ALK). PD-L1 expression has been proportionally correlated with the expression of *NMP-ALK* fusion gene and to echinoderm microtubule-associated protein-like 4 (*EML4*)-*ALK* fusion[131,132]. Additionally, silencing or inhibiting of HIF-1a resulted in a reduction of PD-L1 expression, suggesting a possible role of hypoxia in its modulation. Several other pathways have been related to an induction of PD-L1 expression as NF-kB, MAPK, PTEN/PI3K-Akt, Met and the pathways induced by the DNA double strand break[125,126].

Binding of PD-1 to PD-L1 results in the phosphorylation of the tyrosine residues of the cytoplasmic domain of the receptor, thus leading to binding of protein tyrosine phosphatases, such as SHP2. PTPs dephosphorylate and antagonize the positive signals deriving from TCR and CD28, impairing signaling pathways as PI3K/AKT/RAS, ERK and phospholipase Cγ. Overall PD-1 engagement results in decreased T cell activation, proliferation, survival and cytokine production, while T cell apoptosis is enhanced [133,134].

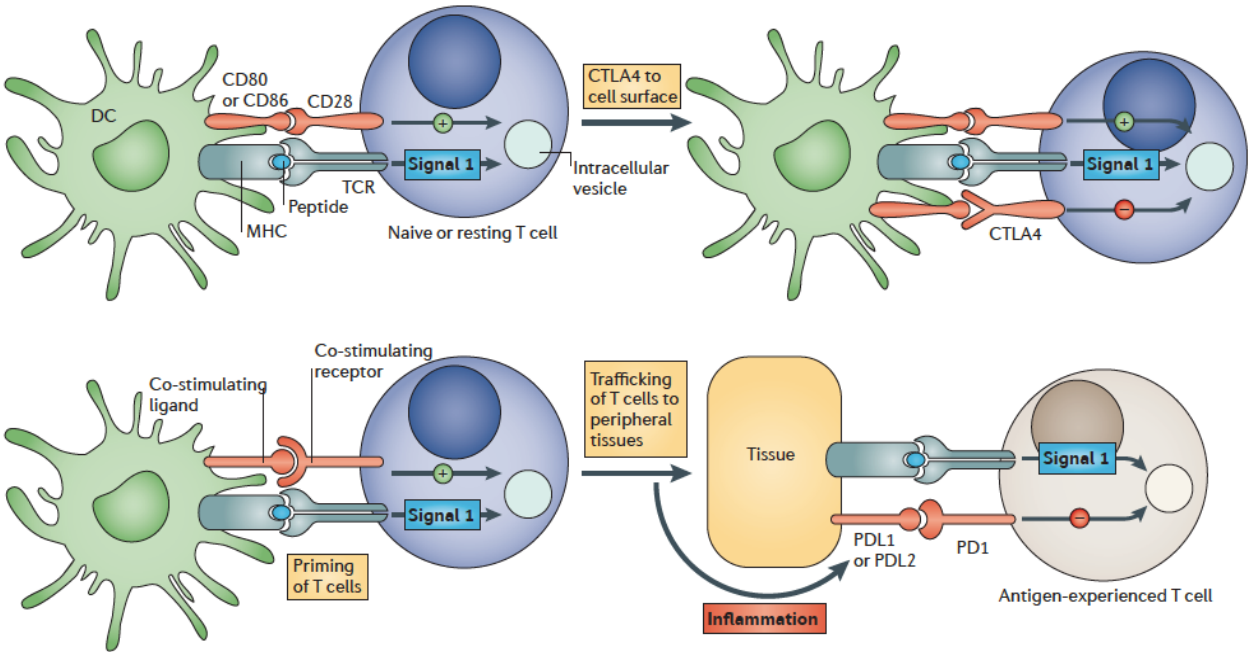

Figure 8. Immune checkpoints regulation of the evolution of the immune response. A) CTLA-4 immune checkpoint is induced in T cells at the initial response. TCR is triggered by the antigen and CTLA-4 is then transported to the cell surface. Thus, CTLA-4 maintains a consistent level of T cell activation. B) PD-1 immune checkpoint checkpoint. Inflammatory signals (as IFN-γ) in the tissues induce the expression of PD-1 ligands. Excessive induction of PD-1 on T cells can induce an exhausted or anergic state in T cells[123].

In RCC patients, PD-L1 positivity associated with dense TILs, has been correlated with unfavorable tumor phenotype and poorer clinical outcome, in contrast with other tumor types as colorectal cancer, non-small cell lung cancer, breast cancer and melanoma [111,114,135–137]. Indeed, PD-L1 expression varies among the different histological subtypes: pRCC and chRCC have reported higher PD-L1 staining than ccRCC in the majority of studies, however data are conflicting [138,139]. Studies agree on the association between PD-L1 expression and a high

number of TILs this resulting a worse patients' prognosis [140–142].

Overall, the association between PD-L1 expression on tumor cells and the high number of TILs in the RCC microenvironment may suggest that this could constitute one of the mechanisms of immune escape, protecting tumor cells from CD8+ cells cytotoxicity [143].

3. GUT MICROBIOTA AND CANCER

Human intestine is inhabited by trillions of micro-organisms organized in complex communities of bacteria, yeast, fungi, protozoa, and viruses collectively referred to as the microbiota [144,145]and whose collection of genomes constitutes the microbiome [144]. Denoting a relevant degree of co-evolution, human gut has adapted to a bi-directional exchange between the host and the flora. While the intestine offers a protected, warm, moisten and nutrient rich environment, microbiota plays an important role in various aspects of human physiology. For instance, gut microbiota assists humans in the digestion of complex carbohydrates, provides short chain fatty acids (SCFAs) and vitamins, and guides the proper development and function of the immune system[144–147]. Collectively, gut microbiota has the metabolic activity of an organ within an organ[148,149]. The immune system tolerates the microbial communities establishing a mutualistic or commensal relationship with the host, while ensuring immunosurveillance against invading pathogens[145,146]. Fundamental conditions for the maintain of a state of homeostasis and symbiotic relationship are the anatomical separation of microbial communities from the host through a multi-level barrier, an eubiotic microbiome and a low host inflammation state[146]. A disequilibrium in these control mechanisms has been associated with microbiota driven inflammation and diseases, including cancer[145,146,150].

Besides the example of some solid tumors, as gastric cancer and gallbladder cancer, whose development is strictly associated to the infection of a defined bacterial pathogen such as *Helicobacter pylori* and *Salmonella enterica* serovar *Thypi* [151,152], the contribution of specific microbes to human tumorigenesis remains elusive. However, there is evidence that a disequilibrium in the intimate relationship between the host and the flora increases susceptibility to infection and is implicated in several autoimmune inflammatory conditions

as irritable bowel syndrome, multiple sclerosis, type I diabetes and rheumatoid arthritis[150,153]. A typical dysbiosis characteristic is the reduced microbial diversity and/or the substantial shift in resident species. Dysbiosis can be caused by several factors including pathogenic organisms, aging, use of antibiotics, diet, exercising habits and smoking [146,154,155]. In addition, chronic inflammatory states, such as Chron's disease, or genetic defects in the intestinal immune system can promote dysbiosis and increase the host's risk to develop neoplasia[150,156]. Collectively, several factors that induce dysbiosis are also implied in cancer development. A wealth of studies related the dysbiosis to the development of intestinal and extraintestinal cancers[157–161], underscoring how microbiota alterations sustain tumor genesis and progression both locally and systemically.

In addition to its role in carcinogenesis, the physiology of the intestinal barrier and its microbiota controls the clinical benefit of anticancer therapies. Several clinical and preclinical studies point out the biological role of gut microbiota in modulating the response to cancer therapy, thus influencing the final clinical outcome of cancer patients[162–168]. Tumor development and progression are strictly interconnected with the immune system, consequently, notable systemic effects of the microbiota on tumor would be mediated through an immune system modulation[144,169]. Initial studies in mice models established a role of gut microbiota in supporting the efficacy of cyclophosphamide chemotherapy through the translocation of specific Gram-positive immunogenic bacteria (*Enterococcus hirae*) that contributes to the elicitation of T helper 17 (T_H17) cell responses against cancer [170]. Consistent with these data, a healthy gut microbiota has been proven to sustain the response to local CgP-oligonucleotide therapies through a modulation of myeloid-derived cells in the tumor microenvironment [171]. This notion was extended to immunotherapy: compelling preclinical studies unveiled the association between gut microbiota composition and response to the checkpoint blockade immunotherapy in patients. An immunostimulatory role was demonstrated for specific bacteria such *Bacteoroides fragilis* and *Bifidobacterium* that were related to an increase in the efficacy of anti-CTLA4 and anti-PD-1 therapies, respectively[163,172]. These mouse studies motivated analogous pursuits, and similar observations were reported across numerous clinical cohorts. They broadly demonstrate the existence of differential gut microbiota "signatures" in patients with a favorable outcome and that these signatures are associated with a stronger systemic immunity and intra tumoral immune infiltrates.

An important factor for microbiota modulation is represented by antibiotic treatment. Indeed, antibiotics alter the balance between the microbial diversity, epithelial cell functions and the local immune system, thus inducing a severe disruption of the homeostasis of the intestinal barrier [173]. Accordingly, the deleterious use of repeated antibiotic medication has been related to an increased frequency of several cancer types, as lung cancer, prostate, bladder cancer and breast cancer[174]. Antibiotic treatment has also been proven to impair the efficacy of anti-cancer treatments, more specifically immune checkpoint inhibitors treatment[166,175,176].

GUT MICROBIOTA AND RCC

RCC has long been considered an immuno-responsive tumor, characterized by an immune infiltrate that has been associated to a prognostic role[112,177]. Investigations of gut bacteria in RCC proved the presence of a causal-effect relationship between the fecal composition and the therapy response outcome, providing evidence that the gut microbiota plays a central role in modulating the response to therapy in RCC[164,167]. Specific gut signatures, characterized by the enrichment in beneficial commensals as *Akkermansia muciniphila* and *Enterococcus hirae* are typical in patients that would later benefit of a better immunotherapy outcome, due to the elicitation of an immune adaptative response against tumor. In addition, it has been proved that TKIs treatment (cabozantinib and axitinib more than sunitinib) induced a microbiota shift favoring a higher abundance of immunostimulatory commensals that could improve the efficacy of a subsequent ICIs therapy including *Akkermansia muciniphila*[167]. Conversely, antibiotic administration before or right after the beginning of immunotherapy is associated with a worse patients' outcome due to the treatment induced decrease in microbiota diversity[166].

Altogether these evidences point the microbiota as a possible approach to stratify patients that can successfully respond to immunotherapy and it could be used as a potential therapeutic target.

4. THERAPEUTIC APPROACH

FIRST LINE TREATMENT SETTING

Localized disease

For localized disease, surgical resection is the standard of care treatment[71]. Partial nephrectomy is recommended over radical nephrectomy, and can be operated via open, laparoscopic or robot-assisted laparoscopic approaches. Adjuvant and neoadjuvant treatment are not recommended outside clinical trials[51,71,178].

Metastatic disease

The management of metastatic disease has undergone through major improvement in the last 30 years. The very first approach that was used for mRCC treatment consisted of the combination of cytokines as interleukin 2 and interferons, mainly IFN-α[179]. The discovery that loss of function of *VHL* led to oncogenesis of ccRCC represented a major breakthrough, opening the way to new therapeutic approaches. In few years (from 2005 to 2008) the standard of care treatment for mRCC switched to antiangiogenic drugs in the first- and second-line setting.

Another important pathway altered in mRCC is the mTOR pathway and several inhibitors have been approved for mRCC systemic treatment as temsirolimus and everolimus.

Lastly, the advent of immune based approaches definitely marked a new treatment era for mRCC patients.

It is of particular relevance for the management of RCC, to understand the need of a personalized approach, which in turn needs an understanding of the variables influencing the prognosis. To this aim, prognostic models are used to direct the therapeutic strategies for kidney cancer patients. MSKCC represented the standard of choice before the advent of targeted therapies, that induced clinicians to develop the IMDC prognostic model. Today this model is the gold standard model that guides the best therapeutic approach.

Currently there are different approaches approved as a first line setting for metastatic ccRCC, depending on the risk assessment.

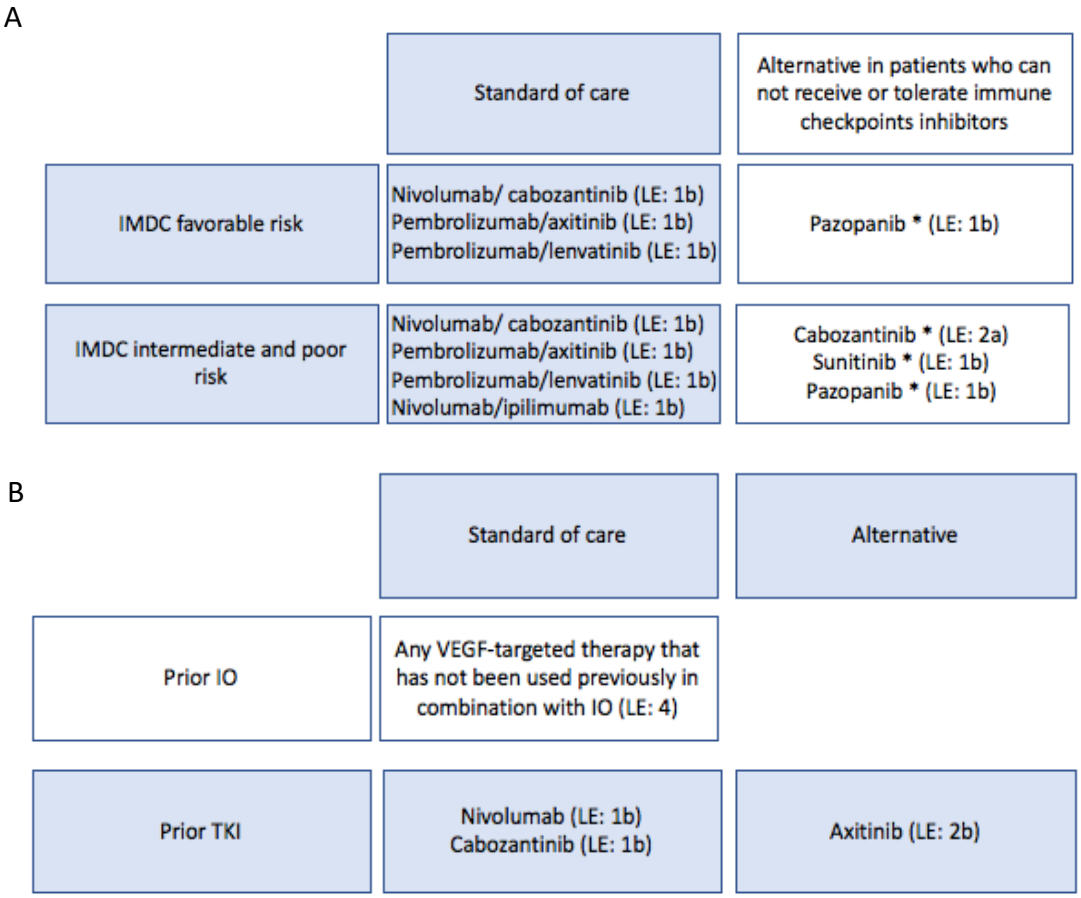

Figure 9. Recommendations from the updated European Association of Urology guideline for the A) first-line treatment, B) second line treatment of metastatic clear-cell RCC[51].

Sunitinib: is an oral small molecule receptor tyrosine kinase inhibitor with direct antiangiogenic and antitumor activity[180]. Sunitinib targets mainly VEGFR in his three isoforms (VEGFR-1, -2, and -3), but has also activity on cKIT, fms-related tyrosine kinase 3 (FLT3), ret proto-oncogene, rearranged during transfection (RET), the platelet derived growth factor receptors (PDGFR-α, -β) and colony stimulating factor 1 receptor (CSF1R)[181]. *In vivo* studies using mouse xenografts derived from rat or human cell lines demonstrated that sunitinib exhibited inhibitory effect against VEGFR-2, PDGFR-β at plasma concentrations of 50-100 ng/ml[182]. The inhibition of these RTKs blocked the downstream signal transduction, thus inhibiting both the tumor-related neoangiogenesis and tumor growth.

In human patients, after having shown efficacy in two different phase II trials conducted on cytokines-refractory patients[183,184] sunitinib was approved for RCC treatment in 2006 both by the Food and Drug Administration (FDA) and the European Medicines Agency (EMA) for the treatment of metastatic RCC. The efficacy of sunitinib treatment was then proved in a phase III trial comparing sunitinib treatment and the standard IFN-α as first line treatment in 750 previously untreated metastatic RCC patients. The primary endpoint of median progression-free survival (PFS) was significantly longer in the sunitinib arm (11 months) compared with the IFN-α arm (5 months), corresponding to a hazard ratio (HR) of 0.42 [95% confidence interval (CI) 0.32–0.54; $p < 0.001$]. Sunitinib also resulted in significantly higher overall response rates (ORRs) than IFN-α (31% versus 6%; $p < 0.001$)[185].

Pazopanib: similarly to sunitinib, pazopanib is an oral small molecule inhibitor of tyrosine kinases which main target is represented by the VEGFRs family (VEGFR-1, -2 and -3), PDGFR-α and -β, cKIT and FGFR-1 and -3[186]. After having proved in two different phase II studies the efficacy of pazopanib in mRCC patients regardless of pretreatment[187,188], its efficacy was then confirmed in the phase III clinical trial VEG105192. A total of 435 RCC patients either treatment naive or pre-treated with cytokines were randomized at a 2:1 ratio into the pazopanib or placebo arms. PFS was considerably higher in the pazopanib arm (9.2 months, 95% CI: 7.4-12.9) vs placebo arm (4.2 months, 95% CI: 2.8-4.2), with HR 0.46 (95% CI: 0.34–0.62)[189].
Pazopanib and sunitinib efficacy as first line therapy for mRCC were compared in the COMPARZ study, a phase III clinical trial. The study demonstrated the non-inferiority of pazopanib to sunitinib based on the PFS (8.4 months versus 9.5 months, respectively). The median OS was 28.3 months in the pazopanib group (95% CI: 26.0–35.5) and 29.1 months in the sunitinib group (95% CI: 25.4–33.1), thus similar between the groups (HR: 0.92; 95% CI: 0.79–1.06)[190,191]. The PISCES study was a unique trial in which 169 patients were randomized to receive either pazopanib or sunitinib for 10 weeks, and after a 2-weeks washout, they switched for the other medication, being at the end asked which medical treatment they preferred. Results indicated that patients tended to prefer pazopanib (70%) over sunitinib (20%) due to higher tolerability[192].

Cabozantinib: is a small molecule tyrosine kinases inhibitor which main targets are VEGFR-1, -2 and -3, MET and AXL[193]. The peculiarity of this molecule consists of the inhibition of MET and AXL, frequently involved in the development of resistance to anti-angiogenic therapies[194]. Cabozantinib has been confronted with sunitinib as initial therapy for mRCC of poor or intermediate risk in the phase II CABOSUN trial, showing an improvement in PFS for patients treated with cabozantinib (8.6 months, 95% CI: 6.8-14.0) versus sunitinib (5.3 months; 95% CI: 3.0-8.2). With a median follow-up of 34.5 months, median OS was 26.6 months (95% CI 14.6-not estimable) with cabozantinib and 21.2 months (95% CI 16.3-27.4) with sunitinib (HR 0.80 [95% CI 0.53-1.21])[195].

Temsirolimus and Everolimus: these two molecules are two derivatives of the rapamycin (sirolimus) a macrolide compound produced by the *Streptomyces hygroscopicus*[196]. They bind selectively to mTORC1 complex, inhibiting its activity and thereby impairing the response of VEGF activation and inhibiting hypoxia-induced activation of HIF-1α[196].

The 2007 Global Advanced Renal Cell Carcinoma (ARCC) phase III trial was the first proving temsirolimus as a valid therapeutic strategy for RCC patients. In this trial, 626 patients with previously untreated poor-risk mRCC were administrated with temsirolimus, IFN-α or combination therapy. Results proved the superiority of temsirolius treatment over IFN-α or combination treatment by a prolongation of OS (10.9 months vs 7.3 and 8.4 respectively) and in PFS (Hudes G. et al., 2007). A subgroup analysis showed that temsirolimus had greater efficacy in patients with non-ccRCC, although the difference was not statistically significative[197]. To date, temsirolimus is one of the agents approved also for the treatment of non-ccRCC[194].

The RECORD-1 sudy, conducted on 416 patients with mRCC randomized 2:1 to everolimus or placebo, demonstrated everolimus efficacy over placebo as a second line treatment after progression on TKIs first setting[198]. On this basis everolimus received FDA approval as second line therapy for advanced RCC patients refractory to anti-angiogenic treatments.

Immunotherapy

The introduction of immunotherapy, and in particular of immune checkpoints inhibitors (ICIs), revolutionized the treatment paradigm for mRCC management. The first agent that has been introduced to the clinic was **Nivolumab**. Nivolumab is a human monoclonal antibody directed against PD-1, thereby inhibiting the binding of PD-1 to PD-L1 and restoring T cell activity. It was firstly approved by FDA for mRCC patients previously treated with anti-angiogenic therapy in 2015[199]. Later in 2018, the association of **Nivolumab and Ipilimumab** was approved as first line setting for patients with intermediate-poor risk advanced RCC. It is the only ICI-ICI combination approved as front-line setting for RCC and it consists of the combination of an anti PD-1 monoclonal antibody (Nivolumab) plus an anti-CTLA-4 monoclonal antibody (Ipilimumab). The combination was approved on the basis of the CheckMate 214 study, a phase III trial involving 1096 patients with previously untreated advanced RCC with clear cell component. Patients were randomized to receive either nivolumab (3 mg/Kg) plus ipilimumab (1 mg/Kg) i.v. every 3 weeks for four doses, followed by nivolumab (3 mg/Kg every 2 weeks), or sunitinib (50 mg orally once daily for 4 weeks, per 6-week cycle). Nivolumab plus Ipilimumab combination led to an improved PFS compared with the sunitinib arm (11.4 vs 8.3 months respectively), and at 2 years the overall survival rate was 75% (95% CI: 70 to 78) for nivolumab plus ipilimumab and 60% (95% CI: 55 to 65) for sunitinib arm; on the other hand, the median overall survival was not reached with nivolumab plus ipilimumab versus 26.0 months with sunitinib (HR for death, 0.63; $p<0.001$). Accordingly, the ORR was 42% versus 27% ($p<0.001$)[200]. Then, in April 2018 the FDA approved the association as firs line setting for intermediate and poor-risk advanced RCC patients. Aside of monotherapies, the association TKIs with ICIs such as Pembrolizumab plus Axitinib, Nivolumab plus Cabozantinib and Pembrolizumab plus Lenvatinib has demonstrated statistical and clinical advantage for patients.

The combination of **Pembrolizumab and Axitinib** has been approved as one of the possible first line settings for advanced RCC. Pembrolizumab is a monoclonal antibody directed against PD-1, thereby inhibiting the binding of PD-1 to PD-L1 and restoring T cell activity. Axitinib is a

second generation multikinase inhibitor, highly selective for VEGFR-1, -2 and -3[201]. The combination was approved on the basis of the KEYNOTE-426 trial, an open-label phase III trial comparing the effects of the pembrolizumab plus axitinib combination (Pembrolizumab 200 mg i.v. every 3 weeks plus Axitinib 5 mg p.o. twice daily), versus sunitinib monotherapy (50 mg p.o. daily, 4 weeks on and 2 off) in previously untreated 861 mRCC patients. The study reported an OS prolongation for patients treated with the combination compared with sunitnib, with an estimated percentage of patients alive after 12 months of 89.9% vs 78.3%, respectively (HR for death, 0.53; 95% CI: 0.38-0.74; p<0.0001)[202]. Improvements were reported also in PFS (15.1 months vs 11.1 months) and ORR (59.3% vs 35.7%). Interestingly, improvements in PFS and OS were reported independently of IMDC risk grade and PD-L1 expression[202].

Another setting is represented by the association of **Nivolumab and Cabozantinib.** Nivolumab, as the above mentioned Pembrolizumab, is a monoclonal antibody targeting PD-1, while Cabozantinib is an anti-angiogenic TKI. Data from the CheckMate 9ER study, an open-label, randomised, phase III study comparing the association of nivolumab and cabozantinib (nivolumab 240 mg i.v. every two weeks plus cabozantinb 40 mg orally daily) versus sunitinib (50 mg orally, daily for 4 weeks per 6 weeks cycle), reported a PFS of 16.6 months for the combination vs 8.3 months for sunitnib monotherapy[203]. At interim analysis, there was also a significant overall survival advantage for Cabozantinib and Nivolumab (18.1 months median follow-up) (HR 0.60; 95% CI 0.40-0.89; p < 0.001)[204]. On this basis, the association has been approved as front-line setting for mRCC.

The association between **Lenvatinib and Pembrolizumab** was tested in the CLEAR study, a phase III clinical study where previously untreated advanced RCC patients were randomized to receive lenvatinib (20 mg orally once daily) plus pembrolizumab (200 mg intravenously once every 3 weeks), lenvatinib (18 mg orally once daily) plus everolimus (5 mg orally once daily), or sunitinib (50 mg orally once daily, alternating 4 weeks receiving treatment and 2 weeks without treatment). Both PFS was longer in patients treated with association of pembrolizumab and levantinib, compared to the sunitinib and lenvatinib plus everolimus arms (23.9 months vs 9.2 and 14.7 months, respectively). OS was reported to improve in the

lenvatinib plus pembrolizumab arm compared with the sunitinib arm, but not with the lenvatinib plus everolimus arm (HR for death, 0.66; 95% CI, 0.49 to 0.88; p=0.005; HR, 1.15; 95% CI, 0.88 to 1.50; p=0.30, respectively)[205].

Overall, currently in Italy there are 7 options approved as first-line setting: sunitinib, pazopanib, cabozantinib (for intermediate-poor-risk patients), pembrolizumab + axitinib, nivolumab + ipilimumab (for intermediate-poor-risk patients), bevacizumab + IFN-α and temsirolimus (for intermediate-poor-risk patients).

SECOND LINE TREATMENT SETTING

The choice of treatment to prefer after the failure of the primary therapy should take into consideration additional elements, as the response and the tolerability of previous therapy. Furthermore, second-line treatment has been dramatically modified by the report of two large trials showing improvement in OS with Nivolumab and Cabozantinib over Everolimus (Checkmate 025 and METEOR respectively)[206,207]. Both trials tested the therapies in patients who had progressed after TKI pre-treatment, either one or two TKIs.

The CheckMate 025 was an open-label phase III study comparing nivolumab with everolimus in patients with advanced RCC who had received previous anti-angiogenic treatment. The ORR was higher with Nivolumab than with Everolimus (25% vs. 5%; odds ratio 5.98; 95% CI: 3.68 to 9.72; p<0.001). Median PFS was 4.6 months (95% CI, 3.7 to 5.4) with Nivolumab and 4.4 months (95% CI, 3.7 to 5.5) with Everolimus (HR, 0.88; 95% CI, 0.75 to 1.03; p=0.11)[206]. The median OS was 5.4 months longer with nivolumab than with everolimus (25.0 months vs. 19.6 months)[206]. The reported benefit of nivolumab therapy compared with everolimus was observe irrespective of the MSKCC prognostic score, number of previous therapies, the region or PD-L1 expression[206].

The METEOR trial was an open-label phase III study comparing cabozantinib to everolimus in patients who had progressed after VEGF-targeted therapy. This study demonstrated the efficacy of cabozantinib, reporting superior OS, PFS and ORR compared to everolimus therapy and leading to his approval by the FDA[207].

Overall, today the therapeutic possibilities are different according to the first line previously received by the patient. After single-agent TKI are recommended Nivolumab or Cabozantinib, and the combination of Lenvatinib and Everolimus represents another option for following treatment lines. On the other hand, after ICI-TKI, only Cabozantinib or Sunitinib represent second-line treatment options. Moreover, after first-line Nivolumab plus Ipilimumab, the therapeutic alternatives are represented by TKI monotherapy or Lenvatinib plus Everolimus combination.

AIM OF THE PROJECT

In the last years, the introduction of immunotherapy revolutionized the clinical approach to many tumours. Metastatic RCC in particular has long been considered an immunogenic malignancy, susceptible to the effect of immunotherapy. However, in spite of the little success observed with the use of cytokines as interleukin 2 (IL-2) and interferon, the approval of immune checkpoint inhibitors (ICIs), represented a real breakthrough and the second paradigm shift in the management of ccRCC after the TKIs era. In addition, the demonstration that TKIs whose main targets is VEGFR, as axitinib, play a role in the immune modulation provided the rationale for the association of TKIs and ICIs and between 2019 and 2021 several of these associations were approved for first line treatment of RCC patients.

In this continuously evolving scenario, we focused our attention on the combination of axitinib plus avelumab or pembrolizumab. Indeed, despite the encouraging results obtained with the first line axitinib-based immuno-therapeutic approach, the individuation of the best therapeutic sequence after a first line remains open and novel biomarkers that could help clarify this therapeutic landscape are needed. To this end, the AXIT study aims to evaluate *in vitro* and *in vivo*, in a syngeneic murine RCC model, the effect of this combination in terms of modulation of the immune response and anti-cancer efficacy to search for preclinical hints that could lead the future clinical choices.

In addition, the impact of the modulation of the gut microbiota in determining the response to cancer treatment has been broadly heralded in the last decade. With regards to RCC, it has been demonstrated that among gut bacteria population, the relative abundance of a beneficial commensal, *Akkermansia muciniphila*, is associated with the elicitation of immune responses beneficial against cancer. On this basis, we also evaluated the impact of gut microbiota on first line standard therapies, exploring the role of *Akkermansia muciniphila* to ICIs therapies in avatar mouse model.

MATERIALS AND METHODS

1. MATERIALS AND ANTIBODIES

Chemical reagents were provided by Sigma-Aldrich Co (Saint Louis, Missouri, USA). Medium, saline solutions, trypsin, FBS (Fetal Bovine Serum), antibiotics were provided by GIBCO, Grand, NY, USA. Petri dishes, sterile test tubes, filters and all the rest of the equipment needed for cell cultures were acquired from Costar, Broadway, Cambridge, MA, USA. Primary antibodies were purchased by Cell Signalling Tecnology, Inc. Antibodies that were used are: PD-L1, Actin. Secondary antibodies peroxidase-coniugated were purchased by Pierce Biotecnology Inc., Rockford, USA. The ImmobilonTM Western Chemiluminescent HRP Substrate kit for the signal revelation by ECL was provided by Millipore Corporation, Billerica, MA, USA. Materials and reagents for electrophoresis and blotting were provided by BIO-RAD, Richmond laboratories, California, USA. The C-DiGitTM Blot Scanner was purchased from Li-COR Bioscences, Inc, Lincoln, NE, USA. The ELISA Kit Quantikine Murine INF-g Immunoassay was purchased from R&D Systems, Minneapolis, MN, USA. The LDH release kit was purchased from Promega, Madison, WI, USA. The antibodies PE-anti-Human PD-1 and PD-L1 or PE-Anti-Mouse PD-1, were purchased from BD Bioscences, San Josè, CA, USA, anti-mouse CD4, anti-mouse TIM-3, anti-mouse CD3ε, anti-mouse CD8a were purchased from Miltenyi Biotech, Germany. Anti-mouse CD25, anti-mouse LAG3 were purchased from BioLegend, San Diego, USA. Anti-mouse CD3 and anti-mouse CD28 and anti-human CD3 and anti-human CD28 were purchased from BioLegend, San Diego, CA, USA. RNA extraction reagents were from Quiagen, Hilden, Germania and kit, reagents and primers for RT-PCR were provided by Applied Bioscences, Waltham, MA, USA and Thermo Fisher Scientific, Waltham, MA, USA.

2. METHODS

2.1 CELL CULTURE

Human ccRCC cell lines 769-P and Caki-2 and murine ccRCC cell line RENCA were purchased from American Type Culture Collection ATCC (Manassas, VA, USA). All cell lines were cultured, as recommended: 769-P and Caki-2 were cultured in RMPI-1640 growth medium or DMEM respectively, supplemented with 1% antibiotics (penicillin 100UI/ml, streptomycin 100μg/ml),

glutamine 2mM (GLN) and 10% of fetal bovine serum (FCS). RENCA cells were cultured in RMPI-1640 growth medium supplemented with 10mM Hepes buffer, 0.1 mM non-essential amino acids, 1 mM sodium pyruvate, 1% antibiotics (penicillin 100UI/ml, streptomycin 100µg/ml), glutamine 4mM (GLN) and 10% of fetal bovine serum (FCS). All cells were maintained under standard cell culture conditions at 37° in a water-satured atmosphere of 5% CO_2 in air. Cells grow in Petri dishes of plastic material (available in different size) and were seeded to different density.

2.2 DRUG TREATMENT

Axitinib (AG-013736), and Avelumab were provided by Pfizer (New York City, NY). Murine anti-PD-1 and anti-CTLA-4 monoclonal antibodies were purchased from BioXCell.
For *in vitro* studies, Axitinib was dissolved in DMSO, and DMSO concentration never exceeded 0.1%(v/v); equal amounts of the solvent were added to control cells.

2.3 ANALYSIS OF CELL PROLIFERATION AND SURVIVAL

Cell proliferation was evaluated by counting the cells in a Bürker haemocytometer with trypan blue exclusion method and by Cristal Violet staining or MTT assay or MTS assay.

2.3.1. CELL COUNTING AND TRYPSINIZATION

Before the counting cells were dissociated using trypsin, a proteolytic enzyme that breaks down proteins to dissociate adherent cells from the vessel in which they are being cultured, the whole process being known as trypsinization. Removed the growth medium, 2ml of 0.1% trypsin-0.02% EDTA in PBS were added at 37° which allows the cells to detach from the plate. Cells were then transferred to sterile tubes and spiked with a volume of medium equal to that of trypsin that inhibits its action. The suspension was centrifuged at 500 x g for 4 minutes, then the supernatant was removed, and cells were re-suspended in fresh complete medium. Cell counting was performed by light microscopy using a Bürker haemocytometer. Finally, cells were seeded at the density desired in plates containing fresh complete medium.

2.3.2. MTT or MTS ASSAY

The MTT (3-(4,5-dimethylthiazol-2-yl)-2,5-diphenyltetrazolium bromide) or MTS (3-(4,5-dimethylthiazol-2-yl)-5-(3-carboxymethoxyphenyl)-2-(4-sulfophenyl)-2H-tetrazolium) assay is a colorimetric assay for measuring cell vitality. The assay is based on the reduction of the yellow tetrazole MTT, to its insoluble formazan, giving a purple colour. MTT reduction is dependent on NAD(P)H-dependent oxidoreductase enzymes expressed in the cell. Therefore, reduction of MTT increases with cellular metabolic activity due to elevated NAD(P)H flux. 3-5 x 10^3 cells were seeded into 96-well plates in quadruplicate and were exposed to various treatments. After 72 h, 100 µl of MTT solution (1mg/ml, Sigma- Aldrich) was added to each well and incubated at 37°C. After 1 h, the insoluble purple formazan product is dissolved in DMSO and the absorbance at 570nm was measured using a microplate-reader (BIORAD).

2.3.3. CRISTAL VIOLET ASSAY

Crystal violet (triphenylmethan dye (4-[(4-dimethylaminophenyl)-phenyl-methyl]-N, N-dimethyl-aniline) assay is a colorimetric assay for measuring cell vitality. Crystal violet dye stains nuclei. Upon solubilisation, the amount of dye taken-up by the monolayer and the intensity of the colour produced are proportional to cell number. After the treatments, medium was removed, and the cells washed twice with cold PBS, fixed with ice-cold methanol for 10 minutes and stained with 0.5% crystal violet in PBS. The unbound dye was removed by washing carefully with water. Bound crystal violet was solubilized with 0.2% TritonX-100 in PBS. Light excitation which increased linearly with the cell number was analysed at 570nm using a microplate-reader (BIORAD).

2.4 WESTERN BLOTTING

2.4.1. PREPARATION OF EXTRACTS

For electrophoretic analysis of proteins, the cell monolayer, after treatment, was washed twice with 2 ml of saline solution in phosphate buffer (PBS) maintained at 4°C. The cell were treated with lysis Buffer (150mM NaCl, 5mM $MgCl_2$, 50mM Tris-HCL pH 7.4, 0.1% Sodiumdodecylsulphate (SDS), 1% Triton-X-100, 100 µg/ml 4- Amidinophenylmethanesulfonyl Fluoride (APMSF), 0.5µg/ml Leupeptin, 0.7µg/ml Pepstatin, EDTA 0.5mM, sodium ortovanadate 1mM, NAF 50 mM, sodium pyrophosphate 5mM, sodium b-glycerophosphate

10mM, sodium deoxycholate 0.5%) and the lysate was collected using “cell scraper”. The extracts obtained were frozen at -80°C for at least 30 minutes, sonicated and centrifuged at 12000 x rpm for 10 minutes at 4°C to separate coarse components from the supernatant containing the proteins. The supernatant was transferred in Eppendorf for the determination of protein content.

2.4.2. DETERMINATION OF THE PROTEIN CONTENT

The protein content of the cell lysate’s solution was determined using the BIO-RAD DC Protein Assay kit (Richmond, CA, USA). 125µl of REAGENT A (alkaline solution of copper’s tartrate) was added to 2µl of sample, vortexed and 1 ml of REAGENT B (Folin reactive) was added in each sample. The samples were incubated in the dark for 15 minutes at room temperature. The protein present in solution gave rise to a reaction that determines the development of a violet coloration whose intensity as proportional to the protein concentration of each sample. The absorption of light by the colour solution was quantified via a single-beam spectrophotometer at a wavelength of 750nm (Beckman Coulter). The protein concentration of each sample was calculated from the measured absorbance, using as standard a protein such as bovine serum albumin (BSA) with which it was built straight calibration.

2.4.3. POLYACRYLAMIDE GEL ELECTROPHORESIS IN SDS (SDS-PAGE)

The same quantity of protein from different samples was taken from cell lysates, previously prepared. The samples were taken at the same volume with the addiction of lysis buffer and supplemented with sample buffer (Tris-HCl 62.5 mM pH 6.8, 2% SDS, 2-5% mercaptoethanol, blue bromine phenol 0.002%, glycerol 20%); following the samples were boiled at 100°C for 2-3 minutes and loaded into gel on SDS polyacrylamide slab gels (8x6x0.15cm) using BIORAD equipment. On each lane the same amount of protein was loaded; proteins were separated on a gel (acrylamide/polyacrylamide 30:0.8) according to the procedure described by Laemmli (Laemmli, 1970), with a constant current of 60mA at 4°C for about an hour. The molecular weight of each band was obtained by comparing the relative mobility of the same and that of standard proteins, coloured and of known molecular weight, which were separated simultaneously with the samples.

2.4.4. ELECTROPHORESIS TRANSFER

Following electrophoresis, the separated molecules were transferred or blotted onto a second matrix, PVDF (polyvinylidene difluoride) membrane, which had to be activated in methanol. The gel was placed in direct contact with a piece of PVDF, and they were “sandwiched” between two electrodes. The transfer was performed by Lightning Blot Protein Transfer System (PerkinElmer). When the electric field was applied, the proteins moved out of the polyacrylamide gel onto the surface of the membrane, where the proteins became tightly attached; the resulting membrane was a copy of the protein pattern that was separated in the polyacrylamide gel itself.

2.4.5. PROTEIN DETECTION

The membranes were incubated with blocking solution (5% non-fat-powdered milk or 5% BSA in TTBS buffered saline composed by Tris 20mM, NaCl 137mM, HCl 1mM and Tween 20 0.1%) for 1 hour at 37°C; this treatment was aimed to block the non-specific binding sites by proteins. The membranes were then incubated with primary antibody overnight at 4°C on a shaker platform. After this time, 3 washes of 5 minutes each were performed with a solution of TTBS. The membranes were then incubated 1 hour with HRP-anti-mouse or HRP-anti-rabbit antibodies (secondary antibodies labelled with peroxidase) at 1:20.000 dilutions. The membranes were washed again with TTBS 1X. Immunoreactive bands were visualized using an enhanced chemiluminescence system: the transferred proteins, complexed with the secondary antibody, reacted with a chemiluminescent substrate like luminol in order to produce immunoreactive bands which were visualized on photographic plates. The intensity of the signal correlates with the abundance of the protein on the blotting membranes. The densitometric analysis of the bands, performed using Quantity One (BIO-RAD) software, allowed the quantification of the light signal that was a function of protein abundance.

2.5 REAL-TIME PCR

For the RealTime PCR, RNA extraction was performed using the “Rneasy Mini Kit” (Qiagen) based on the productor indications and was the quantified by TECAN Infinite M Nano. Quantification consists of reading the optical density at 260 nm, which is in turn converted to RNA concentration. RNA purity rate is determined by comparing the absorbance value read at 260 nm (typical of nucleic acids) and 280 nm (typical of proteins): the optimal value ranges

from 1.8 to 2.0. Retro-transcription was performed using the “High-Capacity cDNA Reverse Transcription Kit” from ThermoFisher, with the “GeneAMP PCR System 2700” (Applied Biosystem) fro 500 ng of RNA in 20 ml. Finally, Real-Time PCR was performed using the SybrGreen reagent using GAPDH and b-actin as control.

2.6 ISOLATION OF PERIPHERAL BLOOD MONONUCLEAR CELLS (PBMCs)

Peripheral blood mononuclear cells were isolated from mice fresh blood. Blood was diluted 1:1 with PBS before addition of Ficoll reagent in a 4:3 proportion with the diluted blood that was added on top of the reagent. After centrifugation, the PBMCs ring (*refer to figure below*) was removed and washed twice with PBS. Cells were then counted with Trypan Blue and activated with anti-CD3 0.2 mg/ml and anti-CD8 2 mg/ml for 24 hours before any other manipulation.

2.7 FLOW CYTOMETRY

Determination of PD-L1 expression on cell surface was assessed by PE-anti-PD-L1 antibodies and flow cytometry analysis. Briefly, PBMCs were activated with with anti-CD3 0.2 mg/ml and anti-CD8 2 mg/ml for 24 hours and treated with Axitinib with or without the anti-PD-1 antibody at 200 μg/ml concentration. Then, cells were harvested, washed with a PBS/EDTA solution and incubated for 1h with the PE-antibody. Quantification of the expression was performed with the Beckman FC500 flow cytometer and data were elaborated with FCS Express software (Software De Novo, CA, USA). Mean fluorescence intensity values have been converted in molecules of equivalent fluorochromes (MEF) using the FluoroSpheres 6-Peak kit (Dako, CA, USA).

2.8 QUANTIFICATION OF SOLUBLE PD-L1

To assay soluble PD-L1 (sPD-L1), cells were seeded in a cell-well culture plate. After 24 h, Axitinib with or without the anti-PD-1 antibody at 200 μg/ml concentration were added for 3 days; at the end, the media were collected and tested for soluble PD-L1 expression by ELISA assay (R&D System, Minneapolis, MN, USA).

2.9 QUANTIFICATION OF IFN-γ PRODUCTION

Quantitative determination of IFN-g in PBMCs cultures supernatants was performed using the ELISA Quantikine Mouse IFN-g Immunoassay. The 96-well plate is provided pre-covered with the polyclonal antibody with specific affinity for IFN-g. After the addition of 100 ml of sample or standard to the wells and a 2h incubation at room temperature, the plate is washed and 200 ml of polyclonal antibody specific for IFN-g and coniugated with enzymes is added. After another 2h incubation and washes the substrate is added: this induces the colorimetric reaction. Absorbance is read at 450 nm and 570 nm.

2.10 CO-COLTURES OF RENCA CELLS AND MURINE PBMCS

To set up a co-culture system, RENCA cells were seeded at $1.5x10^3$ in 24-well plates and then treated with Axitinib 0.5 μM for 72 hours. Murine PBMCs were isolated and activated as described above for 24 hours to guarantee the fullest activation possible. At the end of the treatment with the TKI, activated PBMCs were seeded at a 10:1 ratio of density in relation to the RENCA cells in specific trans wells, which were subsequently inserted in the wells containing the cells (see the figure below), with or without the anti-PD-1 antibody (200 μg/ml). 48 hours after the seeding, culture medium was collected, and IFN-γ production was evaluated. Cellular vitality was assessed on RENCA cells with the crystal violet technique.

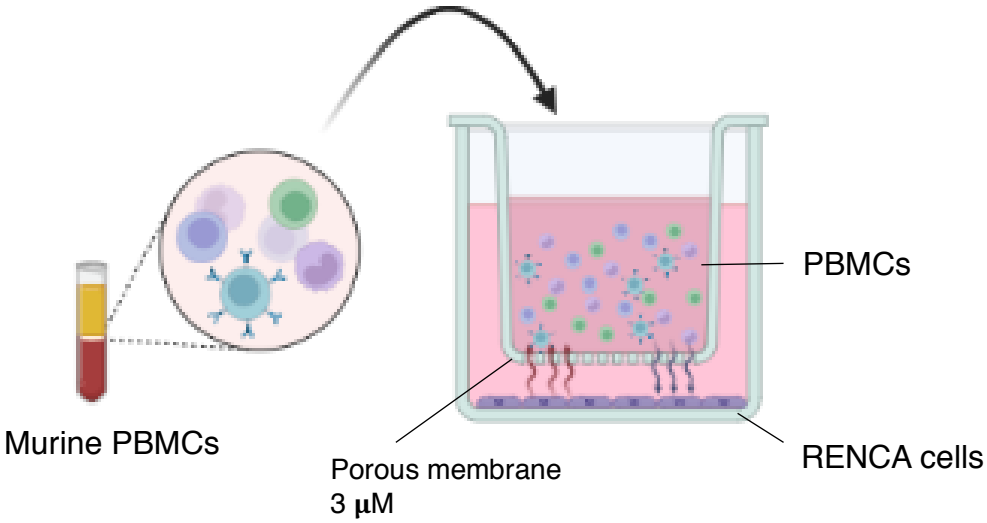

2.11 IN VIVO EXPERIMENTS

Mice. Female Balb/c mice were purchased from Janvier Labs and used between 8 and 16 weeks of age. All mice experiments have been performed at Gustave Roussy Cancer Campus, and mice were housed in SPF conditions.

Fecal Microbiota Transfer. FMT using patients' stool was performed following 3 days of ATBs. Briefly, stools stored at -80°C were unfrozen, diluted if necessary and given to the mice through oral gavage. Engraftment was verified by culturing the fecal pellets resuspended in PBS 1x at 0.1 g/mL on COS plates (5% Sheep Blood Columbia Agar; bioMérieux) plates for 48 hours at 37°C in aerobic and anaerobic conditions.

RENCA-Luc+ orthotopic cancer model. The day of tumor challenge, mice were anesthetized with isoflurane; then, $1x10^4$ RENCA tumor cells resuspended into 30 µL of PBS were injected into the right kidney. The skin incision was then closed with surgical clips. Tumor incidence (at day 7) and development were monitored by in vivo photonic imaging of tumor cell luciferase activity. Briefly, mice received an i.p. injection of the substrate of luciferase (E1605, Promega) at a dose of 150 mg/kg, and in vivo bioluminescence imaging was acquired with an IVIS Spectrum Imaging Series (PerkinElmer). Tumor-bearing mice were randomized to designed groups for treatments at day 7 after tumor challenge (as mentioned previously). Tumor growth was monitored at day 7 and day 15 after treatment start.

Antibiotic treatments. Mice were treated with an antibiotic solution (ATB) containing ampicillin (1 mg/ml), streptomycin (5 mg/ml), and colistin (1 mg/ml), via the drinking water (all purchased from MilliporeSigma). Solutions and bottles were replaced 3 times and once weekly, respectively. Antibiotic activity was confirmed by cultivating fecal pellets resuspended in PBS 1x at 0.1 g/mL on COS plates (5% Sheep Blood Columbia Agar; bioMérieux) plates for 48 hours at 37°C in aerobic and anaerobic conditions.

Feces and plasma collection. Feces were harvested in each mouse and group for metagenomics and metabolomics. Samples were stored at –80°C until processing.

2.12 STATISTICAL ANALYSIS

Statistical analyses were performed using GraphPad Prism 8.0 (GraphPad Software Inc., San Diego, CA, USA). Results are expressed as mean values ± standard deviation for the indicated number of independent measurements. Differences between the registered values and the different experimental conditions have been evaluated by Student T-test or two-way ANOVA

followed by Bonferroni's post-test depending on the assay; p values are underscored in figures texts. $p<0.05$ was considered significative.

RESULTS

1.1. EFFECT OF AXITINIB ALONE OR COMBINED WITH ANTI-PD-L1 IMMUNE CHECK POINT INHIBITOR ON A PANEL OF RCC CELL LINES

In the first part of the research, we evaluated the anti-proliferative effect of axitinib, a second generation multi kinase inhibitor which predominantly targets VEGFR-1, -2, -3 on a panel of RCC cell lines: 769-P and Caki-2 (human) and RENCA (murine).

As shown in Table 1 murine cells have shown to be more sensitive to axitinib than the human cell lines, with an IC_{50} for RENCA of 0.5 mM, while for 769-P and Caki-2 the value was around 4mM and 6mM respectively.

Axitinib IC_{50} values in RCC cell lines	
	IC_{50} (μM)
769P	4.14
Caki-2	6.24
Renca	0.55

Table 1. The table shows IC_{50} values (the drug concentration that inhibits the cellular proliferation of 50%) for axitinib for the three cell lines. 24h after the seeding, cells 769-P, Caki-2 and RENCA cells have been treated with increasing concentrations (0.1 to 50 μM) of axitinib for 72h. Inhibition of cellular proliferation has been evaluated by MTT assay.

Since it has been reported for different target drugs as well as for chemotherapy agents the induction of PD-L1 expression on tumor cells[208–210], we studied the axitinib effect on PD-L1 modulation in RCC cell lines.

Firstly, we demonstrated that IFN-γ, a well-known positive regulator of PD-L1 expression[211] induced PD-L1 total protein in a dose-dependent manner in both 769-P and Caki-2 cells. The induction was less evident in Caki-2 cells, showing a higher basal level as compared to 769-P cells (Figure 1).

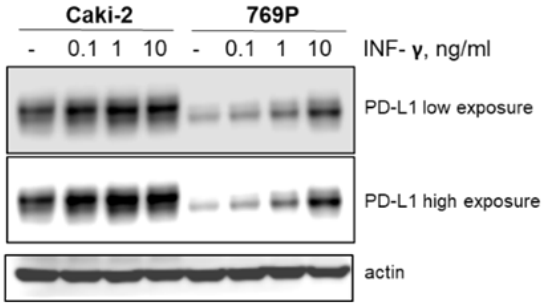

Figure1. Effect of pazopanib and sunitinib on PD-L1 protein expression. 24h after seeding, Caki-2 and 769-P cells were treated with increasing concentrations of IFN-γ for 48h. At the end of the treatment, the cells were lysed and PD-L1 expression was evaluated by Western Blot analysis. Considering the differences in the basal expression of PD-L1 between the two models, two different levels of membrane exposure are shown.

Then, PD-L1 membrane level (mPD-L1) was assessed by flow cytometry in RCC cells after axitinib treatment. In all the cell lines analyzed, PD-L1 expression on tumor cell surface was induced when cells were treated with the highest dose of axitinib, while no significant increase was reported when axitinib was administered 1 mM (Figure 2A). However, the Western-Blot analysis of the total amount of PD-L1 protein expressed by the three RCC cell lines underscored that axitinib did not exert any effect on PD-L1 expression, differently from other target agents or chemotherapy (Figure 2B)[212,213] suggesting that PD-L1 increase on the cell surface was due to protein translocation. Similarly, axitinib treatment did not induce the mRNA expression of PD-L1 in 769-P cells compared to the control (Figure 2C).

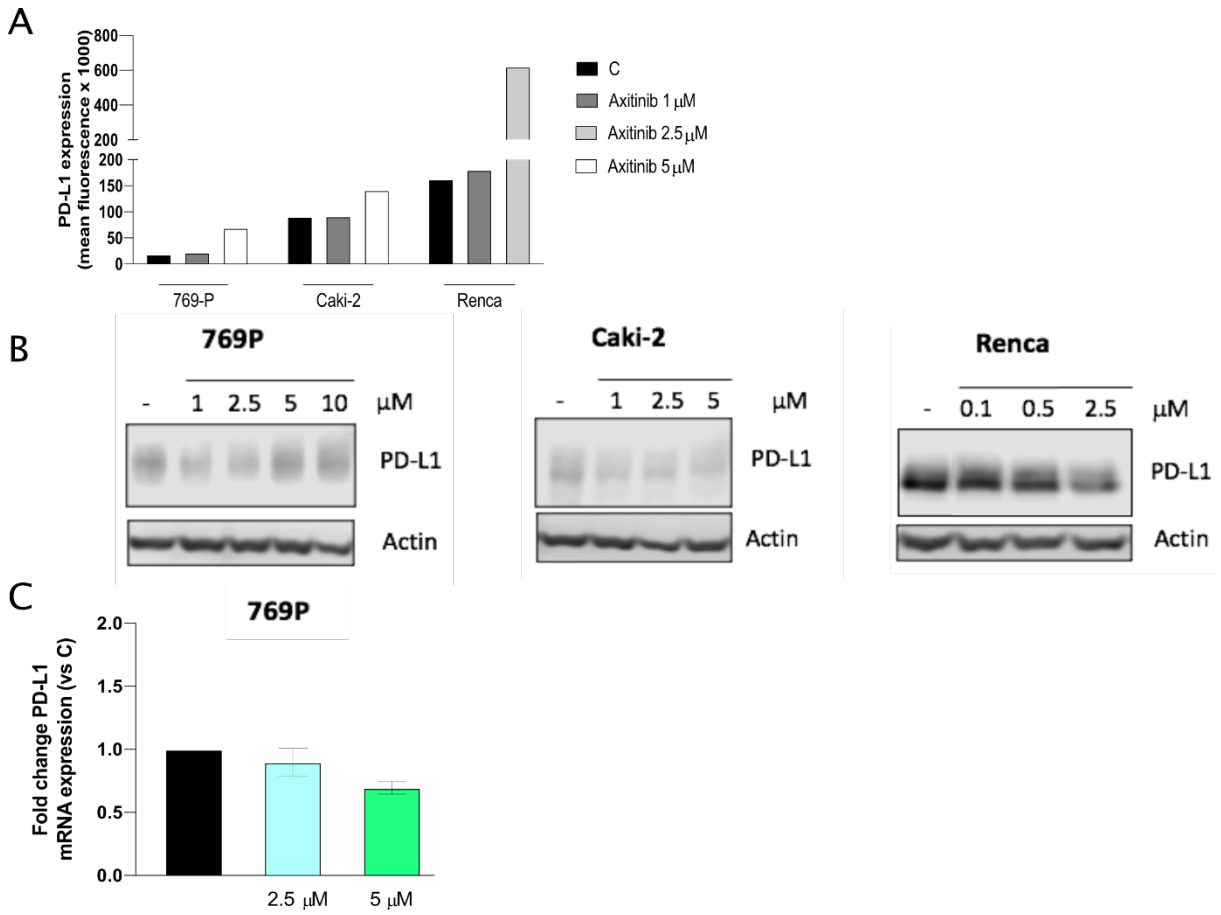

Figure 2. Evaluation of PD-L1 expression after axitinib treatment in a panel of RCC cell lines. A) PD-L1 expression was evaluated in 769-P, Caki-2 and Renca cells after 72 hours of treatment with two different concentrations of axitnib (1 mM and 5 mM or 2.5 mM for Renca cells). Then, cells were harvested, and the analysis was performed by flow cytometry. Results are expressed as mean fluorescence versus untreated cells. B) PD-L1 expression levels following the treatment with axitinib. 24h after the seeding, cells have been treated with increasing concentrations of axitinib for 72 h. Cells were lysed and PD-L1 expression was evaluated by Western Blot analysis. C) 769P cells were treated for 24h with axitinib at the indicated concentrations, then mRNA was extracted, and qRT-PCR was performed to analyze PD-L1 expression. Results are plotted as $2^{-DDCT} \pm$ SD compared to control. The data in A, B, and C are representative of three different experiments.

Subsequently, we investigated the immunomodulatory effect of the association of axitinib and avelumab, an anti-PD-L1 monoclonal antibody already used in the clinical setting, on 769-P and Caki-2 cells. To begin, we tested the effect of the combination: cells were treated with increasing concentrations of avelumab, while axitinib was administrated at the specific IC_{50} previously calculated for each cell line (see Table 1). As expected, the effect consisted of the activity of axitinib alone: avelumab did not show any antiproliferative effect on RCC cells (not shown).

We then assessed the treatment-induced modulation of PD-L1 total expression by Western Blotting on 769-P and Caki-2 cell lines. Cells were treated for 72 hours with a fixed axitinib concentration corresponding to the respective IC_{50} concentration for each model, and with increasing concentrations of avelumab ranging from 2 to 50 µg/ml. Surprisingly, avelumab induced PD-L1 total protein expression in all cell models. When the drugs were given as a combination, PD-L1 expression was significantly reduced, especially in Caki-2 cells (Figure 3).

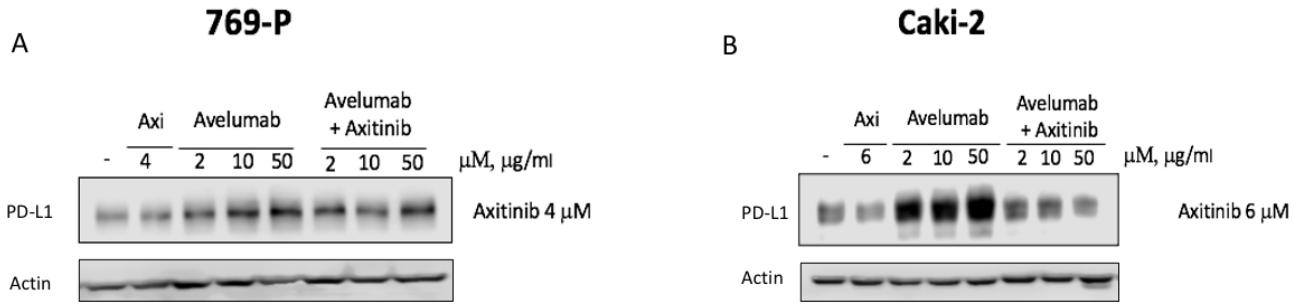

Figure 3. Effect of axitinib and the combination of axitinib and avelumab treatment on PD-L1 expression on RCC cell lines. 24h after the seeding, cells have been treated with axitinib at IC_{50} or the association of increasing concentrations of avelumab and axitinib at IC_{50} for 72 hours. Cells were lysed and PD-L1 expression was evaluated by Western Blot analysis in 769-P (A), Caki-2 (B) cells.

We then evaluated the modulatory effect of TKIs treatments on the soluble form of PD-L1 (sPD-L1), which can also represent a potential tumor marker of sensitivity to anti-PD-L1/PD-1 therapies[214]. The analysis was performed on Renca cells, as they are the model planned to use for *in vivo* experiments. The cells were treated with axitinib or murine anti-PD-1 antibody alone or in combination. As shown in Figure 4, axitinib treatment as well as the combined treatment induced a significant sPD-L1 release, whereas we fail to detect an augmented release of PD-1 after the treatment with ICI alone.

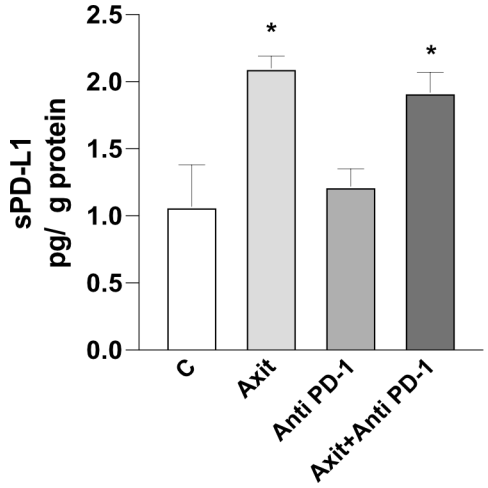

Figure 4. Effect of axitinib and anti-PD-1 ICI on the modulation of sPDL1 expression. 24h after seeding, Renca cells were treated with axitinib (2.5 µM), murine anti-PD-1 (50 µg/ml) alone or in combination for 72h. The media were then collected and sPD-L1 was detected by an ELISA assay (* $p<0.05$ versus C).

1.2. EFFECT OF AXITINIB ON PBMCS

Then, we determined the anti-proliferative and immunomodulatory effects of axitinib on human PBMCs. After the isolation from the buffy coat, PBMCs were activated *in vitro* with anti-CD3 and anti-CD28 antibodies and 24 hours after the activation, cells were exposed to increasing concentrations of axitinib. Notably, individual variability did not play a relevant role as PBMCs tended to be as sensitives to axitinib. Indeed, the two donors reported an IC_{50} value ranging from 0.9-1.7 mM (Figure 5A). Moreover, the anti-proliferative and immunomodulatory effects of axitinib were determined also on murine PBMCs obtained from female Balb/c mice. The effect of drug treatment was evaluated as IFN-γ release, index of lymphocyte activity, from murine PBMCs previously activated *in vitro* with murine anti-CD3 and anti-CD28. As shown in figure 3B, murine PBMCs activity was affected by axitinib in a dose-dependent manner, thus indicating that drug exposure could affect lymphocytes activation (Figure 5B).

A

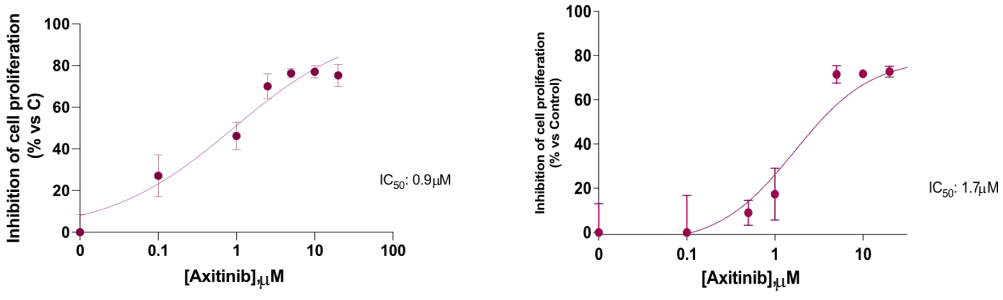

B

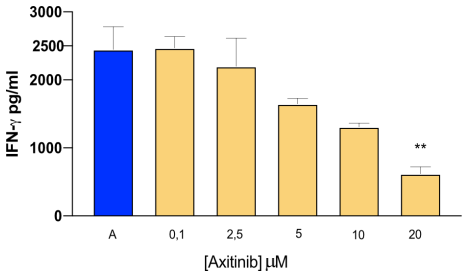

Figure 5. Effect of axitinib on human and murine PBMCs. A) Human PBMCs were isolated from two different healthy donors, activated *in vitro*, and treated with increasing concentrations of axitinib (0.1 to 20 mM) for 72h. Inhibition of proliferation has been evaluated with colorimetric assay MTS. Data are expressed as percentage of inhibition vs. control. B) Effect axitinib on IFN-γ production by PBMCs from Balb/c mice. 24h after isolation and activation, murine PBMCs were treated with increasing concentrations (from 0.1 mM to 20 mM) of axitinib for 72h. IFN- γ release was then measured by ELISA assay. The data in A and B are representative of three different experiments (**p<0.005).

Subsequently, we questioned whether the effect of axitinib on PBMCs activation could be modulated by the association with an anti-PD-1 antibody.

Human PBMCs activated in vitro with anti-CD3 and anti-CD28 were simultaneously treated with axitinib in presence or absence of avelumab at the indicated concentrations for 96 hours and then analyzed for IFN-γ secretion, and for the expression of immunomodulatory surface molecules.

As shown in Figure 6A-B, treatments did not exert any significative effect on cellular activation. Among the total T lymphocytes' population ($CD3^+$ cells), the $CD4^+$ and $CD8^+$ subsets percentages remained unchanged independently of the drug exposition, as well as the IFN-γ release (Figure 6C).

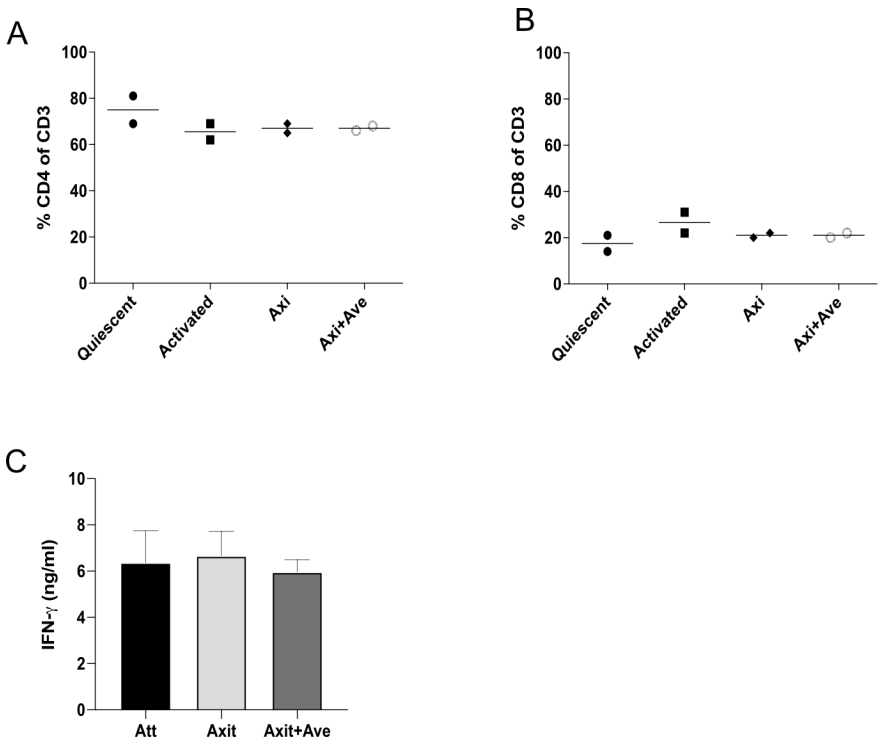

Figure 6. Effect of the combined treatment of axitinib and avelumab on human T cells activation and IFN- γ release in human PBMCs isolated from healthy donors. Following isolation from buffy coats, PBMCs were activated *in vitro* with antibodies against CD3 and CD28 and simultaneously treated with axitinib 1.5μM with or without avelumab 10μg/ml. Following 96 hours of treatment, the cells were harvested and analyzed for the expression of CD3, CD4 and CD8 by flow cytometry and IFN-γ was dosed in the culture media with ELISA method.

In addition, we also examined the treatment effect on modulation of surface proteins expressed on PBMCs and involved in the down regulation of the immune response, as PD-1, Lymphocyte activation gene 3 (LAG-3, CD223) and T cell immunoglobulin 3 (TIM-3). LAG-3, firstly identified on activated human NK and T cells, is a cell surface receptor which negatively regulates antigen-specific T cell responses; TIM-3 is a negative regulator of CD4+ and CD8+ activity[215].

PD-1 was expressed in quiescent cells, while TIM-3 and LAG-3 had no or extremely low expression in these cells. As shown in Figure 7, all three immune checkpoint molecules were induced in activated cells, with some differences between $CD4^+$ and $CD8^+$ cells. In particular, PD-1 expression was higher in $CD4^+$ cells than in $CD8^+$ cells; conversely, TIM-3 and LAG-3 were expressed at higher levels in $CD8^+$ cells. It is worth noting that, even though all these molecules are generally considered as negative regulators of T cell function, their expression has been also associated with activation and differentiation, and TIM-3 and LAG-3, in particular, may play more complex roles, beyond the inhibitory activity, depending on the cell differentiation

stages[216]. Axitinib slightly decreased the percentage of PD-1$^+$CD4$^+$ cells, while had no effect on PD-1 expression in CD8$^+$ cells. The combined treatment of axitinib and avelumab significantly impaired PD-1 expression on CD4+ T cells. TIM-3 expression was reduced at a similar extent in CD4$^+$ and CD8$^+$ cell subsets, however only the combined treatment produced a significative reduction in TIM-3 levels; regarding LAG-3 protein expression we observed a slightly reduction only in CD8$^+$ cells, even if not statistically significative.

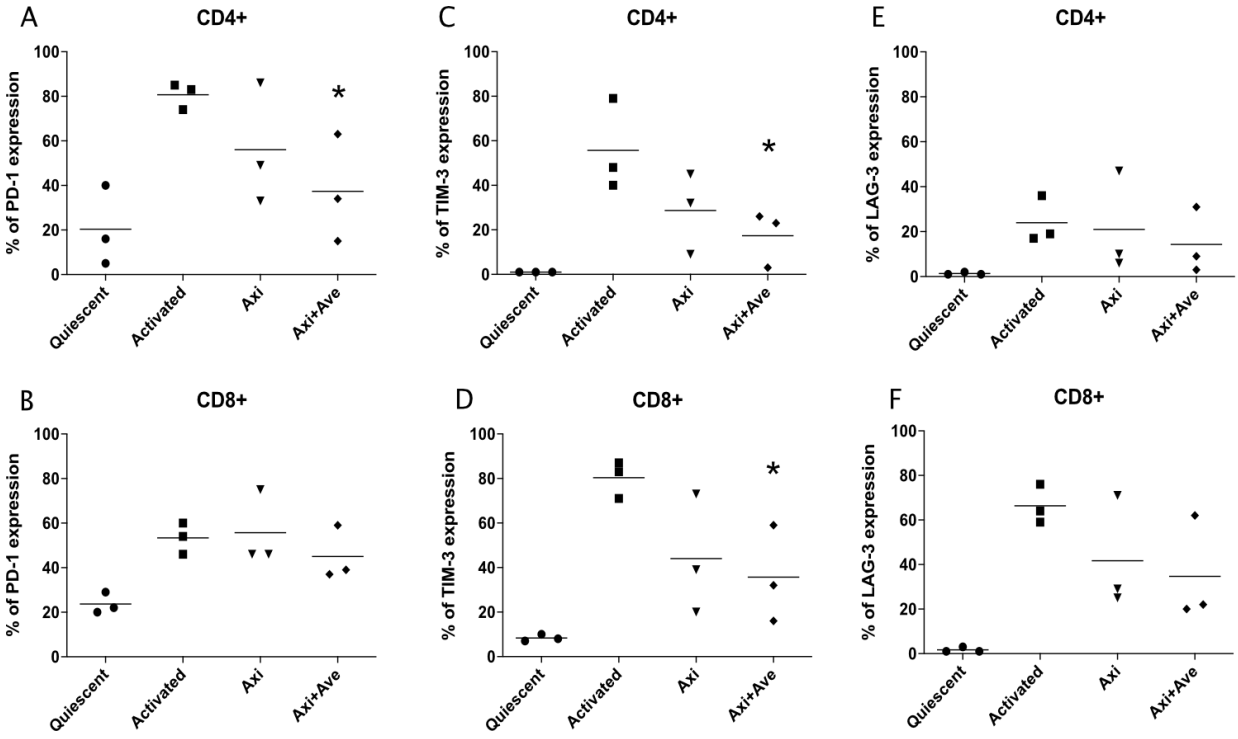

Figure 7. Effect of the combined treatment with axitinib and anti-PD-1 on modulation of human PBMCs surface molecules expression. Following isolation from healthy donors buffy coats, PBMCs were activated in vitro with antibodies against CD3 and CD28 and simultaneously treated with axitinib M with or without avelumab g/ml. Following 96 hours of treatment, the cells were harvested and analyzed for the expression of the indicated surface immunomodulatory molecules in the two subsets populations by flow cytometry (*p<0.05).

Analyses of the modulation of surface molecules induced on lymphocytes surfaces were replicated on murine PBMCs. As shown in Table 3, axitinib reduced the *in vitro* activation of T cells decreasing the percentage of CD25-expressing cells both in CD4$^+$ and CD8$^+$ populations. CD25 is the alpha chain of the interleukin-2 receptor, normally expressed on activated T lymphocytes and it is involved in their growth and proliferation[217]. Therefore, the decrease of CD25 expression indicated a decrease in the activated lymphocyte population (Table 2). Here, the exposure of PBMCs to axitinib, alone or in combination with the anti-PD-1, resulted in a

lower activation of PBMCs, consistently with the decrease in IFN-γ production already reported for PBMCs exposed to axitinib (Figure 5B).

Murine T cells activation		
Conditions	% of PBMC population	
	CD4/ CD25	CD8/ CD25
Control	74	10
Axi 2.5uM	37	5
Axi 2.5uM+ Anti-PD-1 200ug/ml	28	6

Table 2. Effect of the combined treatment with axitinib and anti-PD-1 on murine T cells activation. PBMCs were isolated from fresh blood, activated in vitro with murine antibodies against CD3 and CD28 and simultaneously treated with axitinb 2.5 μM with or without the anti-PD-1 monoclonal antibody at 200 μg/ml. Following 96 hours of treatment, the cells were harvested and analyzed for the expression of CD25, CD4 and CD8 expression by flow cytometry. The data are representative of two different experiments.

As shown in Table 3, in the two subsets of activated ($CD25^+$) immune cells analyzed, $CD4^+$ and $CD8^+$, we observed a reduction of PD-1 levels induced by axitinib and, in the $CD8^+$ population, also by the combinatorial treatment. However, the low or totally absence of signal registered in for the analysis of PD-1 expression after the combination could be also explained by the concurrent binding of the anti-PD1 to the same site. For both populations considered, TIM-3 expression was strongly reduced by axitinib and almost annulled when the cells were exposed to the combination. LAG-3 expression was significantly reduced by the treatments only in $CD25^+/CD4^+$ cells.

E*xpression of membrane proteins on activated CD4+ and CD8+* cells						
Conditions	% of CD4/CD25 cells			% of CD8/CD25 cells		
	PD1	**TIM3**	**LAG3**	**PD1**	**TIM3**	**LAG3**
Control	95	11	96	92	37	99
Axi 2.5uM	68	2	73	62	10	98
Axi 2.5µM+ Anti-PD-1 10ug/ml	-	-	73	11	1	97

Table 3. Effect of the combined treatment with axitinib and anti-PD-1 on modulation of surface molecules expression. PBMCs were isolated from fresh blood, activated in vitro with murine antibodies against CD3 and CD28 and simultaneously treated with axitinb 2.5 µM with or without the anti-PD-1 monoclonal antibody at 200 µg/ml. Following 96 hours of treatment, the cells were harvested and analyzed for the expression of the indicated surface immunomodulatory molecules by flow cytometry. The data are representative of two different experiments.

Overall, in spite of the different sensitivity of murine PBMCs compared to human PBMCs to axitinib exposure in terms of activation, in both models axitinib induced the down regulation of co-inhibitory molecules as PD-1, TIM-3 and LAG-3. The association with avelumab or the anti-PD-1 analogue amplified this effect, thus suggesting that the combination might effectively restore T cells activity.

1.3. OPTIMIZATION OF A MURINE CO-CULTURE SYSTEM

Further investigations of the *in vitro* effects of the anti-angiogenic treatments were performed in a co-culture setting of murine lymphocytes and RENCA cells. The co-culture systems allows a more complete overview of the complex interplay between the immune cells and the cancer cells.

Before the application of the full schedule of treatment to this system, a number of factors were evaluated, in order to obtain the optimal conditions for PBMC/cancer cell interaction:

- the minimum concentration of anti-CD3 and anti-CD28 necessary to obtain a full T cell activation,

- the PBMC to cancer cell ratio,
- the type of co-culture system (co-culturing the cells in the same well or in a transwell system),
- the time of contact.

Firstly, we assessed the minimum concentration of anti-CD3 and anti-CD28 required to fully activate lymphocytes, in order to better mimic the immune cells activation in the body. Murine PBMCs treated with decreasing concentrations of anti-CD3 starting from the recommended concentration of 5 mg/ml were tested for activation via dosing of IFN-γ release. Interestingly, anti-CD28 alone did not seem to particularly influence PBMCs activation, while anti-CD3 at a concentration of 0.2 mg/ml was already sufficient to provide a full T cell activation (Figure 8). For further experiments, anti-CD3 and anti-CD28 concentrations were 0.2 mg/ml and 2 mg/ml respectively.

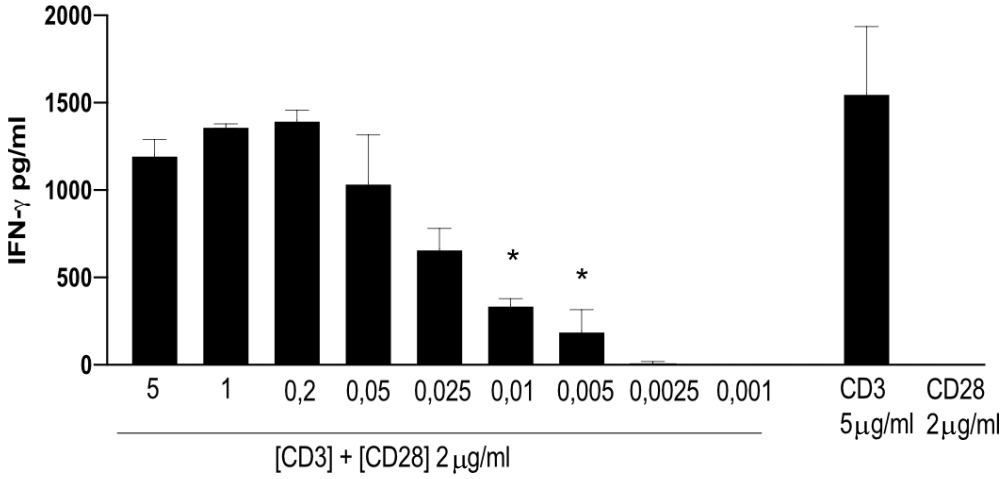

Figure 8. Evaluation of the minimum concentration of anti-CD3 and anti-CD28 required to fully activate lymphocytes. After isolation from mice blood, murine PBMCs were treated with the association of anti-CD28 2 mg/ml and decreasing concentrations of anti-CD3, the main responsible of PBMCs activation. 72 hours after the activation, media were collected, and IFN-γ release was measured by ELISA assay.

Second step of the optimization consisted of the determination of the right time of contact and PBMC/cancer cell ratio. To this aim, we tested different PBMC to cell ratios for different times of contact (24, 48 or 72 hours). The effect due to the contact of PBMCs with cancer cells was evaluated as antiproliferative activity, LDH release (index of cell cytotoxicity) and IFN-γ production. It emerged that the optimal time of contact was 48 hours, and the best PBMC to cancer cell ratio was 10:1 with anti-CD3 administered at 0.2 mg/ml (Figure 9). Moreover, due

to the aggressiveness of the non-specific cytotoxic effect exerted by PBMCs against RENCA cells, the optimal setting consisted of a co-culture using a transwell system, that avoids the direct cell to cell contact while guaranteeing the fluid exchange.

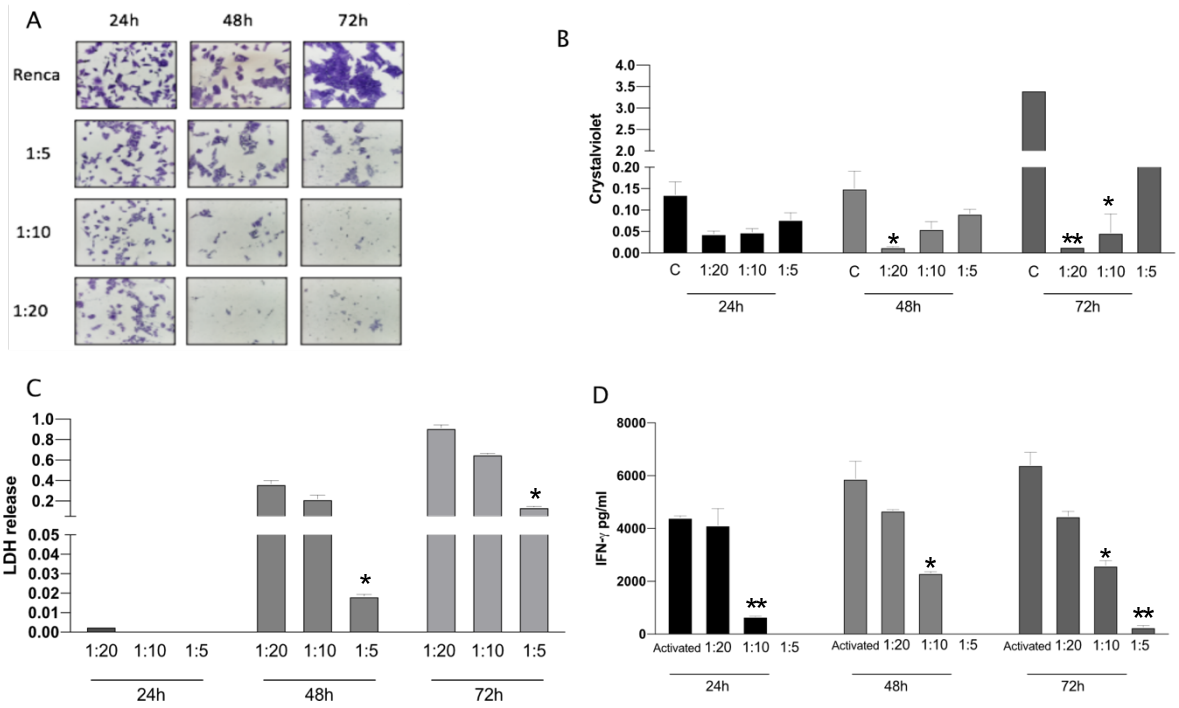

Figure 9. Determination of the right time of contact and PBMC/cancer cell ratio in a murine co-colture system. Renca cells were seeded at different concentrations in order to obtain the desired cancer cells/PBMCs ratio (1:20, 1:10, 1:5). 24h after seeding, Renca cells were added with PBMCs, previously isolated and activated in vitro for 24 hours with anti-CD-3 0.2 mg/ml, for another 24, 48 or 72 hours. Supernatants were then collected and LDH and IFN-γ were dosed (C and D) while cells were fixed with methanol and stained with crystalviolet (A). For simplicity, only the graphs of the condition activated with anti-CD3 0.2 mg/ml are reported. The data in A, B, C and D are representative of three different experiments.

Last evaluation consisted of the investigation of the modulation of PD-L1 and PD-1 on PBMCs and RENCA cells, respectively, in the defined setting: 10:1 PBMCs to cancer cell ratio in a transwell system and a 24 hours PBMCs pre activation (anti-CD3 0.2 mg/ml and anti-CD8 2 mg/ml) before co-culture. As shown in Figure 10A, PD-L1 expression on RENCA cells was strongly induced by the presence of PBMCs, presumably due to the production of IFN-γ by PBMCs. On the other hand (Figure 10B), PD-1 expression on lymphocytes augmented with time after cell activation, consistently with previously reported evidences of this mechanism[218], whereas its expression decreased after the contact with the cells, and this effect was more evident after 72 hours of contact. A possible explanation of this phenomenon

could be that the tumor cells can release the soluble form of PD-L1, whose binding with PD-1 could cause an internalization of the complex ligand-receptor[219] .

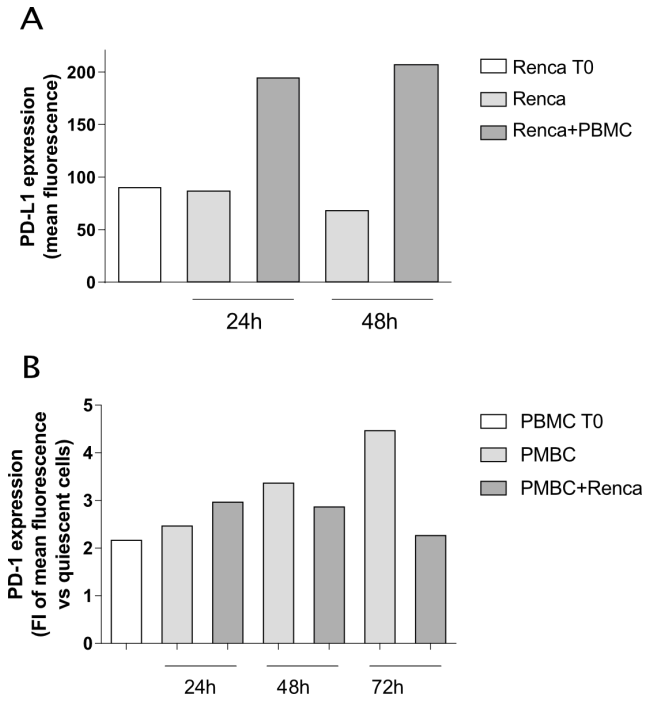

Figure 10. Evaluation of PD-1 and PD-L1 expression in a murine co-culture system. A) PD-L1 expression was evaluated in Renca cells in the presence or absence of PBMCs previously activated for 24 hours. Cells and PBMCs were maintained in contact for 24 or 48 hours, then cells were harvested and the analysis was performed by flow cytometry. B) PD-1 expression on lymphocytes was evaluated in the presence or absence of Renca cells. PBMCs and Renca cells were co cultured for 24, 48 or 72 hours, then PBMCs were harvested and the analysis was performed by flow cytometry. The data in A and B are representative of three different experiments.

The modulatory effects of the immune checkpoint inhibitors on the cytotoxic activity of PBMCs towards tumor cells after exposure to axitinib were evaluated in the correctly settled murine co-culture system. 24 hours after seeding, RENCA cells were treated with axitinib. Following 96 hours of treatment, axitinib was removed from the cells and previously activated PBMCs, were added to RENCA cells using a transwell chamber with or without the murine anti-PD-1 antibody for further 48 hours. As shown in Figure 11A-B, axitinib treatment exerted an anti-proliferative effect on RENCA cells that was increased when anti-PD-1 was administered in addition to PBMCs. On the contrary, the addition of anti-PD1 in the control co-culture system did not affect cell viability. In addition, the combined treatment induced also an increase in IFN-γ release, as shown in Figure 11C. The stronger effect on RENCA cells observed with the schedule might be explained considering that the tendence to increase in

the IFN-γ release could be an indicator of restored PBMCs activity, promoted by the anti PD-1 antibody. The explanation of the anti-proliferative action mediated by the antibody may be related to the previous demonstrated release of soluble PD-L1 by cancer cells: by binding to the sPD-L1 the anti-PD1 prevented the exhaustion of T cells thus maintaining their cytotoxic activity.

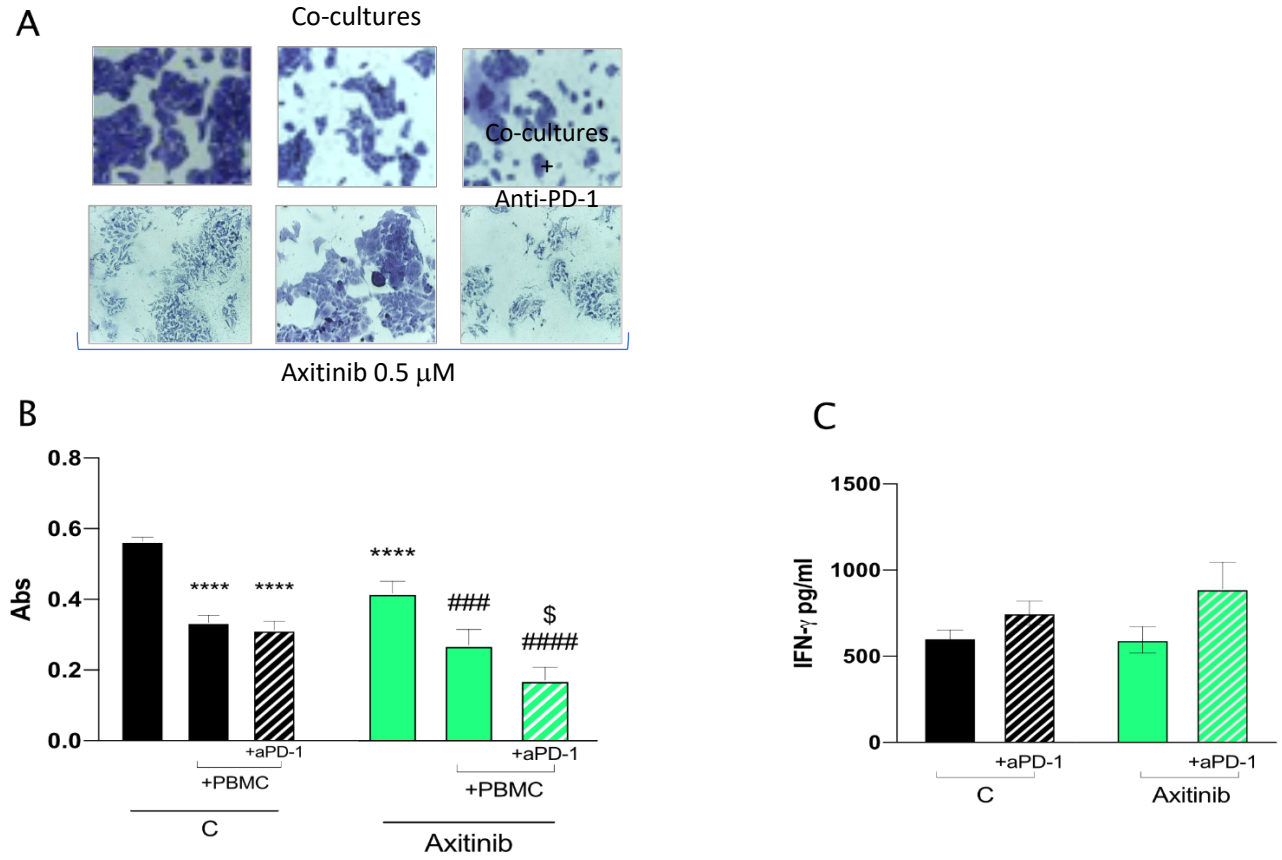

Figure 11. Effect of the treatment schedule in a co-colture system over time. 24h after seeding, Renca cells were treated with axitinib 0.5 mM for 96 h. Then, PBMCs previously isolated and activated in vitro for 24 hours were added to Renca cell colture for another 48 hours in the presence or absence of anti-PD-1 200 mg/ml. Cells were fixed with methanol and stained with crystalviolet (A) and once dried, crystalviolet was dissolved in 0.2% TritonX-100 in PBS and absorbance was read at 570 nm (B). In addition, supernatants were collected and IFN-γ was dosed (C). (**** $p<0.0001$ versus C; ### $p<0.001$ Axitinib versus Axitinib + PBMCs; $ $p<0.05$ Axitinib + PBMCs versus Axitinib + PBMCs + a-PD-1). The data in A, B, and C are representative of three different experiments.

2. GUT MICROBIOTA AND RCC

The importance of the role of the gut microbiota composition has been broadly pointed as a relevant element to consider in cancer patients, as it is able to influence the peripheral immune tonus and the effectiveness of ICI-based therapy[164,165,167].

Particularly, the fecal composition plays a central role in modulating the response to therapy for RCC patients. Specific gut signatures, characterized by the enrichment in beneficial commensals as *Akkermansia muciniphila* and *Enterococcus hirae* are typical in patients that would later benefit of a better immunotherapy outcome, due to the elicitation of an immune adaptative response against tumor. In addition, it has been proved that TKIs treatment (cabozantinib and axitinib more than sunitinib) induce a microbiota shift favoring a higher abundance of immunostimulatory commensals that could improve the efficacy of a subsequent ICIs therapy including *Akkermansia muciniphila* [167]. Conversely, antibiotic administration before or right after the beginning of immunotherapy is associated with a worse patients' outcome due to the treatment induced decrease in microbiota diversity[220] .

Whether gut microbiota can be used as a decision variable to define the better sequence of treatment is still unknown. Thus, we evaluated whether gut microbiota modulation could impact on the efficacy of standard therapies for RCC.

2.1 STANDARD THERAPY AND MICROBIOTA: PERTURBATION OF THE TAXONOMIC COMPOSITION OF MICE MICROBIOTA BY STANDARD THERAPY.

To better assess the causal-effect association between different treatments and sequences of TKIs +/- ICIs and the gut microbiome composition we turned to a preclinical *in vivo* model. The choice of tested drugs was based on the standard of care in first and second line for metastatic RCC patients.

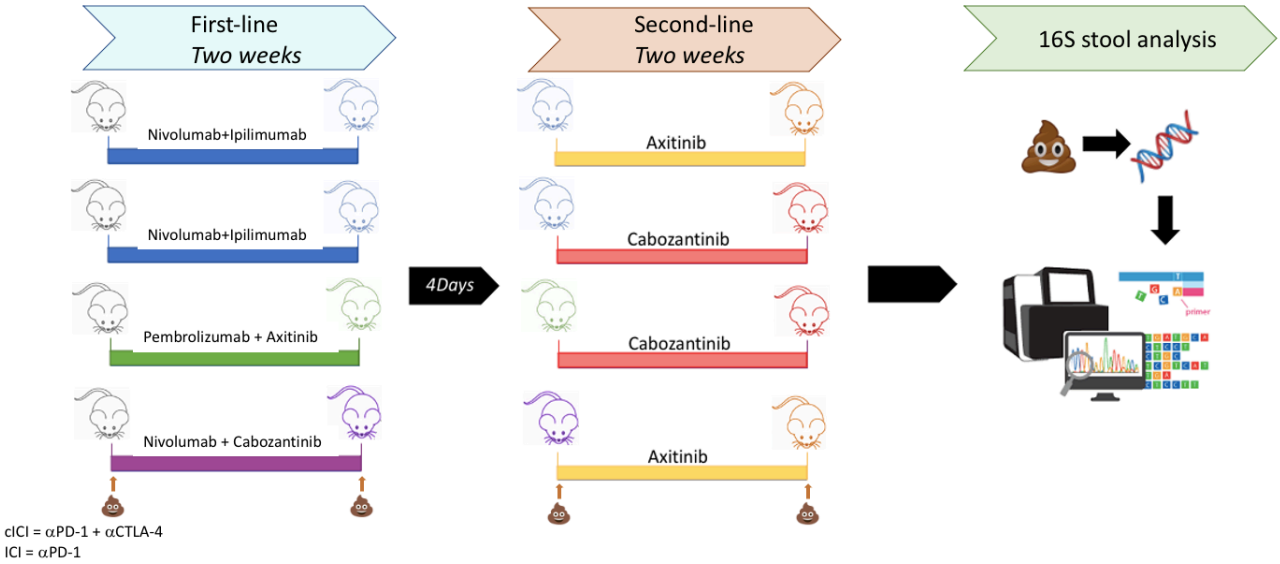

Figure 12. Experimental setting. Specific Pathogen Free (SPF) Balb/c mice received four different treatment sequences of 14 days each. Mice received intraperitoneally anti-CTLA4 and/or anti-PD-1 monoclonal antibodies, while axitinib and cabozantinib were administered daily by oral gavage. Following 4 days of washout, mice orally received either axitinib or cabozantinib on a daily basis for two weeks. Feces were collected every 4 days before treatment administration.

As shown in the Figure 12, Balb/c mice were treated with four different sequences that mimic four different treatment sequences actually used in clinic:

- the association of nivolumab (anti-PD-1) and ipilimumab (anti-CTLA4) followed by either axitinib or cabozantinib,
- the association of pembrolizumab (anti-PD-1) and axitinib followed by cabozantinib,
- the association of nivolumab and cabozantinib followed by axitinib.

A total of 25 specific pathogen free (SPF) Balb/c Mice were treated for 14 days with the "first line" setting followed by 4 days washout and finally for another 14 days with the "second line" setting. Mice were injected intraperitoneally every 4 days for a total of 4 cycles with the murine analogues of the human mAbs pembrolizumab, nivolumab and ipilimumab, while the TKIs cabozantinib and axitinib were orally administrated on a daily basis (Figure 12). Feces were collected every 4 days before treatment administration starting from the beginning of treatment and sent to INRAE for 16S analysis.

To date, deviations of the 16S composition of the stools and deviations at the strain level are ongoing and will be analyzed in collaboration with the group of computational metagenomics lead by prof. Nicola Segata, UNITN, Italy and with dr. Valerio Iebba of the Univeristy of Trieste.

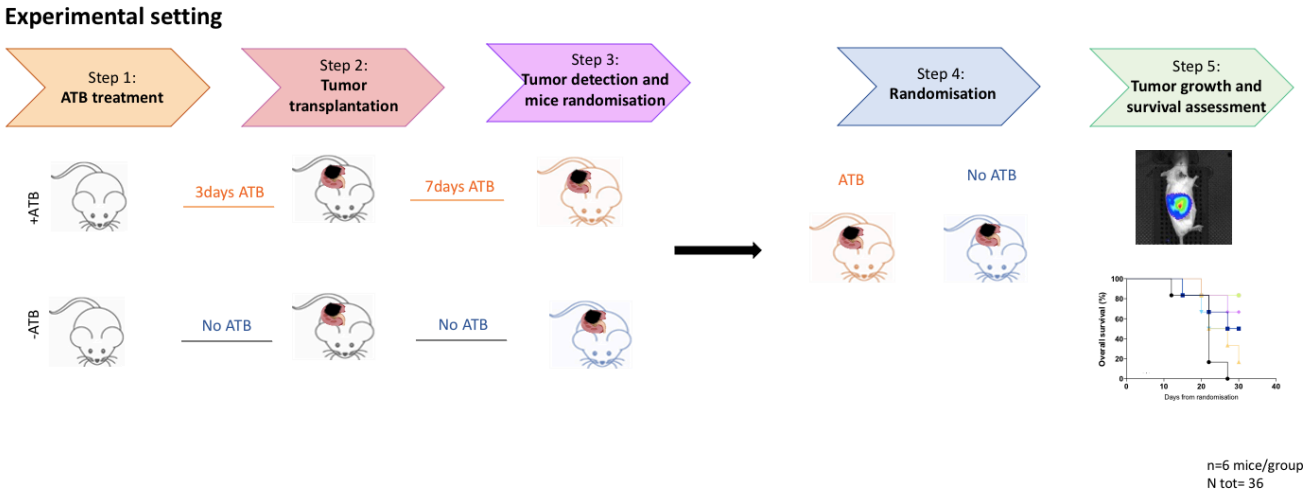

Figure 13. Experimental setting. Specific Pathogen Free (SPF) Balb/c mice were administered with antibiotics (ATB) for 10 days. Luciferase engineered RENCA cells (Luc$^+$RENCA) were orthotopically injected after 3 days of ATBs treatment. From day 7 mice were randomized on the basis of tumor volume measured with whole body bio luminescence and tumor growth was assessed until day 15.

In addition to this, we validated the effect of antibiotic-induced dysbiosis on cancer progression, by comparing tumor progression in mice with a suppressed microbiota.

To this aim SPF Balb/c mice were sterilized by administration of broad-spectrum ATBs (colistin + ampicillin + streptomycin) for a total of 10 days. Following the first 3 days of ATBs therapy, the orthotopic injection of luciferase engineered RENCA cells (Luc$^+$RENCA) was performed in every mouse. Mice were randomized in relation to the tumor size, determined with whole-body bioluminescence, maintaining the stratification in ATB +/- previous administration (Figure 13).

From this experience we can state that ATB previous administration prevented spontaneous remission that we could see in the untreated group (Figure 12B). However, as shown in Figure 12 A, no difference in tumor volumes was observed in animals treated with ATBs respect to untreated ones.

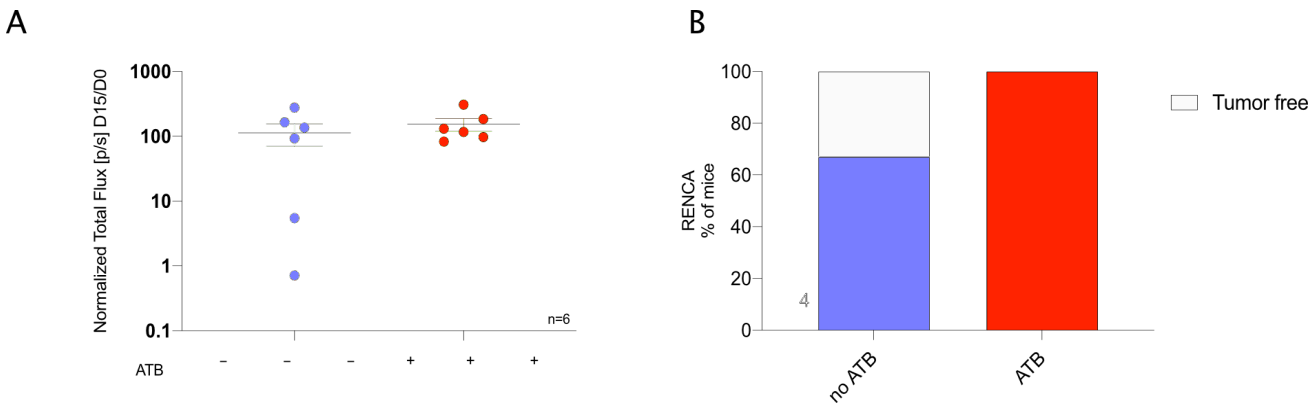

Figure 14. Evaluation of the antibiotic-induced dysbiosis on tumor progression. A) Monitor of RENCA progression using bioluminescence imaging of luciferase activity at Day15. All experiments involved 6 mice per group. C) Tumor free percentage of mice at Day 15. Mice are considered tumor free when the normalized total flux (D0/D15) is < 10.

2.2 VALIDATION OF PROMISING TARGETS (*AKKERMANSIA SPP* AND OTHERS) *IN VIVO* TUMOR MODELS

Starting from the evidence that a microbiota composition that favors a higher abundance of immunostimulatory commensals including *Akkermansia muciniphila* can improve the efficacy of subsequent ICI treatment (Derosa L. et al., 2020), we investigated the possibility to restore the immunotherapy effect in a non-responder avatar mouse phenotype, supplementing mice with this regulatory bacterium. The avatar mouse model allows us to humanize Balb/c guts and to de facto reproduce the gut of the patients thus allowing us to provide cause-effects relationships[164,167,221].

SPF recipient Balb/c mice were treated with ATBs to sterilize their guts and then received fecal microbiota transplantation (FMT) from human stool of a immunotherapy non-responder (NR) patient, identified according to the following characteristics: OS less of 24 months and absence of *Akkermansia* in the stool specimen. Mice were then orthotopically implanted with Luc^{+}RENCA cells two weeks later. Seven days from the tumor injection, mice were randomized in six different groups in relation to the tumor size, determined with whole-body bioluminescence.

A shown in Figure 15, the six groups received either:

- the association of anti-PD-1 plus cabozantinb
- the association of anti-CTLA4 and anti-PD-1
- the association of anti-CTLA4 and anti-PD-1 with different *Akkermansia* strains (SGB9226, SGB5801, SGB9228);

- isotypes antibodies (control group).

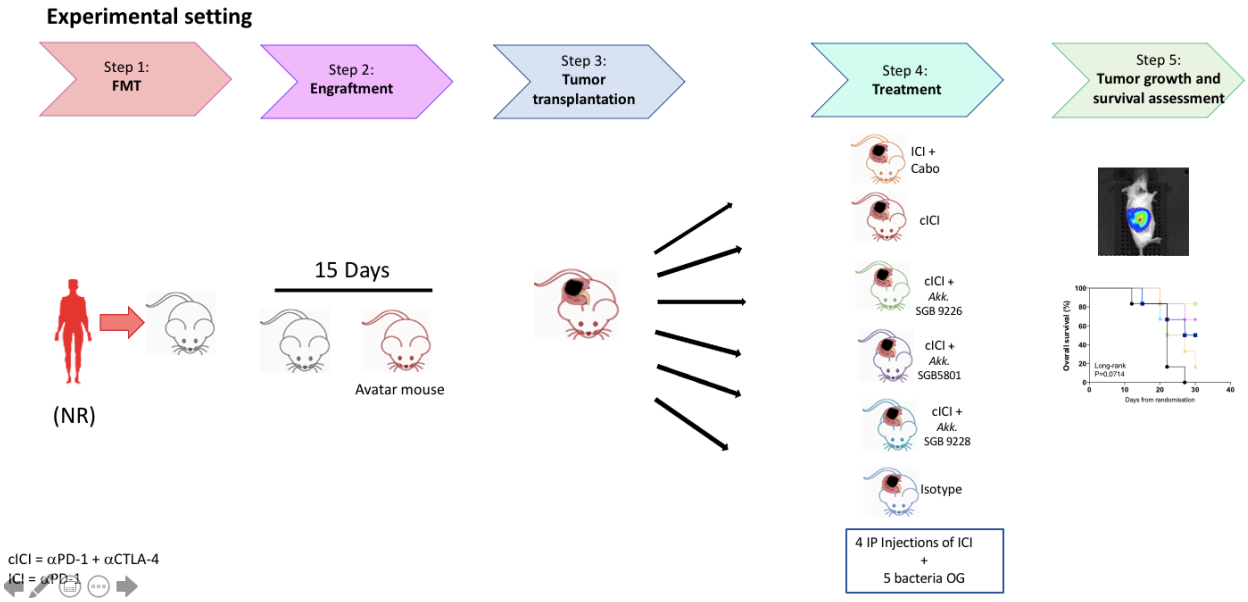

Figure 15. Experimental setting. Fecal Microbial Transplantation (FMT) was performed on specific SPF Balb/c mice following three days of antibiotics. Fifteen days later, luciferase engineered (Luc+) RENCA cells were orthotopically inoculated in mice kidneys, and anti-PD-1 plus anti-CTLA4 (cICB), anti-PD-1 plus Cabozantinib or the isotype control mAb (Iso) were injected intraperitoneally every 4 days. In addition to the injection, three different strains of *Akk* (SGB9226, SGB5801, SGB9228). were orally administrated to the mice.

Mice were intraperitonially injected every 4 days for a total of two weeks with anti-CTLA4 and/or anti-PD1 mAbs with or without a concomitant gavage of bacteria accordingly to the experimental setting (Figure 15). Were required, cabozantinb was administered orally on a daily basis and control group was injected with the isotypes controls of anti-CTLA4 and anti-PD-1 mAbs and gavaged with NaCl. Tumor growth was longitudinally monitored by a follow-up of whole-body bioluminescence after 9 and 15 days from the beginning of the therapy. Mice weight was monitored twice a week.

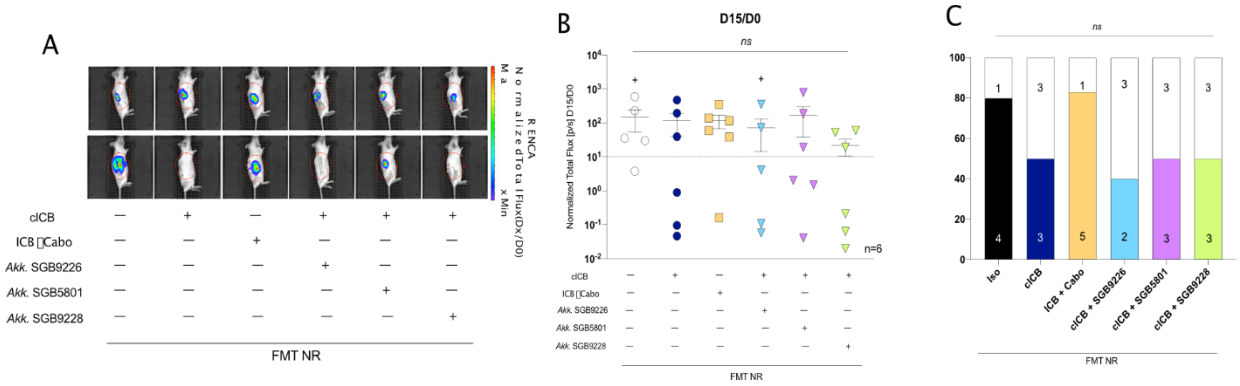

Figure 16. Oral gavage with immunostimulatory strains of *Akkermansia* effect on the restore of the response to cICB therapy. A-B) Longitudinal monitoring of Renca tumor by bioluminescence imaging of luciferase activity. C) Tumor free percentage of mice at Day 15. Mice are considered tumor free when the normalized total flux (D0/D15) is < 10. The experiment involved 6 mice per group.

As shown in Figure 16, in this first experiment, the *Akkermansia* strains SGB9226 and SGB9228 seemed to induce a better response to immunotherapy, while the strain SGB5801 did not exert any additional effect on ICI outcome. More in detail, the beneficial effect exerted by *Akkermansia* administration concomitantly with ICIs therapy was evaluated in terms of tumor size. In particular, implementation of *Akkermansia* SGB9228 strain induced a decrease in tumor size (Figure 16A-C) after 15 days of treatment, and an even greater efficacy in tumor size reduction compared to the control group was reported in the group receiving SGB9226 strain (Figure 16A-C) In addition, the implementation of Akkermansia to immunotherapy resulted in a beneficial effect on mice survival, although not significative. As shown in Fig 17B, the association of ICIs and *Akkermansia* strains SGB9228 and SGB9226 increased mice survival in a comparable way, while the implementation of SGB5801 and the immunotherapy alone showed lower benefit (Figure 17B).

In opposite, the combination of anti-PD-1 and cabozantinib did not induce any improvement in ICI response and tumor sizes were comparable to sizes of the control group (Figure 16A-C). Consistently with these observations, the combination did not seem to induce a beneficial effect on mice survival compared to control and to the other groups (Figure 17A).

It is worth noting the transient decrease in mice weight in this group of animals reported immediately after the first treatment (Figure 17A), probably related to the gastro-intestinal toxicity related to the addition of cabozantinib to the immunotherapy[222].

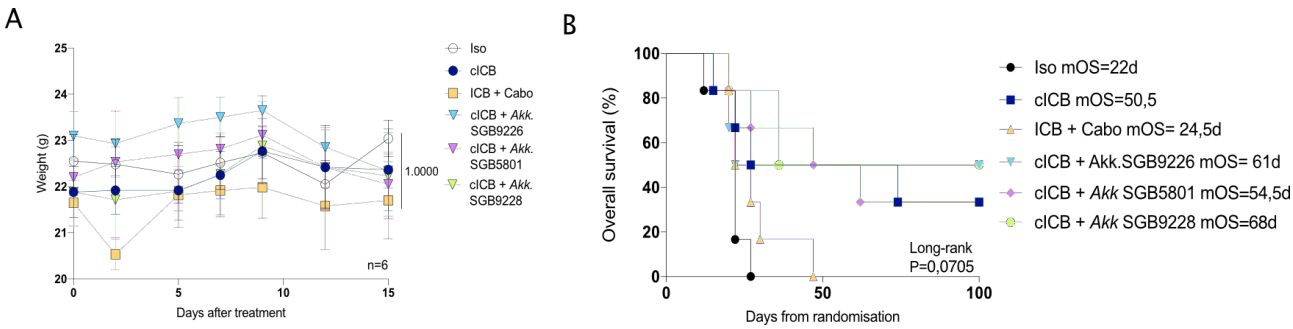

Figure 17. Longitudinal monitoring of oral gavage with immunostimulatory strains of *Akkermansia* effect on the restore of the response to cICB therapy. Longitudinal monitoring of mice well-being was performed by weight assessment (A), with special regards to the weight decrease induced by cabozantinib at day 2. The experiment involved 6 mice per group that were monitored to assess survival, reported as mOS in days (B).

DISCUSSION

The treatment paradigm for RCC has evolved through the years, allowing clinicians to increase the OS and PFS for those patients. Since the success seen in the cytokine era (especially with type I interferon and interleukin 2)[223], later overtaken by the introduction of anti-angiogenic drugs, a true breakthrough was represented by the regulatory approval of the immune checkpoint inhibitors (ICIs). Firstly approved as second line treatment for RCC patients previously treated with TKIs, in the last years several therapeutic associations of ICIs and TKIs were approved as first line standard for advanced RCC patients[224] .

ICIs are agents that act by releasing the latent anti-tumour immunity. The first positive report of nivolumab efficacy was in a second line setting compared to everolimus (Motzer R.J. et al., 2015); after that, several clinical studies, as CheckMate214, JAVELINRenal101, KEYNOTE-426 and IMmotion151 underscored that anti-PD-1 therapy associate with either anti CTLA-4 agents or TKIs were superior to sunitinib monotherapy as first line setting for mRCC[200,225–227].

The mechanism of action of TKIs used in mRCC treatment mainly consist of the impairment of the angiogenesis, thereby reducing tumor growth and proliferation. However, the VEGF protein has been shown to have immunomodulatory properties, in addition to its role in the promotion of angiogenesis. More in detail, it reduces the activity of NF-kB and dendritic cells maturation[228], it attracts the tumor-associated macrophages (TAMs)[229] and it modulates the T cell activity particularly reducing the $CD4^+$ T cells function and increasing the expression of suppressive immunomodulatory molecules as PD-1, CTLA-4, TIM-3 and LAG-3 on $CD8^+$ T cells, thereby contributing to T cell exhaustion[230,231]. It also contributes to the modulation of adhesion molecules and chemokine expression which in turn decreases the recruitment of immune cells within the tumour[232,233]. Overall, VEGF has a prominent role in the generation of an immunosuppressive environment around the tumor. In this scenario, TKIs as sunitinib, pazopanib, and axitinib have been proved to have an immunomodulatory role.

The immunological effects of Axitinib has been investigated in pre-clinical studies, proving that it hampers MDSCs through the downregulation of STAT3 in a *in vivo* xenograft model (Yuan H. et al., 2014) and promotes NK cell degranulation on human RCC cell lines[233,234]. In addition, a preclinical study suggested that its therapeutic efficacy was not only related to the VEGF pathway inhibition, but also through the induction of anti-tumor immunity, exerted by a

significant reduction of immune-suppressive cells (like tumor-promoting mast cells and TAMs), together with an increased T cell response[235]. These findings provided the rationale for a synergistic combination of axitinib and ICIs, and the efficacy of this association has been proved in several clinical studies[225,226]. The axitinib-based immunotherapies are now approved as first line setting for mRCC.

In this rapidly evolving scenario, there is still scarcity of evidences concerning the best strategy to adopt in patients that progress after a first line treatment consisting of the association of TKIs and immunotherapy. To date, the second line therapy should be any VEGF target therapy that has not already be used in association with immunotherapy. Therefore, it is imperative to define new tailored approaches able to identify the better treatment to choose among further TKIs, ICIs, or also mTOR inhibitors after a previous axitinib-based first line setting. In this context, preclinical *in vitro* and *in vivo* studies could help identify immunomodulating mechanisms, revealing the molecular and immune context generated by the drug exposure in the tumor and the host.

Our research focused on the investigation of the immunomodulatory effect of axitinib alone or in combination with anti-PD-(L)1 agents on a panel of RCC cell lines and PBMCs, both humane and murine (the latter chosen for the *in vivo* studies). The first assessment consisted of the evaluation of the antiproliferative effect of axitinib on a panel of RCC cells lines both human (769-P and Caki-2) and murine (RENCA): murine cells line proved to be more sensitive to axitinib, with IC_{50} values reduced of about ten folds compared to the concentrations reported for the human cell lines tested after 72 hours of treatment (0.5 mM for RENCA cells versus 5 mM for human cells).
As previously said, several evidences are in favour to an influence of anti-angiogenic treatment on TME[233,235]. Particularly, patients exposed to sunitinib treatment reported an increased PD-L1 expression on tumor cells as well of PD-1 expression on TILs compared to treatment naive patients[236]. On these bases we investigated whether axitinib treatment could impact on PD-L1 expression on RCC cells, confirming that the membrane expression of PD-L1 was increased after axitinib exposure, with a stronger effect on the murine cell line. However, a deeper investigation of the phenomenon through Western Blot analysis and RT-PCR could not support the hypothesis of an increased genic transcription or a stabilization of the protein at a

cytoplasmatic level induced by the axitinib administration. Thus, we hypothesize that PD-L1 increase of expression at a membrane level seems to be correlated to a protein translocation to the membrane induced by the exposure to axitinib. It is worth of note that PD-L1 expression as well as the regulation of the protein stability and its membrane translocation are the result of multiple layers of regulation, that involve a number of regulating proteins as well as the activation of many intracellular signalling pathways[237]. In this complex scenario, recent findings have identified two proteins, members of the CKLF-like MARVEL transmembrane domain-containing family (CMTM) family, CMTM6 and CMTM4, as critical regulators of the cell-surface expression of PD-L1 both in cancer cells as well as in immune cells and whose activity may be modulated after drug exposure[238]. We cannot exclude that this mechanism might be involved in the increased membrane expression of PD-L1 induced by axitinib in RCC cell lines and further investigations are needed to clarify this aspect.

The up-regulation of the membrane level of PD-L1 could represent a "side-effect" of the therapy, as this immune checkpoint has been indicated as the responsible of the lymphocyte exhaustion and its increase after anti-angiogenic treatment could be interpreted as an increase of tumor immune evasion. Nonetheless, PD-L1 is the target of ICIs with anti-PD-1 or anti-PD-L1 antibodies, and consequently an increase of the expression of this protein at a membrane level could induce a greater sensitivity of tumor cells towards ICIs, thereby providing a rationale for the association with anti-PD-L1 agents as avelumab. Avelumab is a monoclonal antibody that targets PD-L1, blocking its interaction with its receptor PD-1, and that is also able to induce antibody-dependent cellular cytotoxicity (ADCC)[239]. ADCC is particularly important as concours to eliminate tumor cells, preventing them a further utilization of alternative immune checkpoints[240]. On the basis of JAVELINRenal101 study, Avelumab association with axitinib has been officially approved in 2019 by EMA and FDA as a first line setting for advanced RCC[225]. Thus, we evaluated the modulation of PD-L1 expression following the combined treatment with axitinib and avelumab. The Western blot analysis of PD-L1 expression revealed that the combinatorial treatment prevented the induction of PD-L1 expression reported when cells were exposed to avelumab alone. It is worth of note that the evaluation of membrane levels of PD-L1 is complicated by the fact that avelumab and the anti-PD-L1 antibody used for detection recognize the same epitope on PD-L1 molecule and compete for the binding site, and this technical aspect hinders the feasibility of the analysis.

The immune system plays a central role in determining the response to therapies ultimately enabling the restoration of an efficient cytotoxic effect against tumor cells. The investigation of sensitivity to axitinib of peripheral blood mononuclear cells (PBMCs) activated *in vitro* underscored that TKIs treatment induces an antiproliferative effect on these cells and, especially in murine PBMCs, a reduction of both $CD4^+$ and $CD8^+$ lymphocytes activity (measured as IFN-g production and as CD25 expression on lymphocytes). Conversely, human PBMCs activity (measured as IFN- g secretion) is not affected by the treatments. On the other hand, the exposure to axitinib alone or in presence of avelumab modulates the expression of co-inhibitory receptors reducing the expression of PD-1 and TIM-3 on $CD4^+$ and of TIM-3 and LAG-3 in $CD8^+$ cells; the reduced expression of immune check point regulators is more pronounced when PBMCs are exposed to the combined treatment with axitinib and avelumab. The reduction of TIM-3 on T cell populations has already been found in glioblastoma patients treated with axitinib, and disease progression was associated with a significantly increase in the number of Tregs and with an augmented level of PD-1 expression on $CD4^+$ and $CD8^+$ T cells[241]. Our findings on PBMCs from healthy donors demonstrate that axitinib alone and to a major extent the combination of axitinib and avelumab can prevent T cell exhaustion.

A better assessment of the immunomodulatory effects of the treatment can be obtained in a co-culture setting. The co-culture allows a more complete overview of the complex panorama of interactions happening between the immune cells and the tumor cells, while remaining an *in vitro* technique. We performed an optimization of the system before studying the full schedule, in order to obtain the optimal conditions to evaluate the interplay between tumor cells and PBMCs. The setting of fundamental parameters comprised the minimum concentration of activating antibodies necessary to obtain a full T cell activation, the PBMC to cancer cell ratio, the use of a transwell system and time of contact. Activated PBMcs release IFN-γ, a well-known inducer of PD-L1 expression, therefore our investigation included the study of the modulation of PD-L1 levels on RENCA cells in the presence or absence of activated PBMCs in a co-culture setting, in parallel with the modulation of PD-1 expression levels on PBMCs induced by the same culturing conditions. The latter is of particular relevance as it is known that PD-1 expression on lymphocytes tends to increase following activation until the eventual exhaustion[242,243], and our findings confirm this trend, underscoring an increase in PD-1 levels on lymphocytes membranes already after 48 hours of co-culture with RENCA cells.

Lastly, the co-culture was performed using the RENCA cells and consequently murine PBMCs, isolated from Balb/c fresh blood and activated *in vitro*. Balb/c mice are syngeneic with RENCA cells, thus preventing an excessive activation of PBMCs against tumor cells. Co-culturing RENCA cells with murine PBMCs we could demonstrate that adding an anti-PD-1 agent to pre-axitinib treated cells enables an increase of the lymphocyte activity (measured as IFN-γ, production), thus significantly inhibiting the tumor cells proliferation. The increase of lymphocyte activity could be related to the binding of the anti-PD-1 agent to the soluble form of PD-L1, whose release by tumor cells in the media has already been reported for other TKIs[208].

These findings underline the immunomodulatory role of TKI (in particular axitinib) both on tumor cells as well as on lymphocytes activation status and exhaustion timing. In particular the negative immunomodulatory effect induced on tumor cells due to the increased expression of membrane PD-L1, could be the reason of a better outcome of anti-PD-1/PD-L1 treatment; on the other hand, the immunostimulatory role of axitinb could enhance the response to immunotherapy.

In the second part of the research, the attention has been focused on the relationship between gut microbiota and RCC. Several arguments are in favour of a role of the intestinal microbiota in oncogenesis and response to therapy and diverse cause-effect relationships have been established between the gut bacteria composition and the clinical outcome in patients and mice.

The first evidence showing a relation between fecal composition and clinical outcome was that cyclophosphamide induces the translocation of immunogenic bacteria (*E. hirae*) that contributes to the elicitation of T cell responses against cancer[170]. This notion was extended to ipilimumab in 2015[244]. Further studies unveiled the association between gut microbiota composition and response to anti-cancer therapy in patients. The observation that antibiotic treatment hinders immunotherapy efficacy for RCC and Non-Small Cell Lung Cancer (NSCLC) patients[220] paved the way to a deeper investigation of the role of microbiota in the response to immunotherapy. The discovery that gut microbiota composition, independently of treatment type (chemotherapy, radiotherapy, TKIs, immunotherapy), drives patients' outcome to therapy represented a milestone[164,165,167,245]. Among beneficial commensals associated to a better outcome to therapy, emerged *E. hirae*, *A. senegalensis* and *A.*

muciniphila that elicit an adaptive immune response beneficial against RCC[164,167]. In 2022 came the validation of the predictive role of *A. muciniphila* in NSCLC patients: *A. muciniphila* presence in patients gut before the beginning of the anti-PD-1 treatment was associated with a better overall response rate and to a better overall survival regardless of PD-L1 expression[245].

Overall, it appears that a dysbiotic microbiota composition enriched in *Enteroclaster gen*, lacking immunostimulatory bacteria or overrepresenting harmful species causes treatment failure.

In this context, we aimed to evaluate the gut microbiota modulation and impact on the efficacy of standard therapies used for advanced RCC treatment, as whether gut microbiota can be used as a decision variable to define sequence is still unknown. The observation that TKIs treatment induces a prototypic microbiota shift that favors some immunostimulatory commensals as *A. senegalensis* and *A. muciniphila* was demonstrated both in *in vivo* preclinical experiemnts on Balb/c and C57BL/6 mice and by the analysis of stool specimens of RCC patients that received TKIs as first line treatment[167]. On these bases we evaluated whether standard therapies could induce a taxonomic deviation of stool composition in Balb/c mice treated with a sequential approach that mimics the first- and second-line standard approaches adopted for RCC. A perturbation of the taxonomic composition of mice microbiota induced by standard therapy could additionally impact on the efficacy of these therapies against RCC. This impacts on the outcome of RCC patients, as a eubiotic gut can contribute to a later benefit to immunotherapy[167]. A further validation of the effect induced by the antibiotic treatment on tumor growth, confirmed even in the mice model, is the observation that pre-treatment with broad spectrum antibiotics has a detrimental effect on tumor growth, preventing the spontaneous remission, corroborating the clinical observations[220].

Akkermansia muciniphila has been broadly recognized as an immunostimulatory commensal whose abundance can impact the efficacy of anti-cancer treatments[164,167,245]. We already discussed that its abundance can be induced by TKIs treatments that could improve the efficacy of subsequent ICIs, therefore we investigated the possibility to restore the immunotherapy effect in a non-responder avatar mouse phenotype, supplementing mice with this regulatory bacterium. The fecal microbiota transplantation (FMT) has been proven to efficaciously transform mice into patients' "avatars" through the implantation in mice gut of patients intestinal microbiota[164,165,167,245]. Interestingly, among the different A. muciniphila

strains, the more prevalent across human stools was the SGB9226[245], whose abundance has been demonstrated to be related to ICIs outcome in NSCLC patients. On this basis we aimed to provide the proof-of-concept that *Akkermansia spp* can restore eubiosis and increase response to standard therapy *in vivo*. We tested two additional Akkermansia strains, SGB5801 and SGB9228 in a NR (NR: OS<24 months, absence of *Akkermansia* in the stool specimen) avatar model. We provided evidence that a supplementation of *Akkermansia* SGB9226 and the rarer strain SGB9228 tended to increase the benefit of the combination of ICIs in terms of tumor growth and survival, in a NR avatar model. These evidences suggested that an implementation of *Akkermansia* to the standard ICI treatment, or an evaluation of the gut microbiota composition could represent a valuable tool to stratify patients.

CONCLUSION AND FUTURE PERSPECTIVES

To conclude, our investigation demonstrated that axitinib, by increasing the expression of PD-L1 on cell surfaces, has a role in modulating the antitumoral immune response. In addition, in a co-culture setting that allow us to further explore the complex interactions occurring between tumor cells and immune system, we provided evidence of the grater anti-proliferative efficacy of the combined treatment of axitinib and ICIs directed against the PD-1/PD-L1 axis compared to single treatments.

The investigation of the microbiota role as a potential hint to identify the best sequential treatment for RCC led us to corroborate the observation that antibiotic treatment has a negative impact on tumor growth and prevents remission in a validated preclinical model for RCC. Conversely, the enrichment of beneficial commensal *Akkermansia muciniphila* in non-responders patients "avatar" mice models seemed to show a tendence in reduce tumor growth. Overall, these evidences suggest that microbiota modulation could represent an additional clinical tool to identify patients that will later benefit more from following therapies.

These represent the premises for the last phase of the study: the setting of an in vivo pre-clinical study on Balb/c mice injected with RENCA cells in order to test the therapeutic sequence after axitinib-based immuno-therapeutic combinations and to lately identify parameters that would help future clinical chioces.

BIBLIOGRAPHY

1. Padala SA, Barsouk A, Thandra KC, et al. Epidemiology of renal cell carcinoma. *World J Oncol*. 2020;11(3):79-87. doi:10.14740/WJON1279
2. Sung H, Ferlay J, Siegel RL, et al. Global Cancer Statistics 2020: GLOBOCAN Estimates of Incidence and Mortality Worldwide for 36 Cancers in 185 Countries. *CA Cancer J Clin*. 2021;71(3):209-249. doi:10.3322/caac.21660
3. D'Avella C, Abbosh P, Pal SK, Geynisman DM. Mutations in renal cell carcinoma. *Urol Oncol Semin Orig Investig*. 2020;38(10):763-773. doi:10.1016/j.urolonc.2018.10.027
4. Moch H, Cubilla AL, Humphrey PA, Reuter VE, Ulbright TM. The 2016 WHO Classification of Tumours of the Urinary System and Male Genital Organs—Part A: Renal, Penile, and Testicular Tumours. *Eur Urol*. 2016;70(1):93-105. doi:10.1016/j.eururo.2016.02.029
5. Hsieh JJ, Purdue MP, Signoretti S, et al. Renal cell carcinoma. *Nat Rev Dis Prim*. 2017;3:1-19. doi:10.1038/nrdp.2017.9
6. Díaz-Montero CM, Rini BI, Finke JH. The immunology of renal cell carcinoma. *Nat Rev Nephrol*. 2020;16(12):721-735. doi:10.1038/s41581-020-0316-3
7. Choueiri TK, Motzer RJ. Systemic Therapy for Metastatic Renal-Cell Carcinoma. *N Engl J Med*. 2017;376(4):354-366. doi:10.1056/NEJMra1601333
8. Siegel RL, Miller KD, Fuchs HE, Jemal A. Cancer Statistics, 2021. *CA Cancer J Clin*. 2021;71(1):7-33. doi:10.3322/caac.21654
9. Testa U, Pelosi E, Castelli G. Genetic Alterations in Renal Cancers: Identification of The Mechanisms Underlying Cancer Initiation and Progression and of Therapeutic Targets. *Medicines*. 2020;7(8):44. doi:10.3390/medicines7080044
10. Qi X, Li Q, Che X, Wang Q, Wu G. The Uniqueness of Clear Cell Renal Cell Carcinoma: Summary of the Process and Abnormality of Glucose Metabolism and Lipid Metabolism in ccRCC. *Front Oncol*. 2021;11. doi:10.3389/fonc.2021.727778
11. Capitanio U, Bensalah K, Bex A, et al. Epidemiology of Renal Cell Carcinoma [Figure presented]. *Eur Urol*. 2019;75(1):74-84. doi:10.1016/j.eururo.2018.08.036
12. SEER cancer statistics 1975-2017.
13. Kabaria R, Klaassen Z, Terris MK. Renal cell carcinoma: Links and risks. *Int J Nephrol Renovasc Dis*. 2016;9:45-52. doi:10.2147/IJNRD.S75916
14. Chittiboina P, Lonser RR. Von Hippel-Lindau disease. In: *Handbook of Clinical Neurology*. Vol 132. Elsevier B.V.; 2015:139-156. doi:10.1016/B978-0-444-62702-5.00010-X
15. Linehan WM, Schmidt LS, Crooks DR, et al. The metabolic basis of kidney cancer. *Cancer Discov*. 2019;9(8):1006-1021. doi:10.1158/2159-8290.CD-18-1354
16. Menko FH, Maher ER, Schmidt LS, et al. Hereditary leiomyomatosis and renal cell cancer (HLRCC): renal cancer risk, surveillance and treatment. *Fam Cancer*. 2014;13(4):637-644. doi:10.1007/s10689-014-9735-2

17. Hunt JD, Van Der Hel OL, McMillan GP, Boffetta P, Brennan P. Renal cell carcinoma in relation to cigarette smoking: Meta-analysis of 24 studies. *Int J Cancer*. 2005;114(1):101-108. doi:10.1002/ijc.20618
18. Keizman D, Gottfried M, Ish-Shalom M, et al. Active Smoking May Negatively Affect Response Rate, Progression-Free Survival, and Overall Survival of Patients With Metastatic Renal Cell Carcinoma Treated With Sunitinib. *Oncologist*. 2014;19(1):51-60. doi:10.1634/theoncologist.2012-0335
19. Patel NH, Attwood KM, Hanzly M, et al. Comparative analysis of smoking as a risk factor among renal cell carcinoma histological subtypes. *J Urol*. 2015;194(3):640-646. doi:10.1016/j.juro.2015.03.125
20. Budny A, Grochowski C, Kozłowski P, et al. Obesity as a tumour development triggering factor. *Ann Agric Environ Med*. 2019;26(1):13-23. doi:10.26444/aaem/100664
21. Bergström A, Hsieh C-C, Lindblad P, Lu C-M, Cook NR, Wolk A. Obesity and renal cell cancer – a quantitative review. *Br J Cancer*. 2001;85(7):984-990. doi:10.1054/bjoc.2001.2040
22. Esmaeili S, Davoodi SH, Malek-Shahabi T, Malekshahi-Moghadam A, Shahbazi R. *Certain Types of Cancer*. Vol 4.; 2013.
23. Bhaskaran K, Douglas I, Forbes H, dos-Santos-Silva I, Leon DA, Smeeth L. Body-mass index and risk of 22 specific cancers: a population-based cohort study of 5·24 million UK adults. *Lancet*. 2014;384(9945):755-765. doi:10.1016/S0140-6736(14)60892-8
24. Hursting SD, Dunlap SM. Obesity, metabolic dysregulation, and cancer: A growing concern and an inflammatory (and microenvironmental) issue. *Ann N Y Acad Sci*. 2012;1271(1):82-87. doi:10.1111/j.1749-6632.2012.06737.x
25. Stone TW, McPherson M, Gail Darlington L. Obesity and Cancer: Existing and New Hypotheses for a Causal Connection. *EBioMedicine*. 2018;30:14-28. doi:10.1016/j.ebiom.2018.02.022
26. Turco F, Tucci M, Di Stefano RF, et al. Renal cell carcinoma (RCC): Fatter is better? A review on the role of obesity in RCC. *Endocr Relat Cancer*. 2021;28(7):R207-R216. doi:10.1530/ERC-20-0457
27. Albiges L, Ari Hakimi A, Xie W, et al. Body mass index and metastatic renal cell carcinoma: Clinical and biological correlations. *J Clin Oncol*. 2016;34(30):3655-3663. doi:10.1200/JCO.2016.66.7311
28. Bergerot PG, Bergerot CD, Philip EJ, et al. Targeted therapy and immunotherapy: Effect of body mass index on clinical outcomes in patients diagnosed with metastatic renal cell carcinoma. *Kidney Cancer*. 2019;3(1):63-70. doi:10.3233/KCA-180047
29. Sanchez A, Furberg H, Kuo F, et al. Transcriptomic signatures related to the obesity paradox in patients with clear cell renal cell carcinoma: a cohort study. *Lancet Oncol*. 2020;21(2):283-293. doi:10.1016/S1470-2045(19)30797-1
30. Behrens G, Leitzmann MF. The association between physical activity and renal cancer: Systematic review and meta-analysis. *Br J Cancer*. 2013;108(4):798-811. doi:10.1038/bjc.2013.37
31. Liu B, Mao Q, Wang X, et al. Cruciferous vegetables consumption and risk of renal cell carcinoma: A meta-analysis. *Nutr Cancer*. 2013;65(5):668-676. doi:10.1080/01635581.2013.795980
32. Heng DYC, Xie W, Regan MM, et al. External validation and comparison with other models of the International Metastatic Renal-Cell Carcinoma Database Consortium prognostic model: A population-based study. *Lancet Oncol*. 2013;14(2):141-148. doi:10.1016/S1470-2045(12)70559-4

33. Weikert S, Boeing H, Pischon T, et al. Fruits and vegetables and renal cell carcinoma: Findings from the European Prospective Investigation into Cancer and Nutrition (EPIC). *Int J Cancer*. 2006;118(12):3133-3139. doi:10.1002/ijc.21765
34. MacLeod LC, Hotaling JM, Wright JL, et al. Risk factors for renal cell carcinoma in the VITAL study. *J Urol*. 2013;190(5):1657-1661. doi:10.1016/j.juro.2013.04.130
35. Rumgay H, Murphy N, Ferrari P, Soerjomataram I. Alcohol and cancer: Epidemiology and biological mechanisms. *Nutrients*. 2021;13(9). doi:10.3390/nu13093173
36. International Agency for Research on Cancer. Agents classified by the IARC monographs. *Igarss 2014*. 2012;1-105(1):1-5.
37. Lee JE, Hunter DJ, Spiegelman D, et al. Alcohol intake and renal cell cancer in a pooled analysis of 12 prospective studies. *J Natl Cancer Inst*. 2007;99(10):801-810. doi:10.1093/jnci/djk181
38. Pelucchi C, Galeone C, Montella M, et al. Alcohol consumption and renal cell cancer risk in two Italian case-control studies. *Ann Oncol*. 2008;19(5):1003-1008. doi:10.1093/annonc/mdm590
39. Chow W-H, Dong LM, Devesa SS. Epidemiology and risk factors for kidney cancer. *Nat Rev Urol*. 2010;7(5):245-257. doi:10.1038/nrurol.2010.46
40. Hidayat K, Du X, Zou SY, Shi BM. Blood pressure and kidney cancer risk: Meta-analysis of prospective studies. *J Hypertens*. 2017;35(7):1333-1344. doi:10.1097/HJH.0000000000001286
41. Sanfilippo KM, Mctigue KM, Fidler CJ, et al. Hypertension and Obesity and the Risk of Kidney Cancer in 2 Large Cohorts of US Men and Women Epidemiology/Population. *Abingt Meml Hosp*. 2014. doi:10.1161/HYPERTENSIONAHA
42. Larsson SC, Wolk A. Diabetes mellitus and incidence of kidney cancer: A meta-analysis of cohort studies. *Diabetologia*. 2011;54(5):1013-1018. doi:10.1007/s00125-011-2051-6
43. Harding JL, Shaw JE, Peeters A, Cartensen B, Magliano DJ. Cancer risk among people with type 1 and type 2 diabetes: Disentangling true associations, detection bias, and reverse causation. *Diabetes Care*. 2015;38(2):264-270. doi:10.2337/dc14-1996
44. Pearson-Stuttard J, Zhou B, Kontis V, Bentham J, Gunter MJ, Ezzati M. *Articles Worldwide Burden of Cancer Attributable to Diabetes and High Body-Mass Index: A Comparative Risk Assessment*. Vol 6.; 2018. www.thelancet.com/.
45. Scelo G, Larose TL. JOURNAL OF CLINICAL ONCOLOGY Epidemiology and Risk Factors for Kidney Cancer. *J Clin Oncol*. 2018;36:3574-3581. doi:10.1200/JCO.2018
46. Karami S, Lan Q, Rothman N, et al. Occupational trichloroethylene exposure and kidney cancer risk: A meta-analysis. *Occup Environ Med*. 2012;69(12):858-867. doi:10.1136/oemed-2012-100932
47. Inamura K. Renal cell tumors: Understanding their molecular pathological epidemiology and the 2016 WHO classification. *Int J Mol Sci*. 2017;18(10). doi:10.3390/ijms18102195
48. Muglia VF, Prando A. Renal cell carcinoma: Histological classification and correlation with imaging findings. *Radiol Bras*. 2015;48(3):166-174. doi:10.1590/0100-3984.2013.1927
49. Moch H, Amin MB, Berney DM, et al. The 2022 World Health Organization Classification of Tumours of the Urinary System and Male Genital Organs—Part A: Renal, Penile, and Testicular Tumours. *Eur Urol*.

2022;82(5):458-468. doi:10.1016/j.eururo.2022.06.016

50. Delahunt B, Eble JN, Samaratunga H, Thunders M, Yaxley JW, Egevad L. Staging of renal cell carcinoma: current progress and potential advances. *Pathology*. 2021;53(1):120-128. doi:10.1016/j.pathol.2020.08.007
51. Ljungberg B, Albiges L, Abu-Ghanem Y, et al. European Association of Urology Guidelines on Renal Cell Carcinoma: The 2022 Update. *Eur Urol*. 2022;82(4):399-410. doi:10.1016/j.eururo.2022.03.006
52. Pass H, Giroux D, Kennedy C, et al. The IASLC Mesothelioma Staging Project: Improving Staging of a Rare Disease Through International Participation. *J Thorac Oncol*. 2016;11(12):2082-2088. doi:10.1016/j.jtho.2016.09.123
53. Weprin S, Falagario U, Veccia A, et al. Simplified PADUA Renal (SPARE) Nephrometry Scoring System: External Validation, Interobserver Variability, and Comparison with RENAL and PADUA in a Single-center Robotic Partial Nephrectomy Series. *Eur Urol Focus*. 2021;7(3):591-597. doi:10.1016/j.euf.2020.05.016
54. Carteni G. Linee guida AIOM 2019: Tumori al rene. *Assoc Ital di Oncol Medica*. 2019:104.
55. Volpe A, Patard JJ. Prognostic factors in renal cell carcinoma. *World J Urol*. 2010;28(3):319-327. doi:10.1007/s00345-010-0540-8
56. Ficarra V, Righetti R, Martignoni G, et al. *Prognostic Value of Renal Cell Carcinoma Nuclear Grading: Multivariate Analysis of 333 Cases*. Vol 67.; 2001. www.karger.comwww.karger.com/journals/uin.
57. Delahunt B, Sika-Paotonu D, Bethwaite PB, et al. *Fuhrman Grading Is Not Appropriate for Chromophobe Renal Cell Carcinoma*.; 2007.
58. Wagener N, Edelmann D, Benner A, et al. Outcome of papillary versus clear cell renal cell carcinoma varies significantly in non-metastatic disease. *PLoS One*. 2017;12(9). doi:10.1371/journal.pone.0184173
59. Grivas N, Kafarakis V, Tsimaris I, Raptis P, Hastazeris K, Stavropoulos NE. Clinico-pathological prognostic factors of renal cell carcinoma: A 15-year review from a single center in Greece. *Urol Ann*. 2014;6(2):116-121. doi:10.4103/0974-7796.130552
60. Guida A, Le Teuff G, Alves C, et al. *Identification of International Metastatic Renal Cell Carcinoma Database Consortium (IMDC) Intermediate-Risk Subgroups in Patients with Metastatic Clear-Cell Renal Cell Carcinoma*. Vol 11.; 2020. www.oncotarget.com.
61. Heng DYC, Xie W, Regan MM, et al. Prognostic factors for overall survival in patients with metastatic renal cell carcinoma treated with vascular endothelial growth factor-targeted agents: Results from a large, multicenter study. *J Clin Oncol*. 2009;27(34):5794-5799. doi:10.1200/JCO.2008.21.4809
62. Kohn L, Svenson U, Ljungberg B, Roos G. *Specific Genomic Aberrations Predict Survival, But Low Mutation Rate in Cancer Hot Spots, in Clear Cell Renal Cell Carcinoma*.; 2014. www.appliedimmunohist.com.
63. Sekido Y. Molecular Genetics of Malignant Mesothelioma. In: *ELS*. ; 2012. doi:https://doi.org/10.1002/9780470015902.a0022448
64. Gulati S, Martinez P, Joshi T, et al. Systematic evaluation of the prognostic impact and intratumour heterogeneity of clear cell renal cell carcinoma biomarkers. *Eur Urol*. 2014;66(5):936-948. doi:10.1016/j.eururo.2014.06.053
65. Joseph RW, Kapur P, Serie DJ, et al. Clear Cell Renal Cell Carcinoma Subtypes Identified by BAP1 and

PBRM1 Expression. *J Urol*. 2016;195(1):180-187. doi:10.1016/j.juro.2015.07.113

66. Iacovelli R, Nolè F, Verri E, et al. Prognostic Role of PD-L1 Expression in Renal Cell Carcinoma. A Systematic Review and Meta-Analysis. *Target Oncol*. 2016;11(2):143-148. doi:10.1007/s11523-015-0392-7
67. Carretero−González A, Lora D, Sobrino IM, et al. The value of pd-l1 expression as predictive biomarker in metastatic renal cell carcinoma patients: A meta-analysis of randomized clinical trials. *Cancers (Basel)*. 2020;12(7):1-16. doi:10.3390/cancers12071945
68. McDermott DF, Huseni MA, Atkins MB, et al. Clinical activity and molecular correlates of response to atezolizumab alone or in combination with bevacizumab versus sunitinib in renal cell carcinoma. *Nat Med*. 2018;24(6):749-757. doi:10.1038/s41591-018-0053-3
69. Motzer RJ, Robbins PB, Powles T, et al. Avelumab plus axitinib versus sunitinib in advanced renal cell carcinoma: biomarker analysis of the phase 3 JAVELIN Renal 101 trial. *Nat Med*. 2020;26(11):1733-1741. doi:10.1038/s41591-020-1044-8
70. Sun R, Breau RH, Mallick R, et al. Prognostic impact of paraneoplastic syndromes on patients with non-metastatic renal cell carcinoma undergoing surgery: Results from canadian kidney cancer information system. *Can Urol Assoc J*. 2021;15(4):0-5. doi:10.5489/CUAJ.6833
71. Escudier B, Porta C, Schmidinger M, et al. Renal cell carcinoma: ESMO Clinical Practice Guidelines for diagnosis, treatment and follow-up. *Ann Oncol*. 2019;30(5):706-720. doi:10.1093/annonc/mdz056
72. Vaupel P, Mayer A. Hypoxia in cancer: Significance and impact on clinical outcome. *Cancer Metastasis Rev*. 2007;26(2):225-239. doi:10.1007/s10555-007-9055-1
73. Banumathy G, Cairns P. Signaling pathways in renal cell carcinoma. *Cancer Biol Ther*. 2010;10(7):658-664. doi:10.4161/cbt.10.7.13247
74. Hoerner CR, Miao SY, Hsieh JJ, Fan AC. *Targeting Metabolic Pathways in Kidney Cancer Rationale and Therapeutic Opportunities*.; 2020. www.journalppo.com.
75. Clark PE. The role of VHL in clear-cell renal cell carcinoma and its relation to targeted therapy. *Kidney Int*. 2009;76(9):939-945. doi:10.1038/ki.2009.296
76. Linehan WM, Srinivasan R, Schmidt LS. The genetic basis of kidney cancer: A metabolic disease. *Nat Rev Urol*. 2010;7(5):277-285. doi:10.1038/nrurol.2010.47
77. Masoud GN, Li W. HIF-1α pathway: Role, regulation and intervention for cancer therapy. *Acta Pharm Sin B*. 2015;5(5):378-389. doi:10.1016/j.apsb.2015.05.007
78. Stanca Melincovici C, Boşca AB, Şuşman S, et al. Vascular endothelial growth factor (VEGF)-key factor in normal and pathological angiogenesis. *Rom J Morphol Embryol*. 2018;59(2):455-467. http://www.rjme.ro/.
79. Yang J, Yan J, Liu B. Targeting VEGF/VEGFR to modulate antitumor immunity. *Front Immunol*. 2018;9(MAY):1-9. doi:10.3389/fimmu.2018.00978
80. Hamrah P, Chen L, Cursiefen C, Zhang Q, Joyce NC, Dana MR. Expression of vascular endothelial growth factor receptor-3 (VEGFR-3) on monocytic bone marrow-derived cells in the conjunctiva. *Exp Eye Res*. 2004;79(4):553-561. doi:10.1016/j.exer.2004.06.028
81. Ferrara N. Vascular endothelial growth factor: Basic science and clinical progress. *Endocr Rev*.

2004;25(4):581-611. doi:10.1210/er.2003-0027

82. Takahashi H, Shibuya M. The vascular endothelial growth factor (VEGF)/VEGF receptor system and its role under physiological and pathological conditions. *Clin Sci*. 2005;109(3):227-241. doi:10.1042/CS20040370

83. Koch S, Claesson-Welsh L. Signal transduction by vascular endothelial growth factor receptors. *Cold Spring Harb Perspect Med*. 2012;2(7). doi:10.1101/cshperspect.a006502

84. Hoeben A, Landuyt B, Highley MS, Wildiers H, Van Oosterom AT, De Bruijn EA. Vascular endothelial growth factor and angiogenesis. *Pharmacol Rev*. 2004;56(4):549-580. doi:10.1124/pr.56.4.3

85. Selvaraj SK, Giri RK, Perelman N, Johnson C, Malik P, Kalra VK. Mechanism of monocyte activation and expression of proinflammatory cytochemokines by placenta growth factor. *Blood*. 2003;102(4):1515-1524. doi:10.1182/blood-2002-11-3423

86. Kim WU, Yoo SA, Kwok SK. Proinflammatory role of vascular endothelial growth factor in the pathogenesis of rheumatoid arthritis: Prospects for therapeutic intervention. *Mediators Inflamm*. 2008;2008. doi:10.1155/2008/129873

87. Denko NC. Hypoxia, HIF and metabolism in the solid tumour. *Nat Rev Cancer*. 2008;8(September):705-713.

88. Buti S, Leonetti A, Dallatomasina A, Bersanelli M. Everolimus in the management of metastatic renal cell carcinoma: An evidence-based review of its place in therapy. *Core Evid*. 2016;11:23-36. doi:10.2147/CE.S98687

89. Cantor JR, Sabatini DM. Cancer cell metabolism: One hallmark, many faces. *Cancer Discov*. 2012;2(10):881-898. doi:10.1158/2159-8290.CD-12-0345

90. Kennedy SG, Kandel ES, Cross TK, Hay N. Akt/Protein kinase B inhibits cell death by preventing the release of cytochrome c from mitochondria. *Mol Cell Biol*. 1999;19(8):5800-5810. doi:10.1128/MCB.19.8.5800

91. Mayo LD, Donner DB. The PTEN, Mdm2, p53 tumor suppressor-oncoprotein network. *Trends Biochem Sci*. 2002;27(9):462-467. doi:10.1016/s0968-0004(02)02166-7

92. Zhou BP, Hung M-C. Novel targets of Akt, p21Cip1/WAF1, and MDM2. *Semin Oncol*. 2002;29(3, Supplement 11):62-70. doi:https://doi.org/10.1016/S0093-7754(02)70128-0

93. Liang J, Slingerland JM. Multiple roles of the PI3K/PKB (Akt) pathway in cell cycle progression. *Cell Cycle*. 2003;2(4):339-345.

94. Bellacosa A, Kumar CC, Di Cristofano A, Testa JR. Activation of AKT kinases in cancer: implications for therapeutic targeting. *Adv Cancer Res*. 2005;94:29-86. doi:10.1016/S0065-230X(05)94002-5

95. Muise-Helmericks RC, Grimes HL, Bellacosa A, Malstrom SE, Tsichlis PN, Rosen N. Cyclin D expression is controlled post-transcriptionally via a phosphatidylinositol 3-kinase/Akt-dependent pathway. *J Biol Chem*. 1998;273(45):29864-29872. doi:10.1074/jbc.273.45.29864

96. Yang H, Rudge DG, Koos JD, Vaidialingam B, Yang HJ, Pavletich NP. mTOR kinase structure, mechanism and regulation. *Nature*. 2013;497(7448):217-223. doi:10.1038/nature12122

97. Liu P, Gan W, Chin YR, et al. PtdIns(3,4,5)P3-Dependent Activation of the mTORC2 Kinase Complex. *Cancer Discov*. 2015;5(11):1194-1209. doi:10.1158/2159-8290.CD-15-0460

98. Altomare DA, Testa JR. Perturbations of the AKT signaling pathway in human cancer. *Oncogene*. 2005;24(50):7455-7464. doi:10.1038/sj.onc.1209085

99. Laplante M, Sabatini DM. mTOR signaling in growth control and disease. *Cell*. 2012;149(2):274-293. doi:10.1016/j.cell.2012.03.017

100. Huber TB, Walz G, Kuehn EW. mTOR and rapamycin in the kidney: signaling and therapeutic implications beyond immunosuppression. *Kidney Int*. 2011;79(5):502-511. doi:10.1038/ki.2010.457

101. Jiang N, Dai Q, Su X, Fu J, Feng X, Peng J. Role of PI3K/AKT pathway in cancer: the framework of malignant behavior. *Mol Biol Rep*. 2020;47(6):4587-4629. doi:10.1007/s11033-020-05435-1

102. Hakimi AA, Reznik E, Lee CH, et al. An Integrated Metabolic Atlas of Clear Cell Renal Cell Carcinoma. *Cancer Cell*. 2016;29(1):104-116. doi:10.1016/j.ccell.2015.12.004

103. Gameiro PA, Yang J, Metelo AM, et al. In vivo HIF-mediated reductive carboxylation is regulated by citrate levels and sensitizes VHL-deficient cells to glutamine deprivation. *Cell Metab*. 2013;17(3):372-385. doi:10.1016/j.cmet.2013.02.002

104. Creighton CJ, Morgan M, Gunaratne PH, et al. Comprehensive molecular characterization of clear cell renal cell carcinoma. *Nature*. 2013;499(7456):43-49. doi:10.1038/nature12222

105. Matthew G. Vander Heiden, Lewis C. Cantley and CBT. Understanding the Warburg Effect: The Metabolic Requirements of Cell Proliferation. *Science (80-)*. 2009;324(5930):3828-3828. doi:10.1007/978-3-540-29678-2_5605

106. Linehan WM, Srinivasan R, Schmidt LS. The genetic basis of kidney cancer: A metabolic disease. *Nat Rev Urol*. 2010;7(5):277-285. doi:10.1038/nrurol.2010.47

107. Mier JW. The tumor microenvironment in renal cell cancer. *Curr Opin Oncol*. 2019;31(3):194-199. doi:10.1097/CCO.0000000000000512

108. Fridman WH, Zitvogel L, Sautès-Fridman C, Kroemer G. The immune contexture in cancer prognosis and treatment. *Nat Rev Clin Oncol*. 2017;14(12):717-734. doi:10.1038/nrclinonc.2017.101

109. Fridman WH, Galon J, Pagès F, Tartour E, Sautès-Fridman C, Kroemer G. Prognostic and predictive impact of intra- and peritumoral immune infiltrates. *Cancer Res*. 2011;71(17):5601-5605. doi:10.1158/0008-5472.CAN-11-1316

110. Fridman WH, Pagès F, Sautès-Fridman C, Galon J. The immune contexture in human tumours: Impact on clinical outcome. *Nat Rev Cancer*. 2012;12(4):298-306. doi:10.1038/nrc3245

111. Giraldo NA, Becht E, Vano Y, et al. Tumor-infiltrating and peripheral blood T-cell immunophenotypes predict early relapse in localized clear cell renal cell carcinoma. *Clin Cancer Res*. 2017;23(15):4416-4428. doi:10.1158/1078-0432.CCR-16-2848

112. Thompson RH, Dong H, Lohse CM, et al. PD-1 is expressed by tumor-infiltrating immune cells and is associated with poor outcome for patients with renal cell carcinoma. *Clin Cancer Res*. 2007;13(6):1757-1761. doi:10.1158/1078-0432.CCR-06-2599

113. Yoshihara K, Shahmoradgoli M, Martínez E, et al. Inferring tumour purity and stromal and immune cell admixture from expression data. *Nat Commun*. 2013;4. doi:10.1038/ncomms3612

114. Zhang S, Zhang E, Long J, et al. Immune infiltration in renal cell carcinoma. *Cancer Sci*. 2019;110(5):1564-

1572. doi:10.1111/cas.13996

115. Bukur J, Jasinski S, Seliger B. The role of classical and non-classical HLA class I antigens in human tumors. *Semin Cancer Biol*. 2012;22(4):350-358. doi:10.1016/j.semcancer.2012.03.003

116. Dunker K, Schlaf G, Bukur J, Altermann WW, Handke D, Seliger B. Expression and regulation of non-classical HLA-G in renal cell carcinoma. *Tissue Antigens*. 2008;72(2):137-148. doi:10.1111/j.1399-0039.2008.01090.x

117. Seliger B, Jasinski-Bergner S, Quandt D, et al. *HLA-E Expression and Its Clinical Relevance in Human Renal Cell Carcinoma*. Vol 7.; 2016. www.impactjournals.com/oncotarget.

118. Chevrier S, Levine JH, Zanotelli VRT, et al. An Immune Atlas of Clear Cell Renal Cell Carcinoma. *Cell*. 2017;169(4):736-749.e18. doi:10.1016/j.cell.2017.04.016

119. Kotecha RR, Motzer RJ, Voss MH. Towards individualized therapy for metastatic renal cell carcinoma. *Nat Rev Clin Oncol*. 2019;16(10):621-633. doi:10.1038/s41571-019-0209-1

120. Dyck L, Mills KHG, Dyck L, Mills KHG. Immune checkpoints and their inhibition in cancer and infectious diseases. 2017:765-779. doi:10.1002/eji.201646875

121. Topalian SL, Drake CG, Pardoll DM. Immune checkpoint blockade: A common denominator approach to cancer therapy. *Cancer Cell*. 2015;27(4):450-461. doi:10.1016/j.ccell.2015.03.001

122. Leach DR, Krummel MF, Allison JP. *Enhancement of Antitumor Immunity by CTLA-4 Blockade*. Vol 271.; 1996.

123. Pardoll DM. The blockade of immune checkpoints in cancer immunotherapy. *Nat Rev Cancer*. 2012;12(4):252-264. doi:10.1038/nrc3239

124. Topalian SL. Targeting Immune Checkpoints in Cancer Therapy. *JAMA*. 2017;318(17):1647-1648. doi:10.1001/jama.2017.14155

125. Cha J-H, Chan L-C, Li C-W, Hsu JL, Hung M-C. Mechanisms Controlling PD-L1 Expression in Cancer. *Mol Cell*. 2019;76(3):359-370. doi:10.1016/j.molcel.2019.09.030

126. Yi M, Niu M, Xu L, Luo S, Wu K. Regulation of PD-L1 expression in the tumor microenvironment. *J Hematol Oncol*. 2021;14(1):10. doi:10.1186/s13045-020-01027-5

127. Prestipino A, Emhardt AJ, Aumann K, et al. Oncogenic JAK2(V617F) causes PD-L1 expression, mediating immune escape in myeloproliferative neoplasms. *Sci Transl Med*. 2018;10(429). doi:10.1126/scitranslmed.aam7729

128. Díaz-Montero CM, Rini BI, Finke JH. The immunology of renal cell carcinoma. *Nat Rev Nephrol*. 2020. doi:10.1038/s41581-020-0316-3

129. Dang C V, Le A, Gao P. MYC-induced cancer cell energy metabolism and therapeutic opportunities. *Clin cancer Res an Off J Am Assoc Cancer Res*. 2009;15(21):6479-6483. doi:10.1158/1078-0432.CCR-09-0889

130. Sun C, Mezzadra R, Schumacher TN. Europe PMC Funders Group Regulation and Function of the PD-L1 Checkpoint. 2020;48(3):434-452. doi:10.1016/j.immuni.2018.03.014.Regulation

131. Marzec M, Zhang Q, Goradia A, et al. Oncogenic kinase NPM/ALK induces through STAT3 expression of immunosuppressive protein CD274 (PD-L1, B7-H1). *Proc Natl Acad Sci U S A*. 2008;105(52):20852-20857. doi:10.1073/pnas.0810958105

132. Ota K, Azuma K, Kawahara A, et al. Induction of PD-L1 expression by the EML4-ALK oncoprotein and down stream signaling pathways in non-small cell lung cancer. *Clin Cancer Res*. 2015;21(17):4014-4021. doi:10.1158/1078-0432.CCR-15-0016

133. Sharpe AH, Pauken KE. The diverse functions of the PD1 inhibitory pathway. *Nat Rev Immunol*. 2018;18(3):153-167. doi:10.1038/nri.2017.108

134. Zhu X, Lang J. Soluble PD-1 and PD-L1 : predictive and prognostic significance in cancer. 2017;8(57):97671-97682.

135. Choueiri TK, Fishman MN, Escudier B, et al. Immunomodulatory activity of nivolumab in metastatic renal cell carcinoma (mRCC): Association of biomarkers with clinical outcomes. *J Clin Oncol*. 2015;33(15_suppl):4500. doi:10.1200/jco.2015.33.15_suppl.4500

136. Motzer RJ, Escudier B, McDermott DF, et al. Nivolumab versus Everolimus in Advanced Renal-Cell Carcinoma. *N Engl J Med*. 2015;373(19):1803-1813. doi:10.1056/nejmoa1510665

137. Eichenauer T, Simmendinger L, Fraune C, et al. High level of EZH2 expression is linked to high density of CD8-positive T-lymphocytes and an aggressive phenotype in renal cell carcinoma. *World J Urol*. 2021;39(2):481-490. doi:10.1007/s00345-020-03200-4

138. Walter B, Gil S, Naizhen X, et al. Determination of the expression of PD-L1 in the morphologic spectrum of renal cell carcinoma. *J Cancer*. 2020;11(12):3596-3603. doi:10.7150/jca.35738

139. Chandrasekaran D, Sundaram S, Kadhiresan N, Padmavathi R. Programmed Death Ligand 1; An immunotarget for renal cell carcinoma. *Asian Pacific J Cancer Prev*. 2019;20(10):2951-2957. doi:10.31557/APJCP.2019.20.10.2951

140. Basu A, Yearley JH, Annamalai L, Pryzbycin C, Rini B. Association of PD-L1, PD-L2, and immune response markers in matched renal clear cell carcinoma primary and metastatic tissue specimens. *Am J Clin Pathol*. 2019;151(2):217-225. doi:10.1093/ajcp/aqy141

141. Flaifel A, Xie W, Braun DA, et al. PD-L1 expression and clinical outcomes to cabozantinib, everolimus, and sunitinib in patients with metastatic renal cell carcinoma: Analysis of the randomized clinical trials Meteor and Cabosun. *Clin Cancer Res*. 2019;25(20):6080-6088. doi:10.1158/1078-0432.CCR-19-1135

142. Tatli Dogan H, Kiran M, Bilgin B, et al. Prognostic significance of the programmed death ligand 1 expression in clear cell renal cell carcinoma and correlation with the tumor microenvironment and hypoxia-inducible factor expression. *Diagn Pathol*. 2018;13(1). doi:10.1186/s13000-018-0742-8

143. Möller K, Fraune C, Blessin NC, et al. Tumor cell PD-L1 expression is a strong predictor of unfavorable prognosis in immune checkpoint therapy-naive clear cell renal cell cancer. *Int Urol Nephrol*. 2021;53(12):2493-2503. doi:10.1007/s11255-021-02841-7

144. Matson V, Chervin CS, Gajewski TF. Cancer and the Microbiome—Influence of the Commensal Microbiota on Cancer, Immune Responses, and Immunotherapy. *Gastroenterology*. 2021;160(2):600-613. doi:10.1053/j.gastro.2020.11.041

145. Zitvogel L, Galluzzi L, Viaud S, et al. Cancer and the gut microbiota: An unexpected link. *Sci Transl Med*. 2015;7(271):1-5. doi:10.1126/scitranslmed.3010473

146. Schwabe RF, Jobin C. The microbiome and cancer. *Nat Rev Cancer*. 2013;13(11):800-812.

doi:10.1038/nrc3610

147. Belkaid Y, Hand T. Role of microbiota in immunity and inflammation. *Cell*. 2014;157(1):121-141. doi:10.1016/j.cell.2014.03.011.Role

148. Bocci V. The neglected organ: Bacterial flora has a crucial immunostimulatory role. *Perspect Biol Med*. 1992;35(2):251-260. doi:10.1353/pbm.1992.0004

149. O'Hara AM, Shanahan F. The gut flora as a forgotten organ. *EMBO Rep*. 2006;7(7):688-693. doi:10.1038/sj.embor.7400731

150. Ruff WE, Greiling TM, Kriegel MA. Host–microbiota interactions in immune-mediated diseases. *Nat Rev Microbiol*. 2020;18(9):521-538. doi:10.1038/s41579-020-0367-2

151. Caygill CPJ, Hill MJ, Braddick M, Sharp JCM. Cancer mortality in chronic typhoid and paratyphoid carriers. *Lancet*. 1994;343(8889):83-84. doi:10.1016/S0140-6736(94)90816-8

152. Di Domenico EG, Cavallo I, Pontone M, Toma L, Ensoli F. Biofilm producing Salmonella typhi: Chronic colonization and development of gallbladder cancer. *Int J Mol Sci*. 2017;18(9). doi:10.3390/ijms18091887

153. Kim D, Zeng MY, Núñez G. The interplay between host immune cells and gut microbiota in chronic inflammatory diseases. *Exp Mol Med*. 2017;49(5). doi:10.1038/emm.2017.24

154. Ottman N, Smidt H, de Vos WM, Belzer C. The function of our microbiota: who is out there and what do they do? *Front Cell Infect Microbiol*. 2012;2(August):104. doi:10.3389/fcimb.2012.00104

155. Zitvogel L, Daillère R, Roberti MP, Routy B, Kroemer G. Anticancer effects of the microbiome and its products. *Nat Rev Microbiol*. 2017;15(8):465-478. doi:10.1038/nrmicro.2017.44

156. Kamada N, Seo SU, Chen GY, Núñez G. Role of the gut microbiota in immunity and inflammatory disease. *Nat Rev Immunol*. 2013;13(5):321-335. doi:10.1038/nri3430

157. Zhan Y, Chen PJ, Sadler WD, et al. Gut microbiota protects against gastrointestinal tumorigenesis caused by epithelial injury. *Cancer Res*. 2013;73(24):7199-7210. doi:10.1158/0008-5472.CAN-13-0827

158. Bonnet M, Buc E, Sauvanet P, et al. Colonization of the human gut by E. coli and colorectal cancer risk. *Clin Cancer Res*. 2014;20(4):859-867. doi:10.1158/1078-0432.CCR-13-1343

159. Wang JL, Chang CH, Lin JW, Wu LC, Chuang LM, Lai MS. Infection, antibiotic therapy and risk of colorectal cancer: A nationwide nested case-control study in patients with Type 2 diabetes mellitus. *Int J Cancer*. 2014;135(4):956-967. doi:10.1002/ijc.28738

160. Dapito DH, Mencin A, Gwak GY, et al. Promotion of Hepatocellular Carcinoma by the Intestinal Microbiota and TLR4. *Cancer Cell*. 2012;21(4):504-516. doi:10.1016/j.ccr.2012.02.007

161. Yoshimoto S, Loo TM, Atarashi K, et al. Obesity-induced gut microbial metabolite promotes liver cancer through senescence secretome. *Nature*. 2013;499(7456):97-101. doi:10.1038/nature12347

162. Viaud S, Daillère R, Boneca IG, et al. Harnessing the intestinal microbiome for optimal therapeutic immunomodulation. *Cancer Res*. 2014;74(16):4217-4221. doi:10.1158/0008-5472.CAN-14-0987

163. Vétizou M, Pitt JM, Daillère R, et al. Anticancer immunotherapy by CTLA-4 blockade relies on the gut microbiota. *Science (80-)*. 2015;350(6264):1079-1084. doi:10.1126/science.aad1329

164. Routy B, Le Chatelier E, Derosa L, et al. Gut microbiome influences efficacy of PD-1-based immunotherapy against epithelial tumors. *Science (80-)*. 2018;359(6371):91-97. doi:10.1126/science.aan3706

165. Terrisse S, Derosa L, Iebba V, et al. Intestinal microbiota influences clinical outcome and side effects of early breast cancer treatment. *Cell Death Differ*. 2021;28(9):2778-2796. doi:10.1038/s41418-021-00784-1

166. Derosa L, Hellmann MD, Spaziano M, et al. Negative association of antibiotics on clinical activity of immune checkpoint inhibitors in patients with advanced renal cell and non-small-cell lung cancer. *Ann Oncol*. 2018;29(6):1437-1444. doi:10.1093/annonc/mdy103

167. Derosa L, Routy B, Fidelle M, et al. Gut Bacteria Composition Drives Primary Resistance to Cancer Immunotherapy in Renal Cell Carcinoma Patients. *Eur Urol*. 2020;78(2):195-206. doi:10.1016/j.eururo.2020.04.044

168. Derosa L, Routy B, Thomas AM, et al. Intestinal Akkermansia muciniphila predicts clinical response to PD-1 blockade in patients with advanced non-small-cell lung cancer. *Nat Med*. 2022;28(2):315-324. doi:10.1038/s41591-021-01655-5

169. Hanahan D. Hallmarks of Cancer: New Dimensions. *Cancer Discov*. 2022;12(1):31-46. doi:10.1158/2159-8290.CD-21-1059

170. Viaud S, Saccheri F, Mignot G, et al. The intestinal microbiota modulates the anticancer immune effects of cyclophosphamide. *Science (80-)*. 2013;342(6161):971-976. doi:10.1126/science.1240537

171. Iida N, Dzutsev A, Stewart CA, et al. Commensal bacteria control cancer response to therapy by modulating the tumor microenvironment. *Science (80-)*. 2013;342(6161):967-970. doi:10.1126/science.1240527

172. Sivan A, Corrales L, Hubert N, et al. Commensal Bifidobacterium promotes antitumor immunity and facilitates anti-PD-L1 efficacy. *Science (80-)*. 2015;350(6264):1084-1089. doi:10.1126/science.aac4255

173. Derosa L, Zitvogel L. Antibiotics impair immunotherapy for urothelial cancer. *Nat Rev Urol*. 2020;17(11):605-606. doi:10.1038/s41585-020-0373-1

174. Boursi B, Mamtani R, Haynes K, Yang YX. Recurrent antibiotic exposure may promote cancer formation-Another step in understanding the role of the human microbiota? *Eur J Cancer*. 2015;51(17):2655-2664. doi:10.1016/j.ejca.2015.08.015

175. Pinato DJ, Howlett S, Ottaviani D, et al. Association of prior antibiotic treatment with survival and response to immune checkpoint inhibitor therapy in patients with cancer. *JAMA Oncol*. 2019;5(12):1774-1778. doi:10.1001/jamaoncol.2019.2785

176. Mohiuddin JJ, Chu B, Facciabene A, et al. Association of Antibiotic Exposure with Survival and Toxicity in Patients with Melanoma Receiving Immunotherapy. *J Natl Cancer Inst*. 2021;113(2):162-170. doi:10.1093/jnci/djaa057

177. Şenbabaoğlu Y, Gejman RS, Winer AG, et al. Tumor immune microenvironment characterization in clear cell renal cell carcinoma identifies prognostic and immunotherapeutically relevant messenger RNA signatures. *Genome Biol*. 2016;17(1). doi:10.1186/s13059-016-1092-z

178. Linee guida Tumori del Rene AIOM 2021. 2021:1-25.

179. Dutcher JP, Flippot R, Fallah J, Escudier B. On the Shoulders of Giants: The Evolution of Renal Cell Carcinoma Treatment-Cytokines, Targeted Therapy, and Immunotherapy. 2020. doi:10.1200/EDBK_

180. Chow LQM, Eckhardt SG. Sunitinib: From rational design to clinical efficacy. *J Clin Oncol*. 2007;25(7):884-896. doi:10.1200/JCO.2006.06.3602

181. Nassif E, Thibault C, Vano Y, et al. Sunitinib in kidney cancer: 10 years of experience and development. *Expert Rev Anticancer Ther*. 2017;17(2):129-142. doi:10.1080/14737140.2017.1272415

182. Mendel DB, Laird AD, Xin X, et al. In vivo antitumor activity of SU11248, a novel tyrosine kinase inhibitor targeting vascular endothelial growth factor and platelet-derived growth factor receptors: determination of a pharmacokinetic/pharmacodynamic relationship. *Clin cancer Res an Off J Am Assoc Cancer Res*. 2003;9(1):327-337.

183. Motzer RJ, Rini BI, Bukowski RM, et al. *Sunitinib in Patients With Metastatic Renal Cell Carcinoma*. Vol 295.; 2006. www.jama.com.

184. Motzer RJ, Michaelson MD, Redman BG, et al. Activity of SU11248, a multitargeted inhibitor of vascular endothelial growth factor receptor and platelet-derived growth factor receptor, in patients with metastatic renal cell carcinoma. *J Clin Oncol*. 2006;24(1):16-24. doi:10.1200/JCO.2005.02.2574

185. Motzer RJ, Hutson TE, Tomczak P, et al. *Sunitinib versus Interferon Alfa in Metastatic Renal-Cell Carcinoma*. Vol 356.; 2007. www.nejm.org.

186. Kumar R, Knick VB, Rudolph SK, et al. Pharmacokinetic-pharmacodynamic correlation from mouse to human with pazopanib, a multikinase angiogenesis inhibitor with potent antitumor and antiangiogenic activity. *Mol Cancer Ther*. 2007;6(7):2012-2021. doi:10.1158/1535-7163.MCT-07-0193

187. Hutson TE, Davis ID, Machiels JPH, et al. Efficacy and safety of pazopanib in patients with metastatic renal cell carcinoma. *J Clin Oncol*. 2010;28(3):475-480. doi:10.1200/JCO.2008.21.6994

188. Hainsworth JD, Rubin MS, Arrowsmith ER, Khatcheressian J, Crane EJ, Franco LA. Pazopanib as second-line treatment after sunitinib or bevacizumab in patients with advanced renal cell carcinoma: A sarah cannon oncology research consortium phase ii trial. *Clin Genitourin Cancer*. 2013;11(3):270-275. doi:10.1016/j.clgc.2013.04.006

189. Sternberg CN, Davis ID, Mardiak J, et al. Pazopanib in locally advanced or metastatic renal cell carcinoma: Results of a randomized phase III trial. *J Clin Oncol*. 2010;28(6):1061-1068. doi:10.1200/JCO.2009.23.9764

190. Motzer RJ, Hutson TE, Cella D, et al. Pazopanib versus Sunitinib in Metastatic Renal-Cell Carcinoma. *N Engl J Med*. 2013;369(8):722-731. doi:10.1056/nejmoa1303989

191. Motzer RJ, Hutson TE, McCann L, Deen K, Choueiri TK. Overall Survival in Renal-Cell Carcinoma with Pazopanib versus Sunitinib. *N Engl J Med*. 2014;370(18):1769-1770. doi:10.1056/nejmc1400731

192. Escudier B, Porta C, Bono P, et al. Randomized, controlled, double-blind, cross-over trial assessing treatment preference for pazopanib versus sunitinib in patients with metastatic renal cell carcinoma: PISCES study. *J Clin Oncol*. 2014;32(14):1412-1418. doi:10.1200/JCO.2013.50.8267

193. Yakes FM, Chen J, Tan J, et al. Cabozantinib (XL184), a novel MET and VEGFR2 inhibitor, simultaneously suppresses metastasis, angiogenesis, and tumor growth. *Mol Cancer Ther*. 2011;10(12):2298-2308. doi:10.1158/1535-7163.MCT-11-0264

194. Khanna A, Crane A, Yerram N, et al. *Contemporary Management of Advanced Renal Cell Carcinoma*. Vol

16.; 2018.

195. Choueiri TK, Hessel C, Halabi S, et al. Cabozantinib versus sunitinib as initial therapy for metastatic renal cell carcinoma of intermediate or poor risk (Alliance A031203 CABOSUN randomised trial): Progression-free survival by independent review and overall survival update. *Eur J Cancer*. 2018;94:115-125. doi:10.1016/j.ejca.2018.02.012

196. Rini BI. Temsirolimus, an inhibitor of mammalian target of rapamycin. *Clin Cancer Res*. 2008;14(5):1286-1290. doi:10.1158/1078-0432.CCR-07-4719

197. Dutcher JP, De Souza P, McDermott D, et al. Effect of temsirolimus versus interferon-α on outcome of patients with advanced renal cell carcinoma of different tumor histologies. *Med Oncol*. 2009;26(2):202-209. doi:10.1007/s12032-009-9177-0

198. Motzer RJ, Escudier B, Oudard S, et al. Phase 3 trial of everolimus for metastatic renal cell carcinoma: Final results and analysis of prognostic factors. *Cancer*. 2010;116(18):4256-4265. doi:10.1002/cncr.25219

199. Xu JX, Maher VE, Zhang L, et al. FDA Approval Summary: Nivolumab in Advanced Renal Cell Carcinoma After Anti-Angiogenic Therapy and Exploratory Predictive Biomarker Analysis. *Oncologist*. 2017;22(3):311-317. doi:10.1634/theoncologist.2016-0476

200. Motzer RJ, Tannir NM, McDermott DF, et al. Nivolumab plus Ipilimumab versus Sunitinib in Advanced Renal-Cell Carcinoma. *N Engl J Med*. 2018;378(14):1277-1290. doi:10.1056/nejmoa1712126

201. Gross-Goupil M, François L, Quivy A, Ravaud A. Axitinib: A review of its safety and efficacy in the treatment of adults with advanced renal cell carcinoma. *Clin Med Insights Oncol*. 2013;7:269-277. doi:10.4137/CMO.S10594

202. Rini BI, Plimack ER, Stus V, et al. Pembrolizumab plus axitinib versus sunitinib for advanced renal-cell carcinoma. *N Engl J Med*. 2019;380(12):1116-1127. doi:10.1056/NEJMoa1816714

203. Choueiri TK, Powles T, Burotto M, et al. Nivolumab plus Cabozantinib versus Sunitinib for Advanced Renal-Cell Carcinoma. *N Engl J Med*. 2021;384(9):829-841. doi:10.1056/nejmoa2026982

204. Motzer RJ, Powles T, Burotto M, et al. Nivolumab plus cabozantinib versus sunitinib in first-line treatment for advanced renal cell carcinoma (CheckMate 9ER): long-term follow-up results from an open-label, randomised, phase 3 trial. *Lancet Oncol*. 2022;23(7):888-898. doi:10.1016/S1470-2045(22)00290-X

205. Motzer R, Alekseev B, Rha S-Y, et al. Lenvatinib plus Pembrolizumab or Everolimus for Advanced Renal Cell Carcinoma. *N Engl J Med*. 2021;384(14):1289-1300. doi:10.1056/nejmoa2035716

206. Motzer RJ, Escudier B, McDermott DF, et al. Nivolumab versus everolimus in advanced renal-cell carcinoma. *N Engl J Med*. 2015;373(19):1803-1813. doi:10.1056/NEJMoa1510665

207. Choueiri TK, Escudier B, Powles T, et al. Cabozantinib versus Everolimus in Advanced Renal-Cell Carcinoma. *N Engl J Med*. 2015;373(19):1814-1823. doi:10.1056/nejmoa1510016

208. Cavazzoni A, Digiacomo G, Alfieri R, et al. Pemetrexed enhances membrane PD-L1 expression and potentiates T cell-mediated cytotoxicity by anti-PD-L1 antibody therapy in non-small-cell lung cancer. *Cancers (Basel)*. 2020;12(3). doi:10.3390/cancers12030666

209. Jiao S, Xia W, Yamaguchi H, et al. PARP Inhibitor Upregulates PD-L1 Expression and Enhances Cancer-

Associated Immunosuppression. *Clin cancer Res an Off J Am Assoc Cancer Res*. 2017;23(14):3711-3720. doi:10.1158/1078-0432.CCR-16-3215

210. Doi T, Ishikawa T, Okayama T, et al. The JAK/STAT pathway is involved in the upregulation of PD-L1 expression in pancreatic cancer cell lines. *Oncol Rep*. 2017;37(3):1545-1554. doi:10.3892/or.2017.5399
211. Garcia-diaz A, Shin DS, Moreno BH, et al. HHS Public Access. 2019;19(6):1189-1201. doi:10.1016/j.celrep.2017.04.031.Interferon
212. Gilad Y, Eliaz Y, Yu Y, Han SJ, O'Malley BW, Lonard DM. Author Correction: Drug-induced PD-L1 expression and cell stress response in breast cancer cells can be balanced by drug combination (Scientific Reports, (2019), 9, 1, (15099), 10.1038/s41598-019-51537-7). *Sci Rep*. 2020;10(1):1-8. doi:10.1038/s41598-020-60964-w
213. Peng J, Hamanishi J, Matsumura N, et al. Chemotherapy induces programmed cell death-ligand 1 overexpression via the nuclear factor-κBto foster an immunosuppressive tumor microenvironment in Ovarian Cancer. *Cancer Res*. 2015;75(23):5034-5045. doi:10.1158/0008-5472.CAN-14-3098
214. Bando Y, Hinata N, Omori T, Fujisawa M. A prospective, open-label, interventional study protocol to evaluate treatment efficacy of nivolumab based on serum-soluble PD-L1 concentration for patients with metastatic and unresectable renal cell carcinoma. *BMJ Open*. 2019;9(12):1-5. doi:10.1136/bmjopen-2019-030522
215. Terenziani R, Zoppi S, Fumarola C, Alfieri R, Bonelli M. Immunotherapeutic approaches in malignant pleural mesothelioma. *Cancers (Basel)*. 2021;13(11). doi:10.3390/cancers13112793
216. Sabins NC, Harman BC, Barone LR, Shen S, Santulli-Marotto S. Differential expression of immune checkpoint modulators on in vitro primed CD4+ and CD8+ T cells. *Front Immunol*. 2016;7(JUN):1-11. doi:10.3389/fimmu.2016.00221
217. Triplett TA, Curti BD, Bonafede PR, Miller WL, Walker EB, Weinberg AD. Defining a functionally distinct subset of human memory CD4+ T cells that are CD25POS and FOXP3NEG. *Eur J Immunol*. 2012;42(7):1893-1905. doi:10.1002/eji.201242444
218. Jubel JM, Barbati ZR, Burger C, Wirtz DC, Schildberg FA. The Role of PD-1 in Acute and Chronic Infection. *Front Immunol*. 2020;11. doi:10.3389/fimmu.2020.00487
219. Takahashi R, Sato Y, Kimishima M, Shiohara T, Ohyama M. Intracellular accumulation of PD-1 molecules in circulating T lymphocytes in advanced malignant melanoma: an implication for immune evasion mechanism. *Int J Clin Oncol*. 2020;25(10):1861-1869. doi:10.1007/s10147-020-01732-8
220. Derosa L, Hellmann MD, Spaziano M, et al. Negative association of antibiotics on clinical activity of immune checkpoint inhibitors in patients with advanced renal cell and non-small-cell lung cancer. *Ann Oncol*. 2018;29(6):1437-1444. doi:10.1093/annonc/mdy103
221. Matson V, Fessler J, Bao R, et al. The commensal microbiome is associated with anti-PD-1 efficacy in metastatic melanoma patients. *Science*. 2018;359(6371):104-108. doi:10.1126/science.aao3290
222. Motzer R, Alekseev B, Rha S-Y, et al. Lenvatinib plus Pembrolizumab or Everolimus for Advanced Renal Cell Carcinoma. *N Engl J Med*. 2021;384(14):1289-1300. doi:10.1056/nejmoa2035716
223. Escudier B, Farace F, Angevin E, et al. Immunotherapy with interleukin-2 (IL2) and lymphokine-activated

natural killer cells: improvement of clinical responses in metastatic renal cell carcinoma patients previously treated with IL2. *Eur J Cancer*. 1994;30A(8):1078-1083. doi:10.1016/0959-8049(94)90460-x

224. Porta C, Schmidinger M. Renal cell carcinoma treatment after first-line combinations. *Lancet Oncol*. 2019;20(10):1332-1334. doi:10.1016/S1470-2045(19)30510-8
225. Motzer RJ, Penkov K, Haanen J, et al. Avelumab plus Axitinib versus Sunitinib for Advanced Renal-Cell Carcinoma. *N Engl J Med*. 2019;380(12):1103-1115. doi:10.1056/nejmoa1816047
226. Rini BI, Plimack ER, Stus V, et al. Pembrolizumab plus Axitinib versus Sunitinib for Advanced Renal-Cell Carcinoma. *N Engl J Med*. 2019;380(12):1116-1127. doi:10.1056/nejmoa1816714
227. Rini BI, Powles T, Atkins MB, et al. Atezolizumab plus bevacizumab versus sunitinib in patients with previously untreated metastatic renal cell carcinoma (IMmotion151): a multicentre, open-label, phase 3, randomised controlled trial. *Lancet*. 2019;393(10189):2404-2415. doi:10.1016/S0140-6736(19)30723-8
228. Gabrilovich D, Ishida T, Oyama T, et al. *Vascular Endothelial Growth Factor Inhibits the Development of Dendritic Cells and Dramatically Affects the Differentiation of Multiple Hematopoietic Lineages In Vivo*.
229. Muramatsu M, Yamamoto S, Osawa T, Shibuya M. Vascular endothelial growth factor receptor-1 signaling promotes mobilization of macrophage lineage cells from bone marrow and stimulates solid tumor growth. *Cancer Res*. 2010;70(20):8211-8221. doi:10.1158/0008-5472.CAN-10-0202
230. Kaur S, Chang T, Singh SP, et al. CD47 Signaling Regulates the Immunosuppressive Activity of VEGF in T Cells. *J Immunol*. 2014;193(8):3914-3924. doi:10.4049/jimmunol.1303116
231. Voron T, Colussi O, Marcheteau E, et al. VEGF-A modulates expression of inhibitory checkpoints on CD8++ T cells in tumors. *J Exp Med*. 2015;212(2):139-148. doi:10.1084/jem.20140559
232. Huang H, Langenkamp E, Georganaki M, et al. VEGF suppresses T-lymphocyte infiltration in the tumor microenvironment through inhibition of NF-κB-induced endothelial activation. *FASEB J*. 2015;29(1):227-238. doi:10.1096/fj.14-250985
233. Hirsch L, Flippot R, Escudier B, Albiges L. Immunomodulatory Roles of VEGF Pathway Inhibitors in Renal Cell Carcinoma. *Drugs*. 2020;80(12):1169-1181. doi:10.1007/s40265-020-01327-7
234. Ozao-Choy J, Ge M, Kao J, et al. The novel role of tyrosine kinase inhibitor in the reversal of immune suppression and modulation of tumor microenvironment for immune-based cancer therapies. *Cancer Res*. 2009;69(6):2514-2522. doi:10.1158/0008-5472.CAN-08-4709
235. Läubli H, Müller P, D'Amico L, Buchi M, Kashyap AS, Zippelius A. The multi-receptor inhibitor axitinib reverses tumor-induced immunosuppression and potentiates treatment with immune-modulatory antibodies in preclinical murine models. *Cancer Immunol Immunother*. 2018;67(5):815-824. doi:10.1007/s00262-018-2136-x
236. Hughes A, Clarson J, Tang C, et al. CML patients with deep molecular responses to TKI have restored immune effectors and decreased PD-1 and immune suppressors. *Blood*. 2017;129(9):1166-1176. doi:10.1182/blood-2016-10-745992
237. Lucibello G, Mograbi B, Milano G, Hofman P, Brest P. PD-L1 regulation revisited: impact on immunotherapeutic strategies. *Trends Mol Med*. 2021;27(9):868-881. doi:10.1016/j.molmed.2021.06.005

238. Mezzadra R, Sun C, Jae LT, et al. Identification of CMTM6 and CMTM4 as PD-L1 protein regulators. *Nature*. 2017;549(7670):106-110. doi:10.1038/nature23669

239. Boyerinas B, Jochems C, Fantini M, et al. Antibody-dependent cellular cytotoxicity activity of a Novel Anti-PD-L1 antibody avelumab (MSB0010718C) on human tumor cells. *Cancer Immunol Res*. 2015;3(10):1148-1157. doi:10.1158/2326-6066.CIR-15-0059

240. Hamilton G, Rath B. Avelumab: combining immune checkpoint inhibition and antibody-dependent cytotoxicity. *Expert Opin Biol Ther*. 2017;17(4):515-523. doi:10.1080/14712598.2017.1294156

241. Du Four S, Maenhout SK, Benteyn D, et al. Disease progression in recurrent glioblastoma patients treated with the VEGFR inhibitor axitinib is associated with increased regulatory T cell numbers and T cell exhaustion. *Cancer Immunol Immunother*. 2016;65(6):727-740. doi:10.1007/s00262-016-1836-3

242. Simon S, Labarriere N. PD-1 expression on tumor-specific T cells: Friend or foe for immunotherapy? *Oncoimmunology*. 2018;7(1):e1364828. doi:10.1080/2162402X.2017.1364828

243. Wherry EJ, Kurachi M. Molecular and cellular insights into T cell exhaustion. *Nat Rev Immunol*. 2015;15(8):486-499. doi:10.1038/nri3862

244. Vétizou M, Pitt JM, Daillère R, et al. Anticancer immunotherapy by CTLA-4 blockade relies on the gut microbiota. *Science (80-)*. 2015;350(6264):1079-1084. doi:10.1126/science.aad1329

245. Derosa L, Routy B, Thomas AM, et al. Intestinal Akkermansia muciniphila predicts clinical response to PD-1 blockade in patients with advanced non-small-cell lung cancer. *Nat Med*. 2022;28(2):315-324. doi:10.1038/s41591-021-01655-5